Simulation of TDP Dynamics during S–laying of Subsea Pipelines

Simulering av TDP Dynamikk under S-legging av offshore srørledninger

Master Thesis

By

Author: Hong, Wei

Supervisor: Professor Svein Sævik

PREFACE

This report is an individual master thesis carried out during the spring of 2010 at the Department of Marine Technology, Norwegian University of Science and Technology, Trondheim. During installation of subsea pipelines, the penetration of the pipe prior to operation has a tendency of being larger than the predicted values. This may have large consequences with respect to intervention work and cost impact. The thesis is to try to explain the behavior that the penetration of the pipe has a tendency of being larger than the predicted values during installation by the dynamics at the touch down point (TDP) induced by 1st order motions from waves using the computer code SIMLA.

I would like to thank my supervisor Professor Svein Sævik, who is a very nice and warm-hearted, for his kind guidance a lot. He helped me a lot with SIMLA, which is his master piece. During the whole semester, I was given sufficient guidance from him.

Finally, my gratitude goes to my parents who are always there support me and love me unconditionally.

ABSTRACT

During the past one and a half decade, pipeline has been proven to the most economical means of large scale overland transportation for crude oil, natural gas and other products. At the same time, more and more problems are encountered. A lot of effort has been put to gain more knowledge about pipeline installation, operation and so on. During installation of subsea pipeline, the penetration of the pipe prior to operation has a tendency of being larger than the predicted values. This may have a great influence on the intervention work and cost impact. It is therefore of interest to investigate whether this behavior can be explained by the dynamics at the touch down point (TDP) induced by 1st order motions from waves.

This thesis work therefore focus on dynamic simulation of pipelines using the computer code SIMLA and put special emphasis on investigating the work done by the pipe onto the soil at TDP as the installation process goes on. For this purpose, a dynamic analysis model for a 32 inch pipeline at 200-300 m water depth is established with SIMLA input code. Both static and dynamic analyses are performed. A comparable very long time analysis time is applied in order to get stable results. The influence of various parameters viz. wave height, wave period and wave direction are investigated in this thesis. The TDP dynamics as a function of sea state is investigated with concentration on the dynamic pipe-soil interaction force and displacement as a function of time.

CONTENT

List of Figures

Chapter 1 Introduction

The first pipeline was built in the United States in 1859 to transport crude oil (Wolbert, 1952). During the past one and a half decade, it has been proven to the most economical means of large scale overland transportation for crude oil, natural gas and other products. The pipeline has been used extensively for many purposes as illustrated in Figure 1.1:

- Export (transportation) pipelines;
- Flowlines to transfer product from a platform to export lines;
- Water injection or chemical injection flowlines;
- Flowlines to transfer product between platforms, subsea manifolds and satellite wells;
- Pipeline bundles.

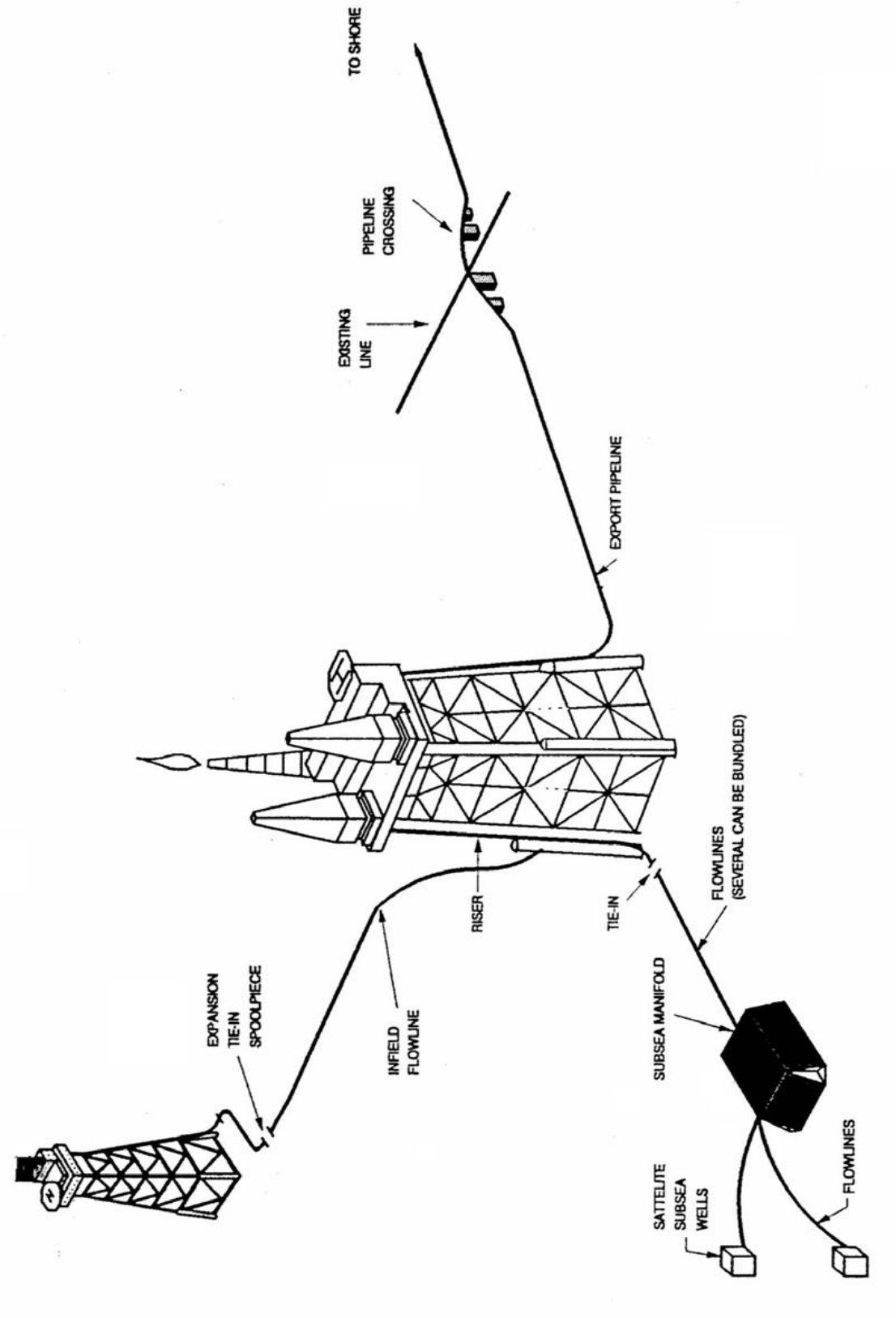

Figure 1.1 Use of Offshore Pipelines (Bai, Yong et al., 2005)

During installation of subsea pipelines, the penetration of the pipe prior to operation has a tendency of being larger than the predicted values. This may have large consequences with respect to intervention work and cost impact. It is therefore of interest to investigate whether this behavior can be explained by the dynamics at the touch down point (TDP) induced by vessel 1st order motions from waves.

The thesis work therefore focuses on dynamic simulation of pipelines using the computer code SIMLA and puts special emphasis on investigating the work done by the pipe onto the soil at TDP as the installation process goes on.

SIMLA is MARINTEK's newly developed computer tool for analysis of offshore pipelines in deep waters and rough environments.

The thesis may be divided into two major parts. The first part describes the background theory material. Brief introduction is given to the offshore pipeline installation technology in which S-lay, J-lay, reel lay method, and tow or pull method are described briefly. During pipeline installation and the subsequent operation phase, the contact of the pipeline and seabed also known as the pipe-soil interaction should be studied. Pipeline resting on the seabed is subjected to hydrodynamic forces arising from the wave and current. The response of the pipeline is nonlinear due to nonlinear hydrodynamic forces and nonlinear interaction between the pipe and soil. Nonlinear finite element method is applied to perform the computing the dynamic response of the pipeline.

The second part focuses on the dynamic simulation of pipelines using the computer code SIMLA. A dynamic analysis model for 32 inch pipeline at 200-300 water depth is established. The influence of various parameters viz. wave height, wave period and wave direction are investigated in this thesis. 4 sea states and 3 wave propagation directions are considered. Thus there are total 12 combinations of sea state and wave propagation direction. The simulations of the 12 cased are performed respectively. Then we try to investigate the TDP dynamics as a function of sea state. Special emphasis is put on the dynamic pipe-soil interaction force and displacement as a function of time.

Chapter 2 Offshore Pipeline Installation Technology

2.1 Introduction

To keep up with the trend of the discovery of oil and gas fields in deeper and deeper water depth up to 3000 m, the pipeline installation technology has beegreatly improved in the past twenty years. There are several methods for pipeline installation as follows:

a) S-lay method

b) J-lay method

c) Reel lay method

d) Tow or pull method including bottom tow, off-bottom tow, mid depth tow, surface tow.

Among those above, S-lay, J-lay, reel lay are the most common methods in practice. S-laying is used in a range of water depth from shallow to deep water, while J-laying and reeling from intermediate to deep water. Tow or pull methods can be used from shallow water to deep water. Herein, the shallow water depth ranges from shore to 500 feet. The range for intermediate water depth is from 500 feet to 1000 feet. And the deep water is water depth greater than 1000 feet. What's more, different vessel types will be adapted depending on the installation methods used and site characteristics (water depth, weather etc).

S-lay/J-lay semisubmersibles;

S-lay/J-lay ships;

Reel ships;

Tow or pull vessels.

Most of the material in this chapter is collected from (Boyun Guo et al., 2005) and (Gilbert Gedeon, 2001).

2.2 S-lay Method

S-lay method is the most common method of pipeline installation in shallow water. S-lay takes its name from the shape the pipe assumes on its way to the seabed. On the deck of the lay-vessel, there is a near horizontal ramp including the firing line consisting of some stations for welding, NDE and field joint application and tension machines. The field joint station is located after the NDE station and the tension machines. As the welding of pipeline goes on, the pipeline is gradually lowered to the seabed behind the vessel by moving the vessel forward. The rollers and the tension machines create a curved support for the pipeline. The welded pipeline is supported on the rollers of the vessel and the stinger, forming the overbend. Then it is suspended in the water all the way to the seabed, forming the sagbend. The overbend and sagbend form the S-shape. In figure 2.1 shows S-laying configuration.

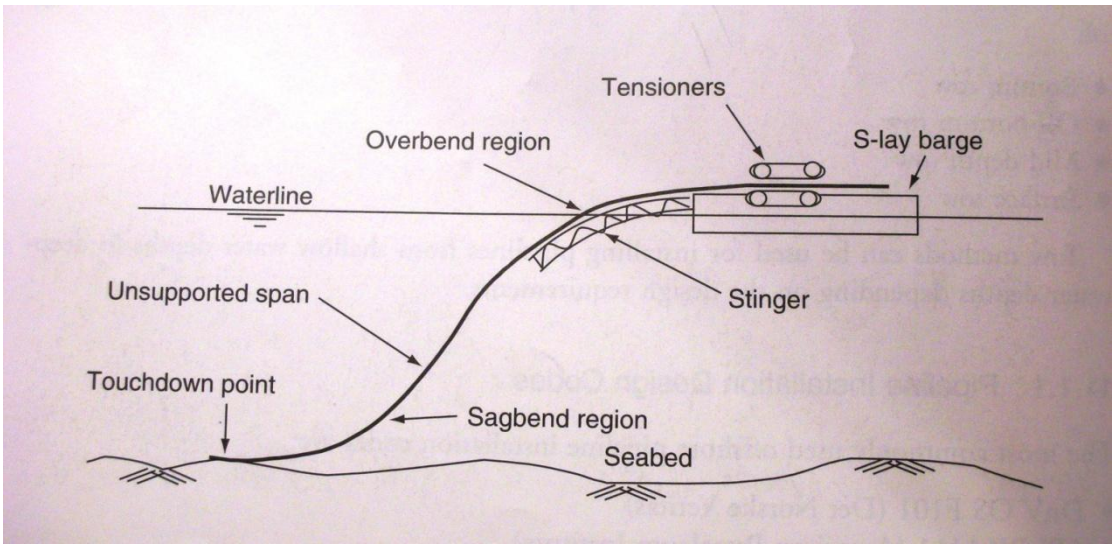

Figure 2.1 S-lay Method for Shallow to Deep Pipelines (Boyun Guo et al., 2005)

The stinger, a truss-like structure equipped with rollers, is used to reduce the

curvature and therefore the bending stress of the pipe as it leaves the vessel. The stinger is normally made up of more than one section. Through moving the sections relative to the vessel and each other, different assemblies can be made. The position of the rollers relative to the section they belong to can be changed too. Thus, a vessel can be configured for a number of different radiuses of curvature. The stinger radius controls the overbend curvature. And the vessel has an upper and lower limit of the departure angle at which the pipeline departs from the stinger due to the limitations for both minimum and maximum radius of curvature for the stinger. A roller/support is normally built up of some wheels, see figure 2.2. (Bai, Yong et al., 2005)

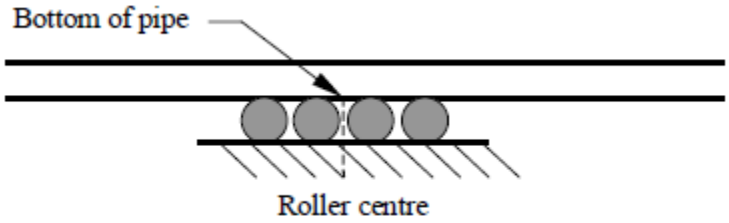

Figure 2.2 Typical Roller/Support for Pipeline (Bai, Yong et al., 2005)

To avoid buckling of the pipe, a tensioning roller and controlled forward thrust must be used to provide appropriate tensile load to the pipeline. By applying tension to the pipeline to support the submerged weight of the suspended part of the pipeline, the curvature of the sagbend and the moment at the stinger tip can be controlled. The tensioner on the vessel pulls the pipeline, keeping the whole section to the seabed in tension. The reaction of this pull is taken up by anchors installed ahead of the vessel, or by thrusters for a dynamically positioned vessel. The required tension depends on the water depth, the submerged weight of the pipeline, the allowable curvature of the overbend and sagbend, and departure angle. The tensioner normally consists of an upper and lower track loops. Wheels in the track loops apply squeeze forces to the tracks which in turn grip the pipeline, see Figure 2.3. (Bai, Yong et al., 2005)

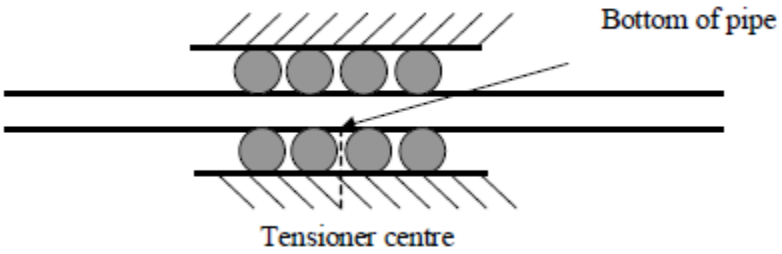

Figure 2.3 Typical Tensioner Support (Bai, Yong et al., 2005)

The deeper the water depths are, the larger the curvature of the pipe becomes. Then longer stinger is required, which will be too long in extremely deep water. What's more, deeper water depths will result in a steeper departure angle of the suspended pipe at the stinger tip, requiring smaller-radius stinger to accommodate the suspended pipe. Meanwhile, in order to support the increased weight of the suspended pipe, greater structural strength will be required. To avoid these difficulties, J-lay method is adopted. J-lay will be briefly introduced in the following section.

2.3 J-lay Method

J-lay method is relatively new for pipeline installation in deeper water to keep up with the trend of the discovery of deepwater oil and gas fields. The method was so-named because the configuration of the pipe resembles "J" as it is being installed. In Figure 2.4 shows the J-lay configuration. Lengths of pipe are joined to each other by welding or other means while supported in a vertical or near-vertical position by a tower and lowered to the seabed. J-lay vessels drop the pipe down almost vertically until it reaches the touchdown point, forming J-shape. In this configuration, the pipeline has a large radius bend from the surface to the seabed. As a result, J-lay induces lower stresses than S-lay in the same water depth. There is no overbend and the stinger is only used to change the angle at the top of the pipeline to a vertical orientation. The horizontal forces required to maintain this configuration are much smaller than those required for S-lay, which means the tensile load and forward thrust can be eliminated. This is favorable for DP vessels and derrick barges to be equipped with a J-lay tower. The J-lay method is slower than the S-lay method and is, therefore, more costly. But since the large J-lay towers are capable of handling prefabricated quad joints (160 feet long), the speed of pipelaying is greatly increased. In deep water, S-lay induces a higher strain than for J-lay. The J-lay is more suitable for deep water like water depths greater than 500 feet, which is

too large for conventionally moored lay vessels to operate because the required tension on anchors and pipe bending stresses are too large. But because of limited pipe angle and the bending stress imposed on the pipe, the J-lay method is difficult to operate in water depths as shallow as 200-500 feet.

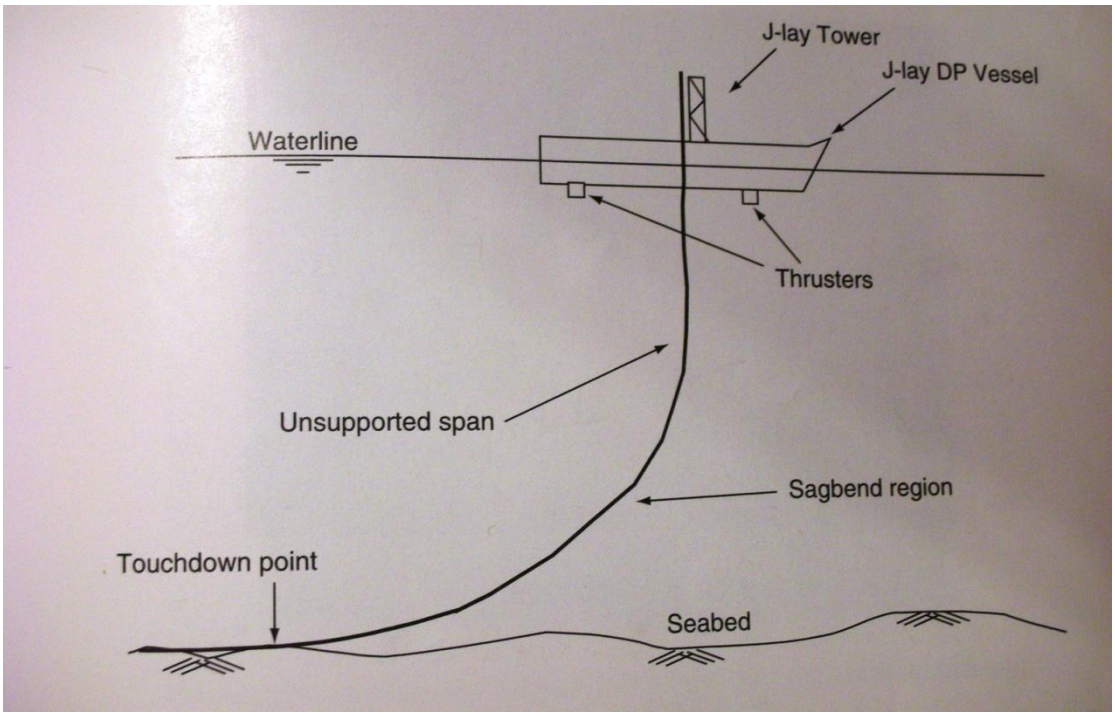

Figure 2.4 J-lay Method for Deep Water Pipelines (Boyun Guo et al., 2005)

2.4 Reel Method

Reel pipelay is a method of installing pipelines by reel vessel. The pipe is welded, coated with a resilient protective coating (flexible epoxy or polyethylene jacket) at an onshore spool base, and spooled onto a drum which is mounted on the deck of a pipelay vessel. After the pipe is loaded onto the drum, the vessel takes it to the offshore location for installation. The pipe is fed off of the drum, straightened, deovalized, and then connected to the wire rope from the seabed pre-installed hold-back anchor. As the pipe stretches from the sea surface to the seabed, a sagbend forms in the pipe. The pipe has to be tensioned to control the sagbend stresses. If the sagbend stresses are too large, the pipe will buckle. The required amount of tension is dependent on the depth of water, the axial strength of the pipe, the allowable stresses for the particular pipe, and the capacity of the tensioning winches. The vessel moves ahead

slowly usually at about one knot depending on weather conditions while it slowly reels out the pipe. When the drum has been emptied, a pullhead connected a wire rope is attached. The A&R wire rope from the reel vessel is played out slowly maintaining sufficient tension in the pipe until the pipe rests on the seabed. A buoy is attached to the end of the A&R cable. Then the reel vessel returns to the spool base to replenish the reel or take on a fully loaded new drum. On returning to the site, it pulls the end of the pipe using the A&R cable, removes the pullhead, and welds it to the pipe on the drum. Then the unreeling process goes on.

The pipe undergoes plastic deformation when it is reeled onto a drum. Thus the pipe experiences some plastic strain. So the diameter of the pipe is restricted by the permissible amount of strain. Usually, the maximum diameter of the pipe is up to 18 inches. And also, due to the limited size of the drum, only short lengths of the pipe can be laid (usually 3-15km depending on pipe diameter). However, it is possible to install larger lines if more drums of pipe are available.

The reeled pipeline can be installed in either S-lay method or J-lay method, depending on the design of the reel vessel and the water depths. Reel vessels are divided into two classes-horizontal reel and vertical reel.

Horizontal reel vessels lay pipelines in shallow to intermediate water depths. S-lay method is adopted. The axis of rotation is vertical with respect to the barge deck. Both anchors and DP can be used for station-keeping of the horizontal reel vessels.

Vertical reel vessels lay is versatile. It can lay pipes from shallow water depths to very deep water depths. This method minimizes bending stresses in the overbend region. If the drum is bottom-loaded, the pipe is fed off horizontally making it well suited for shallow water. For deepwater pipelaying, the drum is top-loaded and the pipe is discharged vertically after it is straightened. For intermediate water depths, the angle of entry can be adjusted according to the engineering calculations and judgments. For deepwater, J-lay method is used. And since bending stresses are minimized by the vertical reel method, no stinger is needed. Only DP is used for station-keeping of the vertical reel vessels.

There are many advantages of the reel method. First, since no on-board welding is needed, the method speeds up the pipeline installation process. The speed of pipelaying with reel method can be up to 10 times faster than conventional pipelaying, which means pipelaying is allowed during a fairly short weather window and the conventional construction season can be

extended by several months.

Most of the welding, x-raying inspection, corrosion coating and testing are accomplished on shore. Thus the labor cost is greatly reduced since labor cost on shore is generally lower than that offshore. Moreover, the processes such as welding, x-raying inspection and so on are performed under controlled conditions onshore. In this way, the quality of the pipeline construction is greatly enhanced.

The principal disadvantage of this method is the difficulty of connecting the ends of the pipeline segments. Re-reeling the pipeline to remove a buckle can be particularly time-consuming. The so-called "weight coated" pipeline could not be reeled because the coating would be destroyed by the bending inherent in this method. Only specifically designed pipe-in-pipe pipelines can be reeled. The pipeline undergoes plastic deformation and then is straightened. Some thinning of the wall and loss of yield strength of the material in localized areas can occur (More detail from Bauschinger effect). When the pipeline is being laid far offshore or a long distance from the spool base, then the method is not that good since plenty of time would be spent in transit to and from the spool base. A DP vertical reel vessel is illustrated in Figure 2.5. (Boyun Guo et al., 2005)

Figure 2.5 Technip's DP Vertical Reel Vessel Deep Blue (J-lay)
(www.technip.com)

2.5 Tow Methods

Compared to the previous three methods, tow method is less commonly used. The fabrication and assembly of the pipeline, that is welding, inspection, joint-coating, and anode installation, are all performed onshore. The fabrication cost is much lower than that offshore. Due to the limited size of the fabrication yard, this method is normally applied to short lines, usually less than 7km. It is particularly well-suited to pipe-in-pipe flowline assemblies, which can be fabricated more efficiently onshore and which contain thermal insulation in the annular space between the inner and outer pipes.

The pipeline can be made up in two ways – perpendicular and parallel to the shoreline.

In the perpendicular launch method, a long enough land to accommodate the longest section of the fabricated pipeline has to be leased. A rail system is installed from the shore end right into the water. First, all the sections that make up the pipeline are fabricated and tested. And then, the first section of the pipeline is lifted by side booms and placed on the rollers of the rail system. The section is attached to the cable from the tow vessel and is pulled into the water, leaving sufficient length onshore to make a welded tie-in to the next section. Then section by section, the whole pipeline is fabricated and pulled into the water. To keep the pipeline under control, a hold-back winch is used during pulling.

In the parallel launch method, the length of the land along the shore should normally be equal to the total length of the pipeline. Compared to perpendicular method, no rail system is needed. After all the sections of the pipeline are welded and tested, the sections are strung along the shoreline. Then all the sections are welded together to make up the pipeline. After that, the pipeline is moved into the water using side-bottom tractors and crawler cranes for the end structures. The front end is attached to the tow vessel, while the rear end is attached to a hold-back anchor. The pipeline is gradually moved laterally into the water by the winches in the anchored tow vessel. At the same time, the curvature of the pipeline is monitored all the time. When the whole length of the pipeline and its end structures are in a straight line, the tow vessel starts to tow the pipeline along the predetermined tow route.

When the pipeline is to be towed into deepwater, pressurized nitrogen can be introduced to the pipeline in order to prevent collapse or buckling under external hydrostatic pressure.

There are four variations of the tow method: bottom tow, off-bottom tow, mid-depth tow, and surface tow. (Boyun Guo et al., 2005)

2.5.1 Bottom tow

In the bottom tow method, the pipeline is towed on or near the seabed along the route that was pre-surveyed to identify any potential seabed hazards. In Figure 2.6 illustrates the bottom tow method. A sea-bottom survey of the pipeline along the tow route from the shoreline to the designated position must be conducted. If the pipeline is launched parallel to the shore, then the whole shallow water area near shore along the length of the pipeline must be surveyed. The route must not cross existing pipelines. If so, some actions like installing and removing structures have to be taken to protect the existing pipelines.

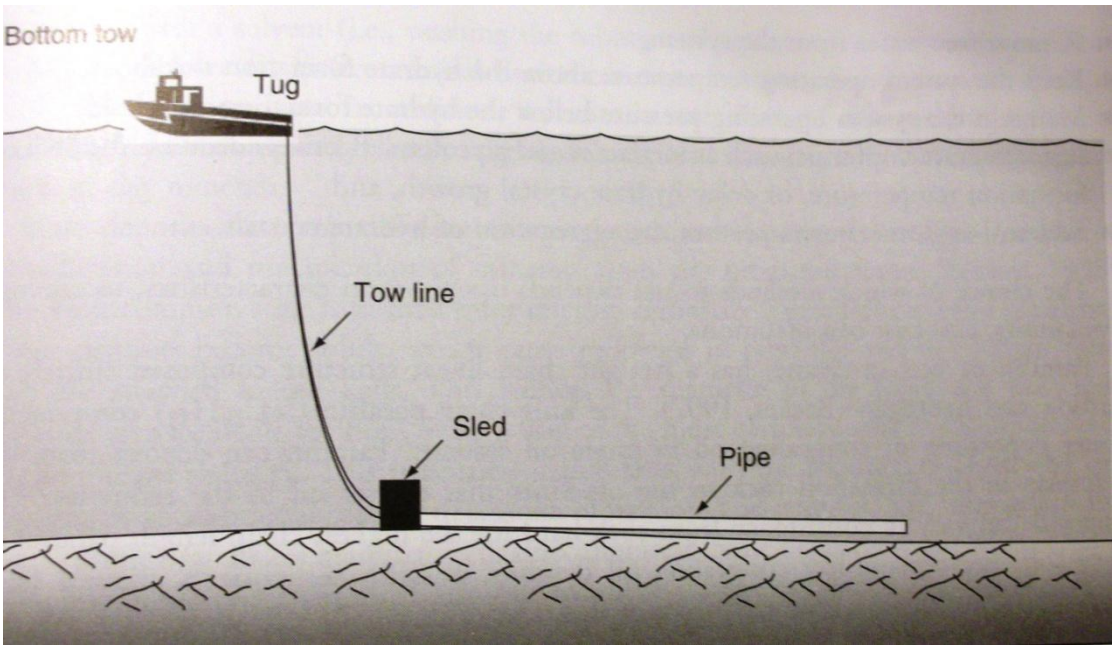

Figure 2.6 Bottom Tow for Pipeline Installation (Boyun Guo et al., 2005)

The length of a single section of the pipeline is limited by the available bollard pull of the vessel. The bollard pull must be greater than the total submerged weight of the pipeline, plus the partially submerged weight of the end structures, times the friction coefficient of the soil. The ends of a bottom-towed pipeline are normally connected by deflect-to-connect method. In this method, the end sections of the pipeline are made to float a few feet above the seabed by providing additional buoy for this length and attaching anchor chains at discrete spacing along this length. The buoy and chains are attached onshore

with chains strapped over the pipeline during towing and deployed in the designated position. This length can then be pulled laterally by attaching cables to the end of the pipeline from the facility. Once the pipeline end structure is secured at the facility, the connection can be made by flanges (in diving depth) or by hydraulically activated connectors (in deepwater).

During tow, the pipeline moves on the seabed. Due to the friction between the pipeline and the seabed, the bottom of the pipeline will have some abrasion. Thus, an additional abrasion-resistant coating is required on the bottom half of the pipeline to protect the normal corrosion-resistant coating like FBE. If concrete weight coating is required for the stability, this can be the abrasion-resistant coating. And additional thickness may be required to allow for abrasion. Several abrasion-resistant coatings that match FBE are available on the market. However, abrasion testing may be required to select the appropriate coating. Moreover, a slick coating on the bottom half of the pipeline can reduce friction and the bollard pull requirement during towing.

For pipelines in shallow water, a trench may be needed due to regulatory requirements or for the stability of the pipeline. In this case, a subsea trenching plow can be attached ahead of the pipeline before pulling it into the designated position. Thus more bollard pull will be needed. A trench can be prepared prior to pulling the pipeline in. It should be noticed that it will be difficult to pull a pipeline into a curved trench. At the same time, a chase vessel is required to keep fishing vessels from crossing the bottom-towed pipeline.

It is worthy to note that the pipeline can be subjected to large wave forces from storms while lying on the beach or near-shore. In this case, a pipe anchor system is required to be available for this kind of emergency. (Boyun Guo et al., 2005)

2.5.2 Off-Bottom Tow

In the off-bottom tow method, as its name indicates, the submerged pipeline is buoyant and floats above the seabed at predetermined height during towing, see Figure 2.7. The buoyancy modules and chains are attached in discrete modules along the length of the pipeline. Once the pipeline is towed on site, the buoyancy modules are removed or flooded and the pipeline settles to the seabed.

Compared to the bottom tow method, the existing pipelines can be crossed with no need of extensive protection structure. This can be done by placing

concrete mats over these pipelines and allowing the hanging chains to drag over the mates. The seabed survey is much simpler that it only needs to consider the obstacles that are higher than the height of the floating pipeline and sudden steep seabed cavities.

Further to abrasion-resistant coating, only a nominal thickness of abrasion-resistant is required which can even be additional FBE coating if no concrete weight coating is needed. And no more additional thickness is required for the concrete weight coating. (Boyun Guo et al., 2005)

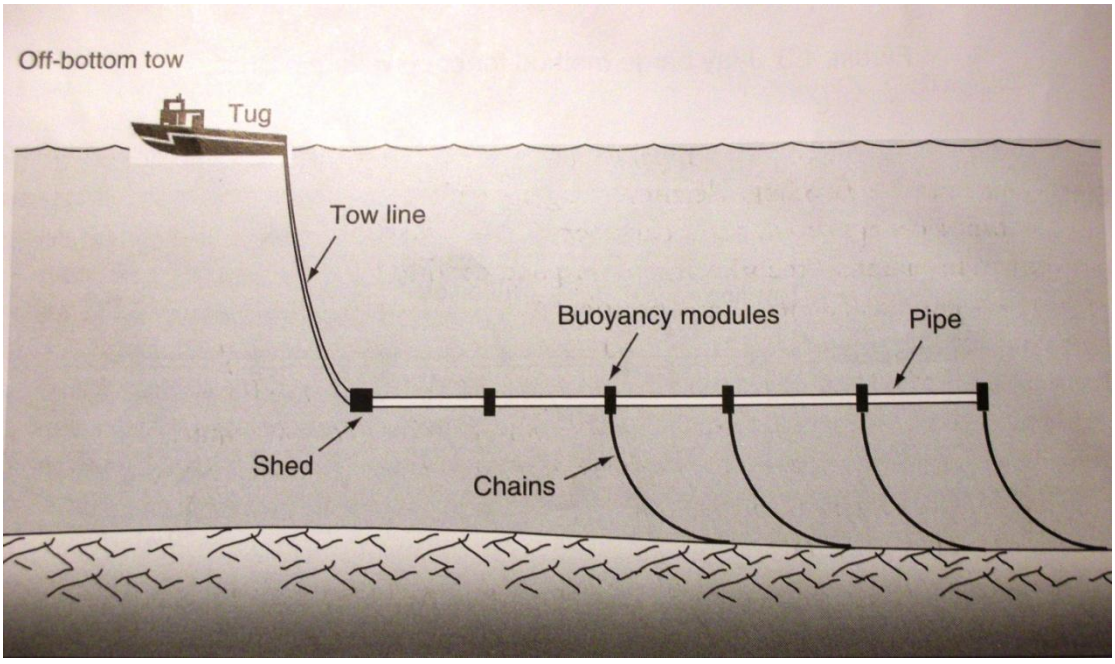

Figure 2.7 Off-bottom Tow for Pipeline Installation (Boyun Guo et al., 2005)

2.5.3 Mid-Depth Tow

In the mid-depth tow method, the entire length of the pipeline is kept at a considerable height above the seabed during towing as can be seen in Figure 2.8. Besides discrete buoyancy and chains, a large tension is applied to the pipeline. The tension is applied by the two tow vessels pulling in opposite directions at each end of the pipeline. Once the pipeline reaches its desired height, the front tow vessel will apply more thrust while the back tow vessel cuts back on its reverse thrust. One more vessel is required to monitor the height of the pipeline in the middle by using a subsea transponder system. The

third vessel sends its signal to the two tow vessels, which see the height in real time and adjust their thrusts appropriately to keep the pipeline within the desired height range. If the pipeline is too long, it will be very difficult to maintain the desired height range and larger tension will be required. This method is not suitable for the pipeline longer than 3 miles.

Only a near shore survey and final infield pipeline route survey are required. Additionally, some discrete areas where the pipeline can be parked in case of emergency must be identified. This method is ideal for areas with extensive rocky outcrops, many existing pipelines, or other obstructions along the tow route. (Boyun Guo et al., 2005)

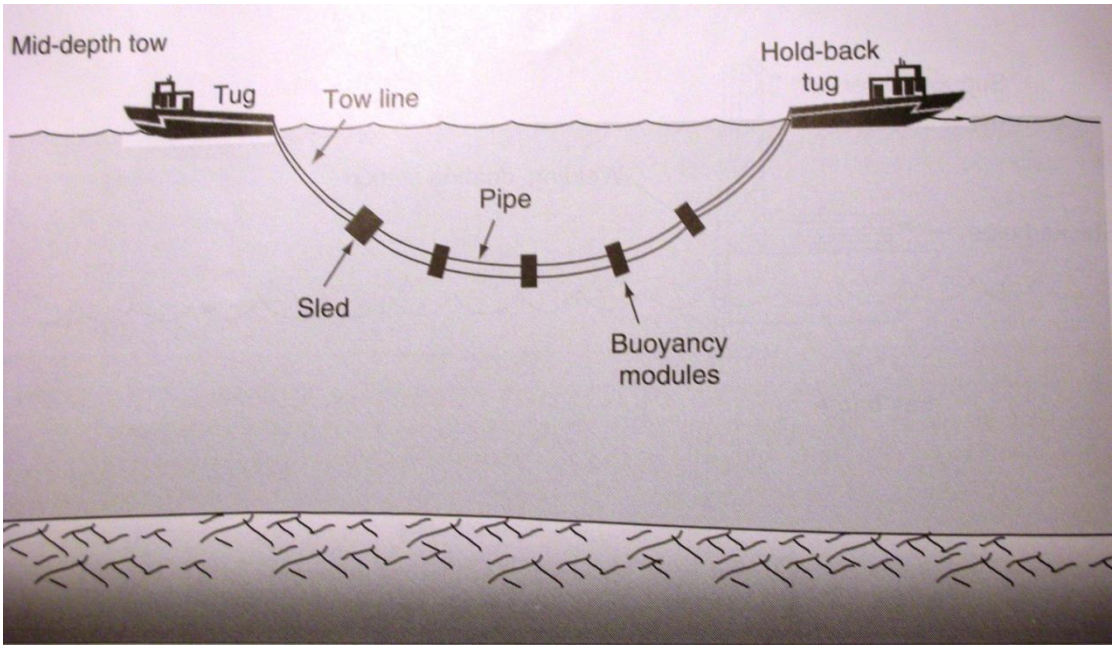

Figure 2.8 Mid-depth Tow for Pipeline Installation (Boyun Guo et al., 2005)

2.5.4 Surface Tow

Surface tow method is similar to mid-depth except that the pipeline will not require any chains. The two vessels keep the pipeline in tension while it is towed on the surface. Only a survey of the final pipeline route is required. This method can be used for shallow water. For deep water, a sophisticated controlled flooding and/or buoyancy removal system is required. Fewer pipelines are installed by this method.

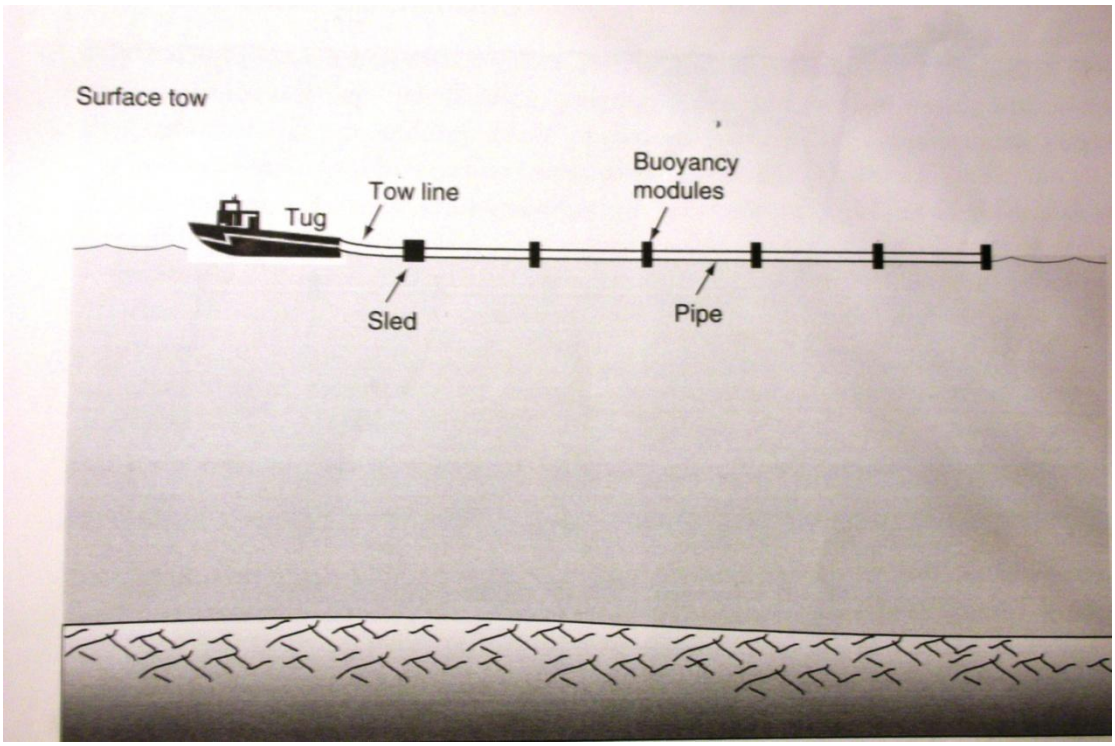

Figure 2.9 Surface Tow for Pipeline Installation (Boyun Guo et al., 2005)

2.6 Vessel Types

Different vessel types are used depending on the pipeline installation methods and site characteristics (water depth, weather etc).

S-lay/J-lay ships;

Reel ships;

Tow or pull vessels.

According to the mooring system, the vessels are classified into two types: conventionally moored lay vessels and dynamically positioned lay vessels.

2.6.1 Conventionally Moored Lay Vessels

For conventionally moored lay vessels, anchors are used for station keeping, associated with anchor chains. Thus, anchor handling vessels are required. It is obvious that the larger the vessel, the greater the target area presented to wind,

wave, and current forces and the heavier the vessel are. As a result, a higher holding is required for the mooring system. The rated holding capacity of an anchor system is a function of the weight and size of the anchor and the tensile strength of the chain that secures the anchor to the vessel. The pipelaying methods have little effect on the required number of anchors. The number of anchors used for a conventionally moored lay vessel is 8-12 anchors, depending on lay barge size.

The limitation of conventionally moored lay vessel is the anchor handling vessel. The deeper the operating water depths, the higher the requirements for the anchor handling vessels. Compared to monohull vessels, semisubmersibles have better sea keeping abilities. They are more suitable to operate in the tough weather conditions. But for shallow water, the cost effectiveness of semisubmersibles is lower than the monohull vessel. (Gilbert Gedeon, 2001)

2.6.2 Dynamically Positioned Lay Vessels

For dynamically positioned lay vessels, the location or position of the vessel is maintained by the vessels' special station-keeping system, which, instead of or in addition to the conventional propeller-rudder system at the stern, employs a system of hull-mounted thrusters near the bow, at mid-ship, and at the stern. In the station-keeping mode, these thrusters, which have the capability to rotate 360^{o} in a horizontal plane, are controlled by a shipboard computer system that usually interfaces with a satellite-based geographic positioning system.

Considering the cost effectiveness, the minimum water depth at which dynamically positioned lay vessels are used is no less than 600 ft. But for reel vessels, sometimes it is used in shallow water. (Gilbert Gedeon, 2001)

Chapter 3 Pipe-Soil Interaction

3.1 Introduction

During the installation and subsequent operation phase, the pipeline is laid to rest on the seabed. Obviously, the mechanical properties of the seabed will affect the pipeline stability significantly. Geotechnical investigation is needed to get the information about the seabed.The pipe-soil soil model consists of seabed stiffness and equivalent friction definition to represent the soil resistance o movement of the pipe. It is important to predict the soil contact pressure, equivalent and soil stiffness accurately. Ole and Torseten (2008) developed a generalized true 3D elastoplastic spring element based on an anisotropic hardening/degradation model for sliding for pipe-soil interaction analysis. The model complies with finite element format allowing it to be directly implemented in a simple way.

3.2 Geotechnical Survey

Geotechnical investigations are performed to obtain information on the physical properties of soil and rock in a site. In subsea geotechnical engineering, seabed materials are considered a two-phase material composed of rock or mineral particles and water. The mechanical properties of the seabed will affect the pipeline stability significantly. Thus, geotechnical survey data provide important information on seabed conditions that can affect both pipeline mechanical design and operations. Seafloor bathymetry would affect pipeline routing, alignment, and spanning. Pipeline should be routed away from any seafloor obstructions and hazards. Spanning analysis should be conducted, based upon geotechnical survey data, to identify any locations where spans will be longer than allowable span lengths. Understanding the soil mechanical properties will help the design of subsea pipelines.

Soil mechanical properties depend largely upon the soil components and their fractions. There are coarse-grained components, like boulder, cobble, gravel, and sand. The fine grained components consist mainly of silt, clay, and organic matter (Lambe and Whitman, 1969). Boulders and cobbles are very stable components. Foundations with boulders and cobbles present good stability. Silt is unstable and, with increased water moisture, becomes a "quasi-liquid" offering little resistance to erosion and piping. Clay is difficult to compact when it is wet, but compacted clay is resistant to erosion. Organic matters tend to increase the compressibility of the soil and reduce the soil stability.

Silt and clay are the major components of seabed soil down to a few feet in depth. Thus, when pipeline is laid on the seabed, it will normally sink into the soil. How much the pipeline will sink depends largely upon the mechanical properties of the soil. The following parameters are normally obtained when performing geotechnical analysis.

Water moisture content is defined as the ratio of the mass of the free water in the soil to the mass of soil solid material. Water moisture content is normally expressed as a percentage. Some soils can hold so much water that their water moisture content can be more than 100%.

Absolute porosity is defined as the ratio, expressed as a percentage, of void volume of soil to the soil bulk volume.

Absolute permeability is defined as a measure of the soil's ability to transmit fluid. To determine the permeability of the soil, a sample is put into a pressure device and water is conducted through the soil. The rate of water flow under a given pressure drop is proportional to the soil permeability.

Liquid limit is determined by measuring the water moisture content and the number of blows required to close a specific groove which was cut through a standard brass cup filled with soil. Liquid limit indicates how much water the soil can hold without getting into the "liquid" state.

Plastic limit is defined as the water moisture content at which a thread of soil with 3.2-mm diameter begins to crumble. Plastic limit is the minimum water content required for the soil to present "plastic" properties.

Plasticity index is defined as the difference between liquid limit and plastic limit.

Liquidity index, LI, is defined as the ratio of the difference between the

natural water moisture content and the plastic limit to the plasticity index.

Activity number is defined as the ratio of plasticity index to the weight percentage of soil particles finer than 2 macros. Activity number indicates how much water will be attracted into soil. (Boyun Guo et al., 2005)

3.2 Pipe-Soil Interaction Model

Once in contact, the interaction between the pipeline and the soil can be described in terms of 3 d.o.f: penetration into the seabed (normal to the seabed), axial movements along the axis of the pipeline and lateral movement perpendicular to the pipeline. The penetration of the pipeline into the seabed has a great influence on the axial and lateral resistance. Many studies about the pipe-soil interaction had been done, referring to (Lyons, 1973), (Lambrakos, 1985), (Karal, 1977), (Brennodden, et al., 1986), (Wagner et al., 1987), (Morris et al., 1988) and (Palmer et al., 1988). These studies show that a pipeline moving cyclically accumulates penetration, which therefore results in an increased lateral soil resistance. H. Brennodden et al. (1985) developed an energy-based pipe-soil interaction model to predict soil resistance to lateral motion of untrenched pipelines based on full- scale pipe-soil interaction tests. The tests confirm that soil resistance is strongly dependent on pipe penetration and soil condition (shear strength of clay and relative density of sand). The total soil resistance into two terms: one is the sliding resistance force and the other is penetration dependent soil resistance force. This method is applied for PONDUS pipe-soil interaction model in SIMLA. The specific information refers to Appendix A. In this section, several methods for calculating the seabed penetration for clay as a function of the static ground pressure exist. Among them, Verley and Lund Method (Verley and Lund, 1995) and the buoyancy method (Håland, 1997) are briefly introduced below. Most of the material in this section is collected from (Bai, Yong et al., 2005).

Figure 3.1 shows the positive direction of the dynamic external forces per unit length acting on the submerged pipe.

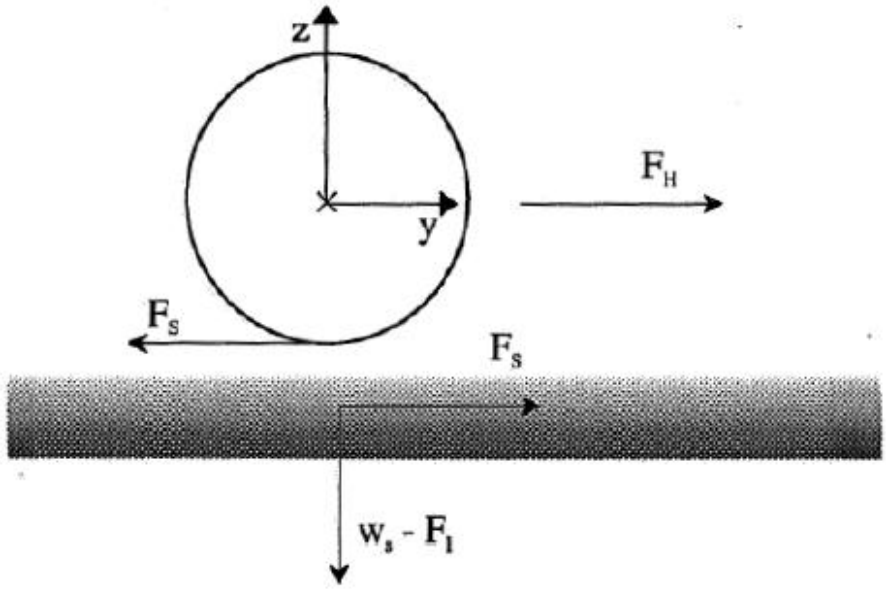

Figure 3.1 External Forces Per Unit Length (Svein, 2008)

3.2.2 Verley and Lund Method

The Verley and Lund method is based on back calculation of pipeline with external diameter from 2.0-1.0 meters, resting on clays with undrained shear strength of 0.8-70 kPa. The formula for calculation of pipeline penetration is given as:

$$\frac{z}{D} = 0.0071 \cdot (S \cdot G^{0.3})^{3.2} + 0.062 \cdot (S \cdot G^{0.3})^{0.7} \quad (3.1)$$

where:

z is the seabed penetration(m);

S is $F_c/(D \cdot s_u)$;

G is $s_u/(D \cdot \gamma')$;

F_c is the vertical contact force (kN/m);

D is the pipeline external diameter (m);

s_u is the undrained shear strength (kPa);

γ' is the submerged soil density (kN/m²).

The Verley and Lund formulation is based on curve fitting to data with $S \cdot D^{0.3} < 2.5$. For larger values the method overestimates penetration. An alternative formulation which is valid for values of $S \cdot D^{0.3}$, is given by:

$$\frac{z}{D} = 0.09 \cdot (S \cdot G^{0.3}) \quad (3.2)$$

3.2.2 Buoyancy method

The method is only used with pipeline resting on very soft clays. The buoyancy method assumes that the soil has no strength and behaves like a heavy liquid. The penetration is estimated by demanding that the soil-induced buoyancy of the pipeline is equal to the vertical contact forces.

$$B = 2 \cdot \sqrt{D \cdot z - z^2} \quad (3.3)$$

$$A_s = (z/6B) \cdot (3 \cdot z^2 + 4 \cdot B^2) \quad (3.4)$$

$$O = A_s \cdot L \cdot \gamma' \quad (3.5)$$

where:

B is the width of pipeline in contact with soil;

A_s is the penetrated cross sectional area of pipe;

O is the buoyancy.

The equivalent friction is mainly based on coulomb friction for sand, cohesion for clay, or combination of the two, the soil density and the contact pressure between the pipe and soil. For the friction model, in the case that the pipeline doesn't penetrate into the seabed much, a pure Coulomb friction model can be appropriate. When the pipeline penetrates into the seabed, the forces required moving the pipeline laterally become larger than the forces needed to move it

in the longitudinal direction. The reason for this effect is passive lateral soil resistance is produced when a wedge of soil resists the pipe's motion. An anisotropic friction model that defines different friction coefficients in the lateral and longitudinal directions of the pipeline is suitable. In SIMLA, the friction is modeled based on the same principles as applied for material plasticity (Levold, 1990).Two major ingredients are included a friction surface and a slip rule. More information is referred to Appendix A. (Bai, Yong et al., 2005)

The breakout force is the maximum force needed to move the pipe from its stable position on the seabed. This force can be significantly higher than the force needed to maintain the movement after breakout due to suction and extra force needed for the pipe to "climb" out of its depression.

(Brennodden, 1991) gives the following equations for the maximum breakout force in the axial and lateral direction:

Axial soil resistance (kN/m):

$$F_{a,max} = 1.05 \cdot A_{c,calc} \cdot s_u \quad (3.6)$$

Lateral soil resistance (kN/m):

$$F_{l,max} = 0.8 \cdot (0.2 \cdot F_c + 1.47 \cdot s_u \cdot A_{c,calc}/D) \quad (3.7)$$

where:

F_c is the vertical contact force (kN/m);

$A_{c,calc}$ equals $2 \cdot R \cdot A\cos(1 - zR)$ (m^2);

z is the seabed penetration;

s_u is the undrained shear strength (kPa).

Chapter 4 Hydrodynamics around Pipes

4.1 Introduction

Pipeline resting on the seabed are subjected to hydrodynamic forces which arise from waves and steady currents that are characteristics of all offshore areas. The hydrodynamic forces are drag and inertia forces that act together laterally on the pipeline, tending to move the pipeline and lift force acting vertically to reduce the submerged weight of the pipeline. Sliding friction between the pipeline and soil provides the resistance of the pipeline on the seabed. Knowledge about the hydrodynamic aspects of pipelines resting on the seabed subjected to the action of regular and random waves is increasing. (Lennon, 1985) reported about three dimensional wave-induced seepages pressures on a buried pipeline in sandy marine soil of finite depth using BIEM. The soil structure and fluid were assumed as incompressible; seabed was horizontal and extended infinitely in both horizontal and vertical directions. The forces on pipeline were found to be a function of relative pipe size, location of wave crest and soil properties. (Spierenburg, 1986) has derived the analytical solution for the hydrodynamic forces on a pipeline. A comparison is also made with numerical solution based on the finite element method. It is concluded that the hydrodynamic force acting upon a submarine pipeline is about 10-30% of the buoyancy of the pipe depending on the maximum wave load and the burial depth. (Magda, 1999) studied the behavior of hydrodynamic uplift force acting on a submarine pipeline in a sandy soil and concluded that the uplift force increased with increase in wavelength and degree of saturation of soil.

4.2 Wave and Current

To determine wave particle velocity, the equations used depend on wave height, water depth, and wave period. Comprehensive studies have been conducted to identify the most suitable wave theories for representing the near-bottom

kinematics due to wave action. The domain of applicability of the various theories is illustrated in Figure 4.1. Linear wave theory provides a good prediction of near-bottom kinematics for a wide range of relative water depth and wave steepness (Dean et al, 1986). Because the influence of nonlinearities considered in higher order wave theories is reduced with depth below the free surface. In (Kirkgoz, 1986), it is said that linear wave theory gave acceptable predictions of near bottom water particle velocities in waves close to the breaking point. Thus, the calculated water particle velocities and accelerations of the surface waves are transferred to seabed level using linear wave theory (Airy wave theory).

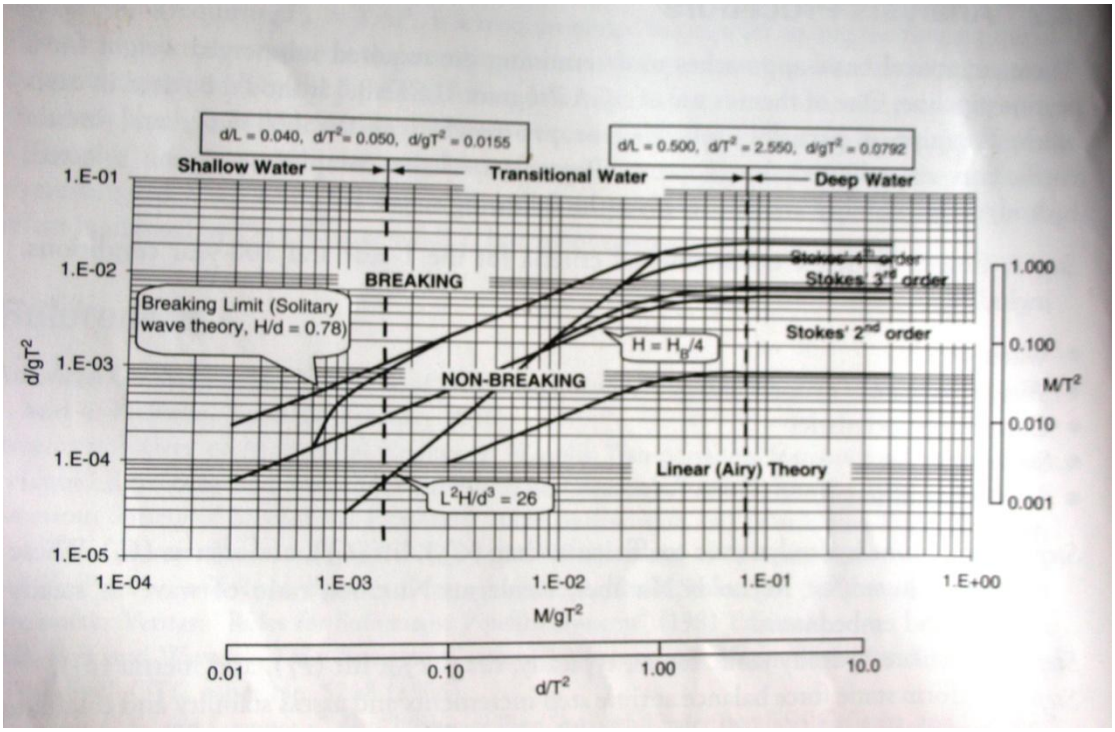

Figure 4.1 Domain of Applicability of the Various Theories

The 2D regular long-crested waves are only simple model that could not give a realistic description of the sea state. The shape of the waves seems more or less random. 2D irregular long-crested waves are used to model a complete sea state. The wave model used in SIMLA is briefly described in the following sections. Most of the material of this chapter is collected from (Svein et al., 2010)

4.2.1 2D Regular Waves

Regular waves are modeled by Airy linear wave theory in SIMLA. The wave

potential φ_0 for a regular wave according to Airy's theory can be expressed as follows:

$$\varphi 0 = \frac{\zeta_a g}{\omega} C_1 \cos(-\omega t + kX\cos\beta + kY\sin\beta + \psi\varphi) \quad (4.1)$$

where ζ_a is the wave amplitude, g is the acceleration of gravity, k is the wave number, β is the direction of wave propagation(where β=o corresponds to wave propagation along the positive X-axis) and ψ_φ is a phase angle lag.

C_1 is given by:

$$C_1 = \frac{\cosh k(Z + D)}{\cosh kD} \quad (4.2)$$

where D is the water depth.

In deep water, C_1 can be approximated by

$$C_1 \approx e^{kZ} \quad (4.3)$$

Then, the particle velocities and accelerations in the undisturbed field are obtained:

$$\upsilon_x = -\zeta_a \omega \cos\beta C_2 \sin\psi \quad (4.4)$$

$$\upsilon_y = -\zeta_a \omega \cos\beta C_2 \sin\psi \quad (4.5)$$

$$\upsilon_z = -\zeta_a \omega C_3 \cos\psi \quad (4.6)$$

$$a_x = \zeta_a \omega^2 \cos\beta C_2 \cos\psi \quad (4.7)$$

$$a_y = \zeta_a \omega^2 \sin\beta C_2 \cos\psi \quad (4.8)$$

$$a_z = \zeta_a \omega^2 C_3 \sin\psi \quad (4.9)$$

where

$$\psi = -\omega t + kX\cos\beta + kY\sin\beta + \psi_\varphi \quad (4.10)$$

According to the approximation we make for the deep water, we can get:

$$C_1 = C_2 = C_3 = e^{kZ} \quad (4.11)$$

In the case of finite water depth, we can get:

$$C_1 = \frac{\cosh k(Z + D)}{\cosh kD} \quad (4.12)$$

$$C_2 = \frac{\cosh k(Z + D)}{\sinh kD} \quad (4.13)$$

$$C_3 = \frac{\sinh k(Z + D)}{\sinh kD} \quad (4.14)$$

The surface elevation is expressed as:

$$\zeta = -\zeta_a \sin\psi = \zeta_a \sin(\omega t - kX\cos\beta - kY\sin\beta + \phi) \quad (4.15)$$

where ϕ=-ψ, phase angle.

The linearized dynamic pressure is given by:

$$p_d = \rho g \zeta_a C_1 \sin\psi \quad (4.16)$$

4.2.2 2D Irregular Waves

The irregular wave formulation is based on the use of wave spectra. Significant wave height, peak period etc define the characteristics of the sea state. In SIMLA, an irregular sea state is described as a sum of two wave spectra: a wind sea contribution and a swell contribution:

$$S_{\zeta,TOT}(\beta, \omega) = S_{\zeta,1}(\omega)\phi_1(\beta - \beta_1) + S_{\zeta,2}(\omega)\phi_2(\beta - \beta_2) \quad (4.17)$$

where $S_{\zeta,1}$ and $S_{\zeta,2}$ describe the frequency distribution of the wind sea and swell, respectively. Spectra included in SIMLA are Pierson-Moscowitz and Jonswap.

ϕ_1 and ϕ_2 describe the directionality of the waves. So far only unidirectional waves are included in SIMLA. β is the direction angle of wave propagation.

Direction of wave propagation β

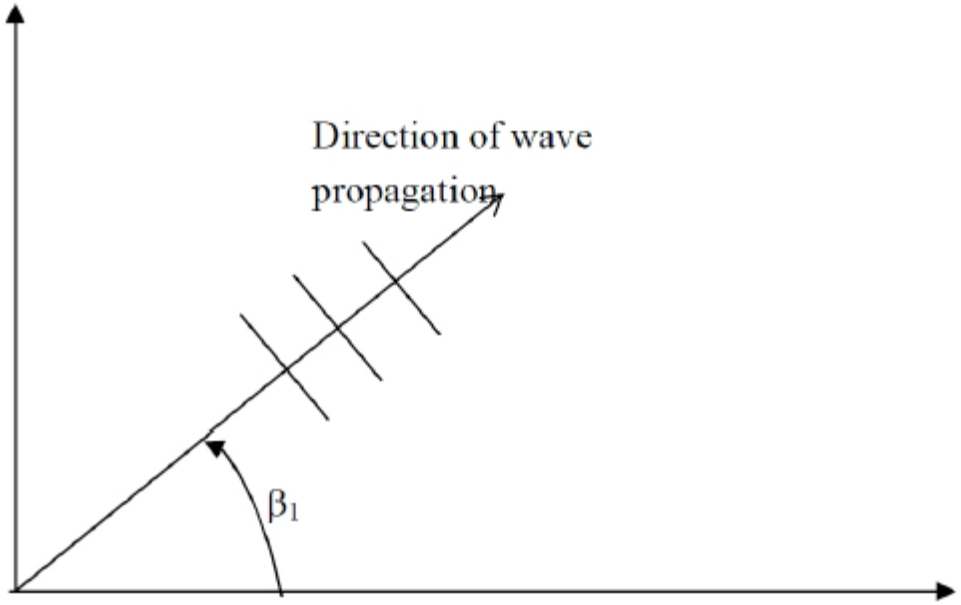

Figure 4.2 Definition of Wave Direction

The spectrum directionality parameters satisfy the relations:

$$\int_{-\frac{\pi}{2}}^{\frac{\pi}{2}} \phi_j(\beta)d\beta = 1.0 \quad (4.18)$$

$$\phi_j(\beta) = 0, \frac{\pi}{2} \leq \beta \leq \frac{3\pi}{2} \quad (4.19)$$

$$\int_0^\infty S_{\zeta,1}(\omega)d\omega + \int_0^\infty S_{\zeta,2}(\omega)d\omega = \sigma_\zeta^2 \quad (4.20)$$

where σ_ζ^2 is the variance of the surface elevation.

In order to generate time series of surface elevation, water particle velocities and accelerations, the short crested irregular sea is discretized into a set of harmonic components. In complex notation, the surface elevation is expressed by:

$$Z_\zeta = \sum_{j=1}^{N_\beta}\sum_{k=1}^{N_\omega} Z_{jk} = \sum_{j=1}^{N_\beta}\sum_{k=1}^{N_\omega} A_{jk}^{\,ei(\omega_k t+\phi_{jk}^p+\phi_{jk})} \quad (4.21)$$

$$A_{jk} = |Z_{jk}| = \sqrt{2S_\zeta(\beta_i,\omega_k)\Delta\beta\Delta\omega} \quad (4.22)$$

$$\arg(Z_{jk}) = \omega_k t + \phi_{jk}^p + \phi_{jk} \quad (4.23)$$

The random phase angles, ϕ_{jk} are sampled from a uniform distributions over $[-\phi,\phi]$. The position dependent phase angle is:

$$\phi_{jk}^p = -k_k X\cos\beta_j - k_k Y\sin\beta_j \quad (4.24)$$

The surface elevation can be expressed as:

$$\zeta(t) I_m Z_\zeta = R_e\left(Z_{\zeta^{e^{-\frac{\pi}{2}}}}\right) = \sum_{j=1}^{N_\beta}\sum_{k=1}^{N_\omega} A_{jk}\sin\left(\omega_k t + \phi_{jk}^p + \phi_{jk}\right) \quad (4.25)$$

The velocity and acceleration components are derived from the surface elevation components.

$$\dot{Z}_{jk} = i\omega_k Z_{jk}\,,\ddot{Z}_{jk} = -\omega_k^2 Z_{jk} \quad (4.26)$$

4.2.3 Steady Currents

When a steady current also exists, the effects of the bottom boundary layer may be accounted for. And the mean current velocity over the pipe diameter may be applied in the analysis. According to (DNV, 1998), this has been included in the finite element model by assuming a logarithmic mean velocity profile.

$$U_c(z_D) = \frac{U(z_r)}{\ln(z_r/z_0)}\left\{\left(\frac{e}{D}+1\right)\ln((e+D)/z_0) - \left(\frac{e}{D}\right)\ln\left(\frac{e}{z_0}\right) - 1\right\} \quad (4.27)$$

where

$U(z_r)$ is the current velocity at reference measurement height;

z_r is reference measurement height (usually 3m);

z_D is height to mid pipe (from seabed);

z_o is the bottom roughness parameter;

e is the gap between the pipeline and the seabed;

D is the total external diameter of pipe (including any coating).

Then the total velocity is obtained by adding the velocities from waves and currents together.

4.3 Hydrodynamic Forces

Hydrodynamic forces arise from water particle velocity and acceleration. These forces can be fluctuating (caused by waves) or constant (caused by steady currents) and will result in a dynamic load pattern on the pipeline. Drag, inertia, and lift forces are of interest when analyzing the behavior of a submerged pipeline subjected to wave and/or current loading. Because of the dynamic nature of waves, the pipeline response when subjected to this type of loading may be investigated in a dynamic analysis. 2D regular or random long-crested waves and the 3D regular or random short-crested waves may be included in the finite element model to supply the wave kinematics in a dynamic analysis. Most of the material is collected from (Bai, Yong et al., 2005).

4.3.1 Hydrodynamic Drag Forces

The drag force, *FD due to water partic*le velocities is given by:

$$F_D = \frac{1}{2}\rho C_D D(U+V)^2 \quad (4.28)$$

where:

F_D is the drag force per unit length;

ρ is the mass density of seawater;

C_D is the drag coefficient;

D is the outside diameter of pipeline (including the coatings);

U is the water particle velocity due to waves;

V is the current velocity.

4.3.2 Hydrodynamic Inertia Force

The inertia force, F_i due to water particle acceleration is given by:

$$F_i = \rho C_M \frac{\pi}{4} D^2 a \quad (4.29)$$

where:

F_i is the inertia force per length;

ρ is the mass density of seawater;

C_M is the inertia coefficient;

D is the outside diameter of pipeline (including the coatings);

a is the water particle acceleration due to waves.

The total force is given by Morison's equation.

The drag and inertia coefficients are given by:

$$C_D = C_D\left(R_e, KC, \alpha, (e/D), (k/D), (A_Z/D)\right) \quad (4.30)$$

$$C_M = C_M\left(R_e, KC, \alpha, (e/D), (A_Z/D)\right) \quad (4.31)$$

Reynolds number indicates the present flow regime, i.e. laminar of turbulent. And it is given as:

$$R_e = \frac{UL}{\nu} \quad (4.32)$$

where:

U is the flow velocity;

L is the characteristics length (Diameter of the pipeline);

ν is the ratio of the viscous force to the inertial force.

The Keulegan-Carpenter number gives information on how the flow separation around cylinders will be for ambient oscillatory planar flow and is given as:

$$KC = \frac{U_M T}{D} \quad (4.33)$$

where:

U_M is the flow velocity amplitude;

T is the oscillatory period;

D is the pipeline diameter.

The current flow ratio may be applied to classify the flow regimes:

$$\alpha = \frac{U_c}{U_c + U_w} \quad (4.34)$$

where:

U_c is typical current velocity normal to pipe;

U_w is the significant wave velocity normal to pipe given for each sea state.

It is obvious to notice that α=0 corresponds to pure oscillatory flow due to waves and α=1 corresponds to pure (steady) current flow.

The presence of a fixed boundary near the pipe (proximity effect) has a pronounced effect on the mass coefficient. The added mass will increase as the pipe approaches solid boundary. The relation is given as follows:

$$C_a = 1 + \frac{1}{\left(10\left(\frac{e}{D}\right) + 1\right)} \quad (4.35)$$

where:

e/D is the gap ratio.

k/D is the roughness number which has a great influence on the flow separation and therefore also on the drag and mass coefficient. k is the characteristics cross-sectional dimension of the roughness on the body surface.

There is a connection between the VIV (Vortex-Induced Vibrations) and the drag forces. A rough approximation can be given as:

$$C_D/C_{D0} = 1 + 2(A_z/D) \quad (4.36)$$

where:

C_D is the drag coefficient with VIV;

C_{D0} is the drag coefficient with no VIV;

A_z is the cross-flow vibration amplitude.

From the expression above, we can tell that larger projected area with diameter up to $D+2A_z$ due to the oscillating cylinder. (Bai, Yong et al., 2005)

4.3.3 Hydrodynamic Lift Forces

4.3.3.1 Lift forces using constant lift coefficients

The lift force per unit length of a pipeline can be calculated according to:

$$F_L = \frac{1}{2}\rho D C_L v_n^2 \quad (4.37)$$

where:

C_L is the lift coefficient for pipe on a surface;

v_n is the transverse water particle velocity (perpendicular to the direction of the lift force);

ρ is the density of seawater;

D is the total external diameter of pipe.

4.3.3.1 Lift force using variable lift coefficients

The hydrodynamic lift coefficient C_L will vary as a function of the gap that might exist between the pipeline and the seabed. It is clearly demonstrated in Figure 4.3 that the lift coefficient decreases significantly with the ratios of e/D, which is true both for the shear and the shear-free flow. (Bai, Yong et al., 2005)

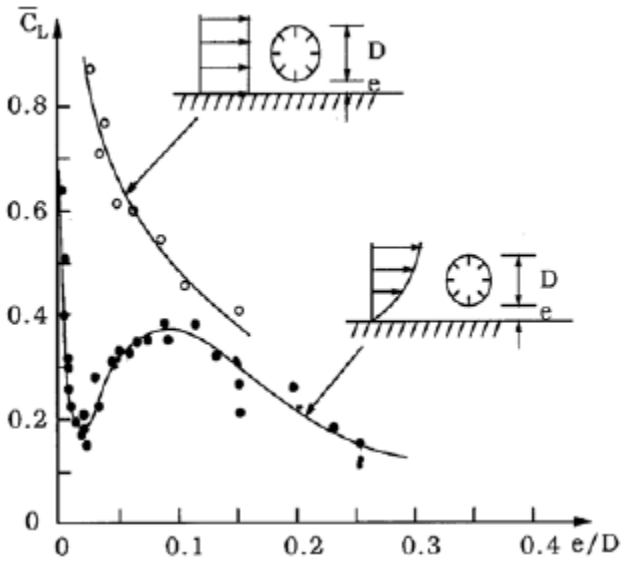

Figure 4.3 C_L in shear and shear-free flow for $10^3<R_e<30\times10^4$(Fredsøe and Sumer, 1997)

Chapter 5 Nonlinear finite element method

5.1 Introduction

Nonlinearies are widespread in mechanical problems. Nonlinear finite element method is a powerful technique for the computational solution for the nonlinear problems. The sources of nonlinearity are mainly geometrical nonlinearity, material nonlinearity and nonlinear boundary conditions. In SIMLA, all these nonlinearies are accounted for. When it comes to large deformations problems, the assumptions about the small displacements and linear material no longer hold. The geometrical and material nonlinearity must be accounted for. In linear analysis, the analytical solutions can be obtained, while it is no longer the case in nonlinear problems. Several solution techniques are used to directly solve the static nonlinear equilibrium equation. Numerical integration will be used to numerical solutions for nonlinear dynamic equilibrium equation. To account for the geometrical nonlinearity, two nonlinear finite element formulations, i.e. the Total Lagrangian (TL) and the Updated Lagrangian (UL) formulations are widely used. Both formulations have been successfully used in many nonlinear problems, see e.g. (Søreide, 1989), (Levold, 1990), (Hibbit et al., 1970), (McMeeking et al., 1975), and (Mattiason, 1983). Egil et al. (1985) described a numerical model for simulating the nonlinear dynamic behavior of submerged pipelines subjected to large transverse impacts and suggested a method for introducing a prescribed displacement or velocity history, without altering the finite element equations proven to work well for highly nonlinear systems. In the following sections, the nonlinear finite element methods applied in SIMLA will be explained briefly. Most material in the following sections are from (Svein, 2008), (T.Moan et al, 2009) and (T.Moan, 2003).

5.2 Total Lagrangian and the Updated Lagrangian (UL) formulations

The difference between the Total Lagrangian and Updated Lagrangian formations is the choice of reference configuration. In a TL formulation, all static and kinematic variables are referred to the initial (C_0) configuration, while in the UL formulation these are referred to the last obtained equilibrium configuration, i.e. the current (C_n) configuration.

Several variations of the TL and UL formulations have been developed to improve the computational efficiency. The basic idea is to separate the rigid body motion from the local or relative deformation of the element. This is done by attaching a local coordinate system to the element and letting it continuously translate and rotate with the element during deformation. The nonlinearities arising from large displacements can be separated from the nonlinearities within the element. Several terms have been introduced to label various formulations. Examples of names are Co-rotational Formulation and Co-rotated Ghost Reference Formulation.

In SIMLA, the present work has been based on the Co-Rotational Formulation referring all quantities to the Co configuration. In the Co-rotational formulation, the last obtained reference configuration is adequately described by the current strains and the equation of incremental stiffness is obtained by making use of principle of virtual work and study the virtual work in an infinitesimal increment. (Svein, 2008)

5.3 Solution Techniques

Various techniques for directly solving the nonlinear problems are available. The following methods are briefly described.

Methods for static analysis

a) Incremental or stepwise procedures (e.g. Euler-Cauchy method)

b) Iterative procedures (e.g. Newton-Raphson)

c) Combined methods (Incremental and iterative methods are combined)

d) Methods based on dynamic analysis (Explicit methods)

5.3.1 Incremental Methods

Incremental methods provide a solution of the nonlinear problem by a stepwise application of the external loading. For each step, the displacement increment is solved. The total displacement is obtained by adding all the displacement increments. The incremental stiffness matrix is calculated based on the known displacement and stress condition before a new load increment is applied. The method is also called Euler-Cauchy method.

As illustrated in Figure 5.1, it is noted that the solution obtained by Euler-Cauchy method has a drift-off from the correct solution. This is because the method does not include the fulfillment of the total equilibrium equation. The accuracy may be increased by reducing the load increment. And also, the load increment should be adjusted according to the degree of nonlinearity. (T.Moan, 2003)

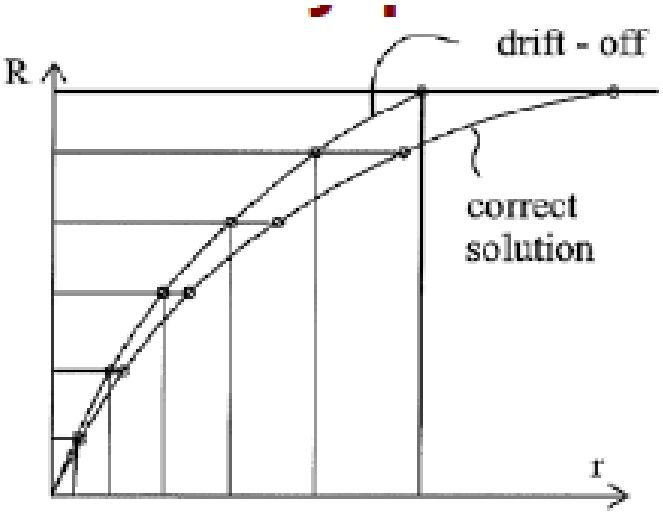

Figure 5.1 Euler-Cauchy Incrementing (T.Moan et al, 2009)

5.3.2 Iterative Methods

Newton-Raphson method is the most frequently used iterative method for solving nonlinear structural problems.

The Newton-Raphson algorithm to solve x for the problem: fx=0 is

$$x_{n+1} = x_n - \frac{f(x_n)}{f'(x_n)} \quad (5.1)$$

where $f'(x_n)$ is the derivative of $f(x_n)$ with respect to x, at $x = x_n$.

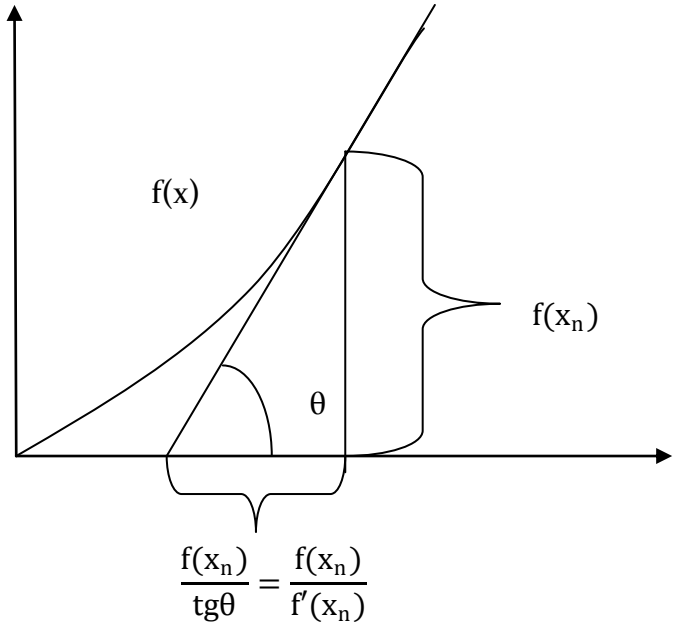

Figure 5.2 Newton-Raphson Algorithm (T.Moan, 2003)

The Newton-Raphson iteration is illustrated in Figure 5.3.The method requires the stiffness matrix is established and that Δr is solved in each iterative step, which is time-consuming. The less frequently updating the stiffness matrix, less effort is needed. Since this approach implies only a limited loss of rate of convergence, such modified Newton-Raphson iteration is beneficial. Two alternatives for modified Newton-Raphson methods are illustrated in the Figure 5.4 below.

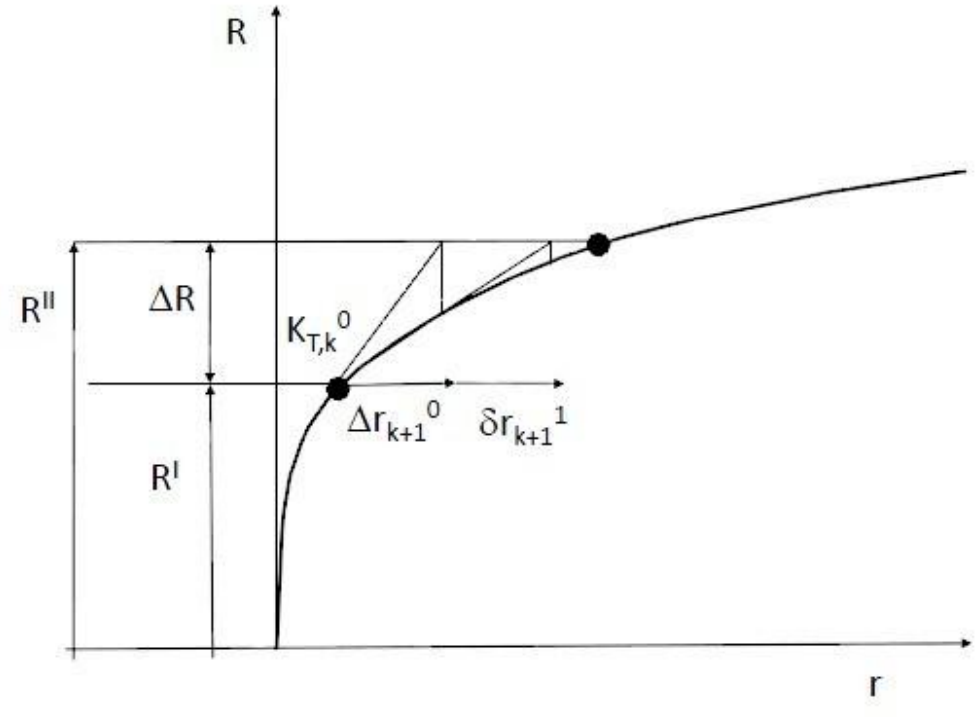

Figure 5.3 Newton-Raphson Iteration (Svein, 2008)

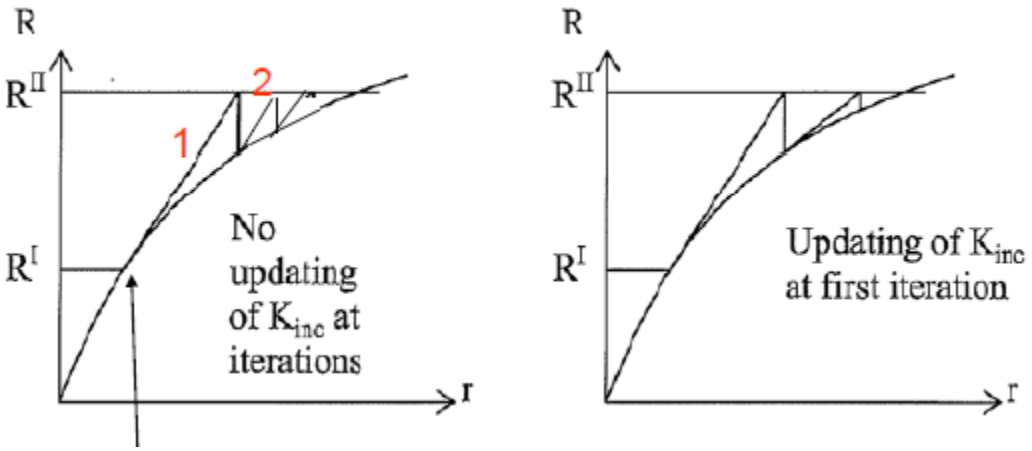

Figure 5.4 Modified Newton-Raphson Methods (T.Moan et al, 2009)

The iteration is stopped when the accuracy is acceptable. The convergence criterion may be based on the change of displacement from on iteration to the next. The convergence criterion may be expressed by

$$\|r_{n+1} - r_n\| < \varepsilon \quad (5.2)$$

where $\|\cdot\|$ is a vector norm and ε is a small, positive number, with the order of 10^{-2}-10^{-4}. The vector norm is a measure of the size of the vector. There are different vector norms that may be applied. One alternative is the modified Euclidean norm defined by:

$$\|r\| = \sqrt{\frac{1}{N}\sum_{k=1}^{N}(r_k/r_{ref})^2} \quad (5.3)$$

where N is the number of components in the vector r and r_{ref} is a reference size, e.g. $\max_N(r_i)$. (T.Moan, 2003)

In SIMLA, the static solution procedure is based on user defined load control with Newton-Raphson equilibrium iteration at each load step. As illustrated in Figure 5.2, the load increment ΔR is given from Equilibrium state I given by load R^I to equilibrium state II given by load R^{II}. The load increment ΔR results in a displacement increment Δr at iteration 0. The internal load vector and the stiffness matrix is updated and iterations are repeated until convergence has been obtained (the unbalance has vanished, i.e. δr_i=0).

The procedure can be written as:

$$\Delta r_{k+1}^{i} = K_{T,k+1}^{-1i}\Delta R_{k+1}^{i} \quad (5.4)$$

Newton-Raphson procedure applied in SIMLA is illustrated step by step as follows:

The procedure is based on co-rotational formulation.

For lode step hoop, k

Iteration hoop, i

Element hoop

Establish the difference between external element loads for load step k and the internal element load for iteration i-1 by $\Delta S^i = S_{ext}^k - S_{int}^{i-1}$.

Transform to global system and add to the global incremental load vector

$\Delta R_i = \Delta R_i + T^T \Delta S^i$.

Establish the tangential element material stiffness matrix by numerical integration k_{TM}^i.

Establish the element initial stress stiffness matrix (based on the current axial force) k_{TS}^i.

Transform to global system and add to global tangential stiffness matrix $K_T^i = K_T^i + T^T k_{TM}^i + k_{TS}^i T$.

End element loop

Adjust global incremental load vector for nodal loads and prescribed displacements, and adjust stiffness matrix for boundary conditions constrains.

Solve equation system $\Delta R_i = R_{ext}^k - R_{int}^{i-1} = K_T^i \Delta r^i$.

Update coordinates and nodal transformations matrices.

Element hoop

Update the element deformations $v^i = v^{i-1} + T\Delta r^i$.

Update the element stresses by evaluating each integration point.

Determine the element forces $S^i(v_i)$.

End element loop

Calculate convergence parameters such as:

Displacement norm=$\sqrt{\sum \Delta r^{i2}} / \sqrt{\sum r^{i2}}$

Force norm=$\sqrt{\sum \Delta R^{i2}} / \sqrt{\sum R^{i2}}$

Energy norm=$\sqrt{\sum \Delta R^i \Delta r^i} / \sqrt{\sum R^i r^i}$

If the convergence criteria are satisfied, go to next load step.

If the convergence criteria are not satisfied, perform new iteration.

End iteration loop, i

End load loop step, k (T.Moan et al, 2009)

5.3.3 Combined Methods

Incremental and iterative methods are often combined. The external load is applied in increments and in each increment equilibrium is achieved by iteration. Figure 5.5 illustrated a combination of Euler-Cauchy incrementation and a modified Newton-Raphson iteration. (T.Moan, 2003)

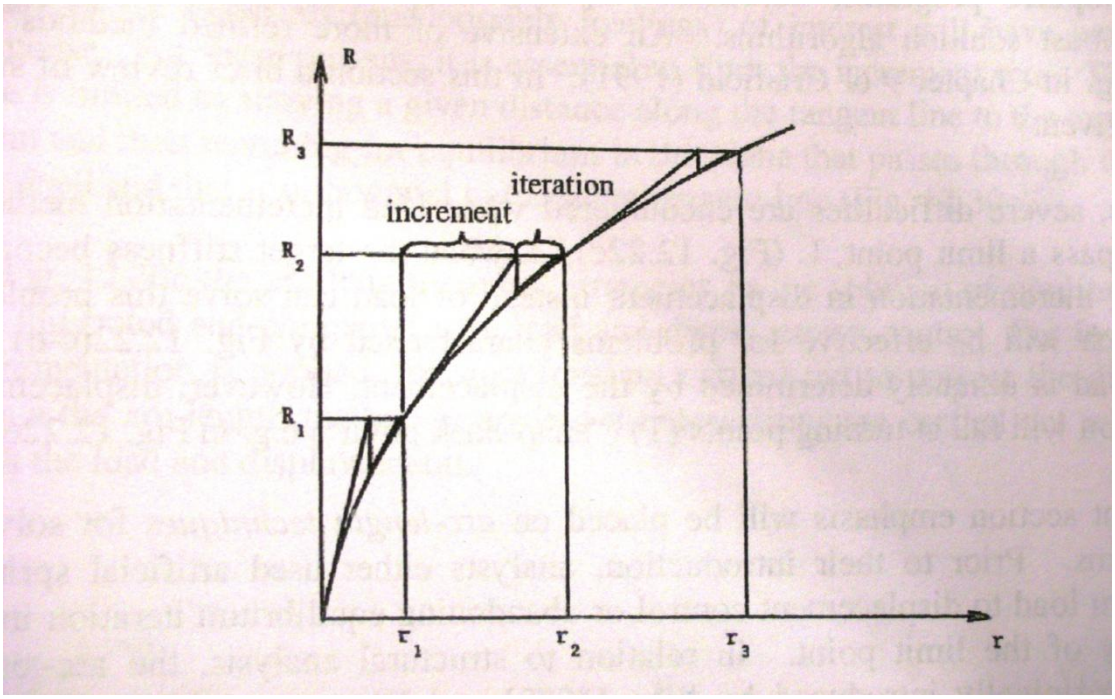

Figure 5.5 Combined Incremental and Iterative Solution Procedures (T.Moan, 2003)

5.3.4 Advanced Solution Procedures

In practice, more advanced techniques are developed to produce effective, robust solution algorithms such as accelerating the iterations,

load/displacement incrementation strategies to allow passing limit, tangent and bifurcation points based on incremental (predictor) and iterative (corrector) techniques and so on.

Line search is used to accelerate convergence by optimizing the parameter ξ such that the increment:

$$s = \Delta r_{n+1}^{i+1} \Delta R_{n+1}^{i+1} \left(r_{n+1}^{i} + \xi \Delta r_{n+1}^{i+1} \right) = 0 \quad (5.5)$$

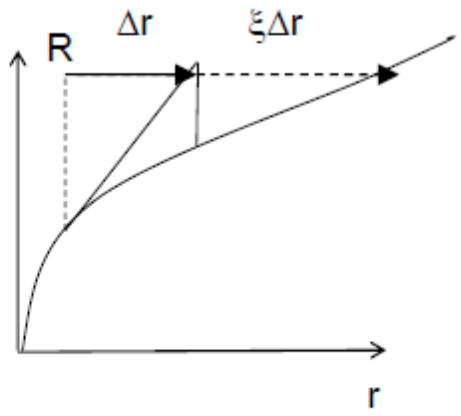

Figure 5.6 Representation of Line Search (T.Moan et al, 2009)

Three load/displacement incrementation strategies are introduced to allow passing limit, tangent, and bifurcation points based on a combined incremental (predictor) and iterative (corrector) approach. (T.Moan et al, 2009)

Load control (automatic load stepping to pass bifurcation, limit and tangent points on load displacement curve);

Displacement control (automatic step length control based on sensing the change in stiffness);

Arc-length control (automatic arc length control by depending upon the desired number of iterations). (T.Moan et al, 2009)

In Figure 5.7 is illustrated the load, displacement and arc-length control strategies in the solution of nonlinear equations. An increment is made along a tangential path, SP. Correction to reach equilibrium is obtained by iteration

controlled by the plane c=0.

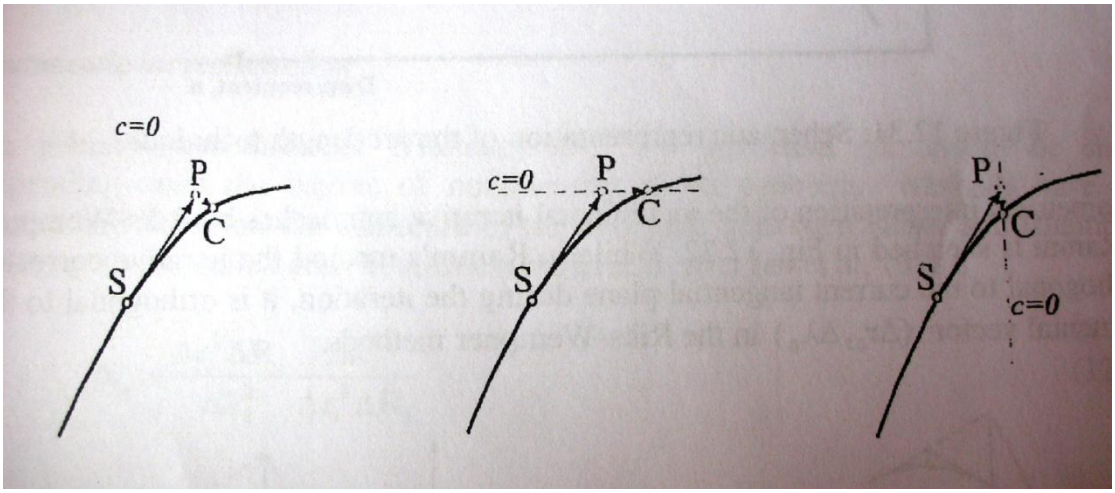

a) load control b) displacement control c)arc-length control

Figure 5.7 Geometric Representations of Different Control Strategies o Nonlinear Solution Methods for Single d.o.f. (T.Moan, 2003)

There are some limitations with load/displacement method. For example, severe difficulties are encountered when load incrementation methods are used to pass a limit point, i.e. when the target stiffness becomes zero. Using incrementation in displacement instead of load can solve this problem. However, displacement incrementation methods will fail at turning points ("snap-back point"). The arc-length method can solve these problems. The arc-length method was originally introduced by (Riks, 1972) and (Wempner, 1971). In this section, this method is briefly reviewed.

In the arc-length method, the global equilibrium equation is written as:

$$g(r,\lambda) = R_{int}(r) - \lambda R_{ref} = 0 \quad (5.6)$$

where R_{ref} is fixed external load vector and the scalar λ is a load level parameter. Equation 5.6 defines a state of "proportional loading" in which the loading pattern is kept fixed.

The arc length is formulated as an additional variable involving both the load and displacement. The increment in the load-displacement space can be described by a displacement vector Δr and a load increment parameter $\Delta\lambda$, such that $\Delta R=\Delta\lambda R_{ref}$.

There are several methods to obtain the arc length. For instance, making the iteration path follow a plane perpendicular to the tangent of the load-displacement curve is shown in Figure 5.8.

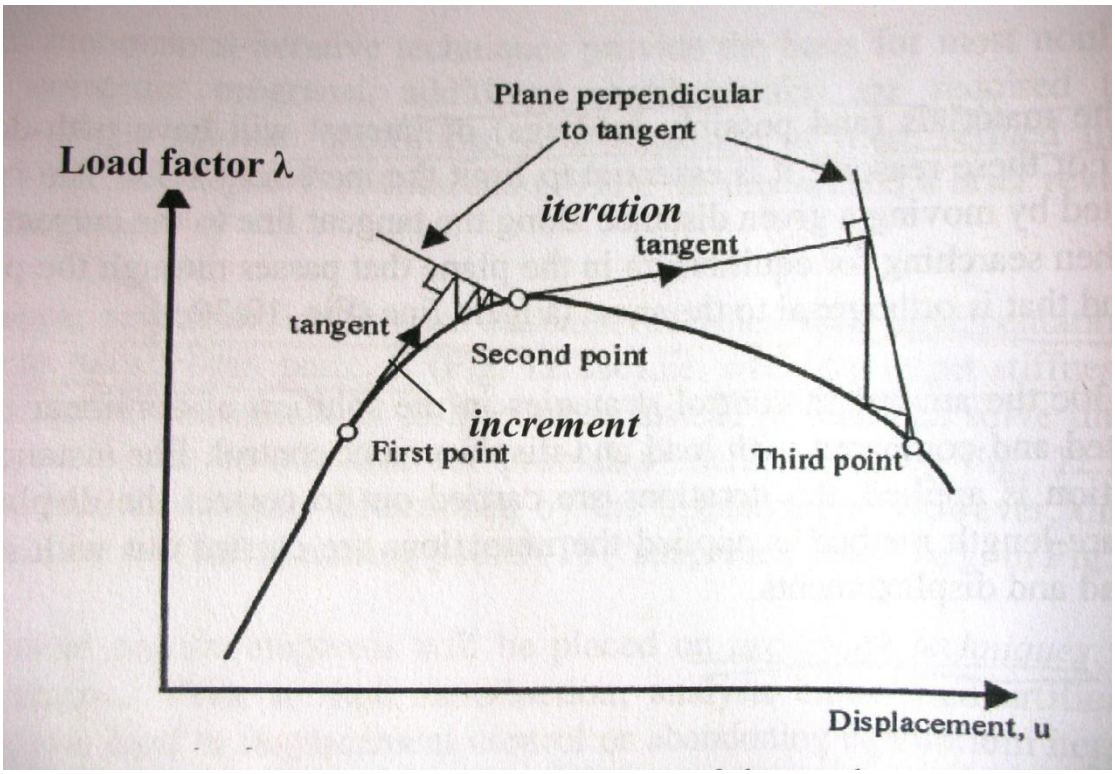

Figure 5.8 Schematic Representation of the Arc-Length Technique (T.Moan, 2003)

A geometrical interpretation of the incremental iterative approaches by Riks-Wempner and Ramm is sketched in Figure 5.8. While in Ramm's method the iterative corrector is orthogonal to the current tangential plane during the iteration, it is orthogonal to the incremental vector (Δr_o, $\Delta \lambda_o$) in the Riks-Wempner methods which are applied in the computer program ABAQUS. (T.Moan, 2003)

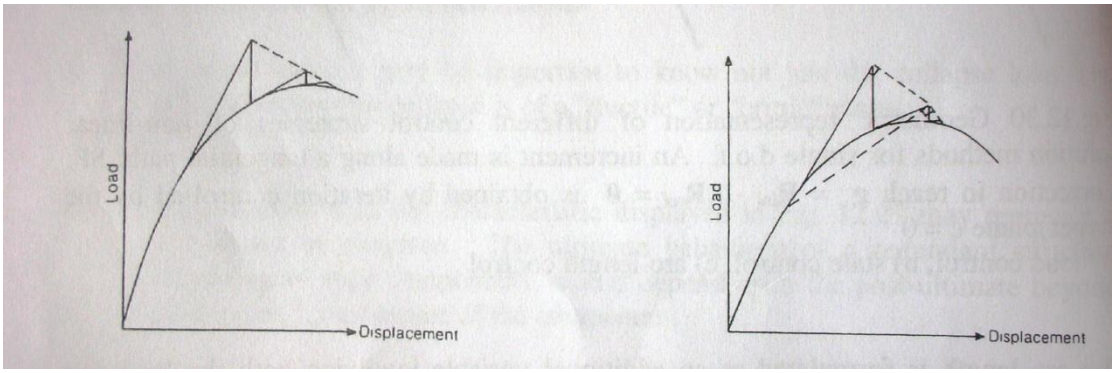

a) Riks-Wempner's Method b) Ramm's Method

Figure 5.9 Arc-Length Control Methods (Crisfield, 1991)

5.3.5 Direct integration Methods

Nonlinear dynamic problems cannot be solved by modal superposition and therefore direct time integration of the dynamic equation of motion is necessary. The direct integration method can be used to treat both geometrical and material nonlinearities. So-called finite difference methods are used for the direction time integration of the dynamic equation of motion. These methods are classified into two: explicit and implicit methods. The material is mainly from (Svein, 2008).

In the explicit methods, the displacements at the new time step will be determined based only on the information from the current time step and previous steps. Explicit methods can be expressed as:

$$r_{i+1} = f(\dot{r}_{i+1}, \ddot{r}_{i+1}, r_i, r_{i-1}, \dot{r}_{i+1}, \ddot{r}_{i+1}, \cdots) \quad (5.7)$$

Explicit methods are conditionally stable and are only stable for very short time steps. If these methods are formulated in terms of lumped mass and lumped damping matrices, it is not necessary to solve a coupled equation system in the time march. This results in very small computational efforts per time step. In the analysis of impulse type response, it is necessary to use small time steps in order to achieve sufficient accuracy. Therefore explicit methods are typically used in explosion and impact analysis.

On the contrary, in implicit methods, the displacements at the next new step depend on quantities at the next time step, together with information from the current step. Implicit methods can be expressed as:

$$r_{k+1} = f(\ddot{r}_{k+1}, \ddot{r}_k, \dot{r}_{k+1}, \dot{r}_k, r_k, \cdots) \quad (5.8)$$

It is noted that the implicit methods use information at the next time step. As a result, they will have better numerical stability than explicit methods. The various implicit methods differ in connection with how the acceleration is assumed to vary between the time steps and at which time the equilibrium equation is fulfilled. For instance, by assuming constant average acceleration between the time steps, the result will be unconditionally stable, which means that numerical stability is obtained regardless of the time step size. It is beneficial to use such methods in case of long analysis durations. When implicit methods are used, it is necessary to solve a coupled equation system at every time step which will be very time-consuming. It will be uneconomical if short time steps are unavoidable due to accuracy. In case of nonlinear systems the guarantee of unconditional stability does not hold, but in practical cases this is not considered to be an issue. (Langen and Sigbjørnsson, 1979)

5.3.5.1 Incremental Time Integration Scheme

In SIMLA, the HHT-α method is used in the time integration scheme. It is a method proposed by Hilbert, Hughes and Taylor. Compared to the well known Newmark-β method, the implicit HHT-α method will damp out high frequency modes and at the same time retain 2nd order accuracy (Mathisen, 1990). In the following, the formulation of the incremental time integration scheme is presented. And the material in this section is collected from (Mathisen, 1990).

In the HHT-α method, the modified equilibrium equation for the system is given as:

$$M\ddot{r}_{k+1} + (1+\alpha)C\,\dot{r}_{k+1} - \alpha C\,\dot{r}_k + (1+\alpha)R^I_{k+1} - \alpha R^I_k = (1+\alpha)R^E_{k+1} - \alpha R^E_k \quad (5.9)$$

where M is the mass matrix, C is the damping matrix, R^I is the internal force vector and R^E is the external force vector. Subscript k+1 refers to the next time step and subscript k to the current time step. The total damping matrix includes both Rayleigh-damping and a diagonal damping matrix:

$$C = C_0 + \alpha_1 M + \alpha_2 K \quad (5.10)$$

where K_T is the global tangent stiffness matrix. The acceleration and velocity at time step k+1 is found by using the same formulas as in the Newmark-β method:

$$\Delta\,\ddot{r}_{k+1} = \Delta\ddot{r}_{k+1} - \Delta\ddot{r}_k = \frac{1}{\Delta t^2\beta}\Delta r_{k+1} - \frac{1}{\Delta t\beta}\dot{r}_k - \frac{1}{2\beta}\ddot{r}_k \quad (5.11)$$

$$\Delta\,\dot{r}_{k+1} = \Delta\dot{r}_{k+1} - \Delta\dot{r}_k = \frac{\gamma}{\Delta t\beta}\Delta r_{k+1} - \frac{\gamma}{\beta}\dot{r}_k - \Delta t\left(\frac{\gamma}{2\beta} - 1\right)\ddot{r}_k \quad (5.12)$$

By subtracting the equilibrium equation at time step k from Equation 5.9 the following relation can be found:

$$\hat{K}_k \Delta r_{k+1} = \Delta\hat{R}_{k+1} \quad (5.13)$$

The effective stiffness matrix $\hat{K}_k$ is:

$$\hat{K}_k = a_0 M + b_0 C + c_0 K_{T,k} \quad (5.14)$$

$$a_0 = \frac{1}{\Delta t^2\beta} + (1+\alpha)\frac{\alpha_1\gamma}{\Delta t\beta} \quad (5.15)$$

$$c_0 = (1+\alpha)\frac{\gamma}{\Delta t\beta} \quad (5.16)$$

$$b_0 = (1+\alpha)\frac{\alpha_2\gamma}{\Delta t\beta} \quad (5.17)$$

The effective load vector$\Delta\hat{R}_{k+1}$ is given as:

$$\Delta\hat{R}_{k+1} = (1+\alpha)\left[R^E_{k+1} - R^E_k + Cb^E_k\right] + Ma_k + R^E_k - R^I_k - C_k\dot{r}_k \quad (5.18)$$

$$a_k = \frac{1}{\Delta t\beta} + (\frac{1}{2\beta} - 1)\ddot{r}_k \quad (5.19)$$

By solving Equation 5.13, the displacements at time step k+1 is obtained. And then the acceleration and velocity is obtained from Equation 5.11 and 5.12. Equation 5.14 accounts for unbalanced forces at time step k such that unbalance in Equation 5.9 will not be accumulated. If α=0, the HHT-α method will coincide with the Newmark-β method. When the HHT-α method is formulated for a linear undamped system in free oscillations, it will be unconditionally stable for the following values of α, β, and γ:

$$-13 < \alpha < 0 \quad (5.20)$$

$$\gamma = 121 - \alpha \quad (5.21)$$

$$\beta = \frac{1}{4}(1-\alpha)^2 \quad (5.22)$$

5.3.5.2 Equilibrium Iteration

Equilibrium iterations are performed to regain the dynamic equilibrium before the time step is increased. In SIMLA, the equilibrium iterations are formulated as a Newton-Raphson iteration method. The governing iteration equation is given as:

$$\hat{K}_k^i \delta r_{k+1}^{i+1} = (1+\alpha)\left[R_{k+1}^E - R_{k+1}^{I,i}, -C\dot{r}_{k+1}^i\right] - M\ddot{r}_{k+1}^i - \alpha(R_k^E - R_k^I - C\dot{r}_k^i) \quad (5.23)$$

K is the effective stiffness matrix given in Equation 5.14. The right-hand side of Equation 5.23 accounts for unbalance in inertia, damping and internal forces. The increment in the acceleration and velocity vectors is found through the contributing terms in Equation 5.11 and Equation 5.12. The updating process can be summarized as:

$$\Delta r_{k+1}^{i+1} = \Delta r_{k+1}^i + \delta r_{k+1}^{i+1} \quad (5.24)$$

$$\Delta \dot{r}_{k+1}^{i+1} = \Delta \dot{r}_{k+1}^i + \frac{\gamma}{\Delta t \beta}\delta r_{k+1}^{i+1} \quad (5.25)$$

$$\Delta \ddot{r}_{k+1}^{i+1} = \Delta \ddot{r}_{k+1}^i + \frac{\gamma}{\Delta t^2 \beta}\delta r_{k+1}^{i+1} \quad (5.26)$$

In SIMLA, the convergence criteria are the same with what described in section 5.3.2. One thing that needs to note is that a predefined number of iterations will be performed and if the equilibrium is not achieved, the time step will be divided before a new trial is initiated. And it is also possible to use norms in terms of energy or forces in SIMLA. (Svein, 2008)

Chapter 6 Modeling in SIMLA

6.1 Introduction

SIMLA is MARINTEK's newly developed computer tool for analysis of offshore pipelines in deep waters and rough environments. Currently available functionality includes pipelaying and inspection of free spans. The SIMLA system architecture is shown in Figure 6.1. In this thesis, the static and dynamic analysis model for a 32inch pipeline at 200-300 water depth is established with the computer code SIMLA. The length of the pipeline is 2190 m. The centre of gravity (COG) is 5 m above the water plane. Free board of the vessel is 10 m. The departure angle is 0.6727 deg. The model is schematically shown in Figure 6.2. In this chapter the information of the model will be described together with SIMLA input code. The material about the input code is collected from (Svein, 2010).

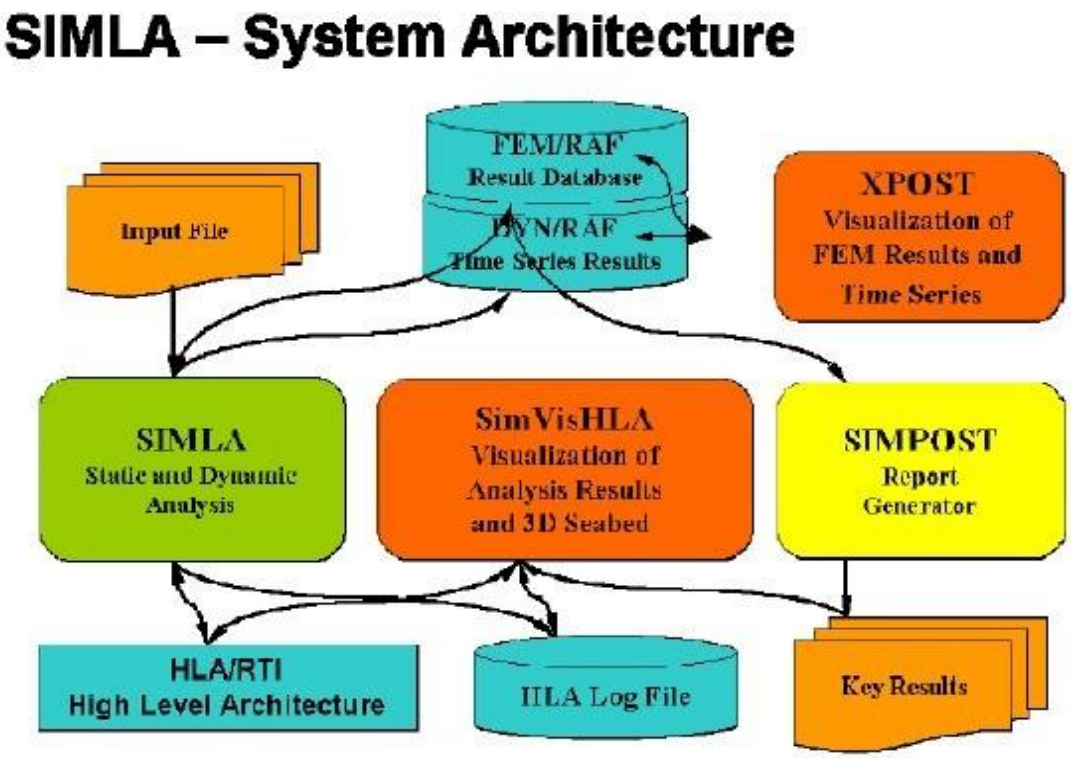

Figure 6.1 SIMLA System Architecture (Svein, 2010)

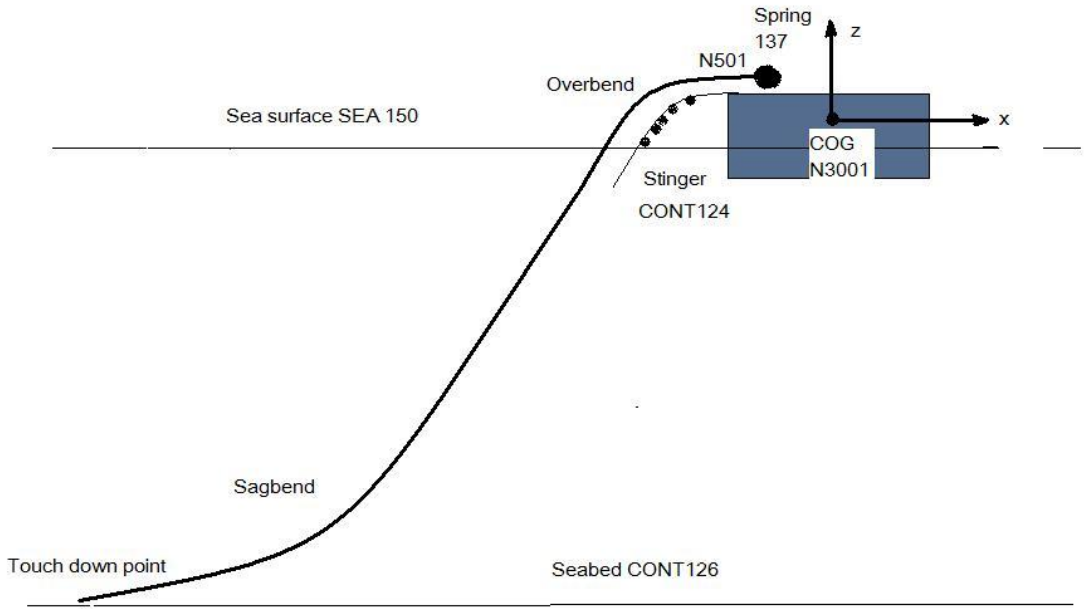

Figure 6.2 S-lay Model (Svein, 2010)

6.1 Element Types Used in the Model

Pipe model

The pipe model is 2190 m long. 500 PIPE elements ID 1-500, that is, 400 PIPE31 linear elements and 100 PIPE33 elastoplastic elements make up of the pipe model. Both PIPE31 and PIPE33 are 3D 2-noded beam elements. Initially, the pipe is a straight line starting at x= 10 m and ending at x=2200 m, node 1-501. Node 501 at x=10m is at the tensioner, where the stinger curve starts.

Stinger model

The stinger is modeled by CONT124 elements where the master node for all the elements is the vessel COG node ID number 3001. Element eccentricity is introduced in these elements in order to position the roller box relative to node ID 3001. Since the pipe centerline is applied as the basis for the geometrical parameters, the radius need to be adjusted by $R_{stinger}$-R_{pipe}-R_{roller} when calculating roller positions to obtain consistency. This is because SIMLA takes the pipe and roller radii into account when calculating contact state. There are 14 roller stations along the stinger. The stinger radius is 185 m and the first roller starts at angle 0 deg. There are two vertical rollers at the last and first roller boxes to avoid transverse displacement. Thus, the total number of contact elements is 18, IDs 2401-2404.

Tensioner model

In order to connect the pipe end node ID 501 to the vessel and to allow tensioner modeling, one SPRING137 element is introduced, end 1 at node ID 3001 which is at the vessel COG and end 2 at pipe node ID 501. In the model, the tensioner node 501 is positioned at x=-89.469 m, and z=5 m relative to the COG (center of gravity) node 3001. An eccentricity of x=-89.469 m and z=4.99 m is introduced in the local element x-direction and at end 1 of spring element ID 3000 to ensure that the element end is positioned at the same point as node 501. Note that z=4.99 m instead of z=5 m is used to avoid zero element length of the spring element SPRING137.

Seabed model

400 CONT126 seabed contact elements numbered from IDs 10001-10400 are connected to the pipe node IDs 1-401. 120 The CONT126 element requires that the seabed geometry is imported from a text file using the COSURFPR card.

The material properties along the route are defined by COSUPR card in which the referenced material name must be defined in the MATERIAL command. The COSURFPR command allows the user to define the contact surface properties relative to the curvilinear position along the contact surface determined by KP points. The contact surface data file is of ASCII type. The route description is based on point. The format is as follows:

x y z nx ny nz

The above line is repeated for the number of points in the route. x, y and z are the coordinate of the point. And nx, ny and nz are the components of the sea bottom normal vector at this point.

Example:

Contact surface data file format:

85699.1406 4235.1299 -2.6577 0.000000 0.000000 1.000000

85700.9141 4237.7715 -2.6551 0.000000 0.000000 1.000000

85702.5859 4240.2622 -2.6526 0.000000 0.000000 1.000000

85704.2578 4242.7524 -2.6502 0.000000 0.000000 1.000000

85705.9297 4245.2432 -2.6477 0.000000 0.000000 1.000000

85707.6016 4247.7339 -2.6452 0.000000 0.000000 1.000000

```
#               name      data file                    nlines kpo xo   yo      fi      id
COSURFPR cosurf1 "OLT_revF_numeric_route.txt"   1       0    0      0       0       100
#           route id    KP1       KP2       matname
COSUPR      100       -100000   10000000      soil1
```

The contact elements need to be activated by using the CONTINT card which

defines the contact interface to optimize the contact search. This also governs for Sea/structure interaction, i.e. all elements that may be submerged must be told to do so by defining an interface between the respective structure element groups and the sea element group.

Example:

```
#              groupn     mname     name     is1 isn   tstx   tsty tstz   maxit   igap
CONTINT seabed       ormpipe1     cosurf1   1   401   3      1    1    50      1.0
CONTINT ormcontact ormcontact ormpipe2 401 501 10000 10000  1   50      1.0
```

SEA model

SEA150 elements, IDs 2101-2221, are used to introduce buoyancy and hydrodynamic loading. In fact, one SEA element is sufficient for the numeric model. In order to get a visual presentation of the wave, 120 elements are used.

The initial coordinates of the elements are specified by the NOCOOR command. There are three types of coordinate definitions: COORDINAES, POLAR, ROTDISP.

Example:

```
#                        no      x              y      z
NOCOOR COORDINAES 1        0              0     10
                         21      192.5983199    0     10
                         41      370.3978694    0     10
                         61      534.5357488    0     10
                         81      686.0616864    0     10
```

```
                    101     825.9447521     0     10
```

The initial orientation of the element coordinate systems is defined by ELORIENT command. For the PIPE and HSHEAR (coating) elements, the orientations are defined by specifying the position of the xy-plane of the local element system relative to the global coordinate system. For the SPRING and CONTACT elements, the orientation of end 1 of the node is defined by specifying a set of three consecutive Euler angles that rotates the local coordinate system to the global coordinate system.

Example:

```
# PIPE element
#                          no    x       y       z
ELORIENT COORDINATES   1     0     10000     10
                          500 2200    10000     10
#SPRING      element
ELORIENT EULERANGLE   3000   0       0       0
```

The element properties are defined by the ELPROP command. In SIMLA, there are 9 types of element properties available: PIPE, BELLMOUTH, COMPIPE, CABLE, ROLLER, USERCONTACT, GENSPRING, COATING, BODY. In this model, PIPE, ROLLER and GENSPRING are used.

```
#          name     type   rad     th     CDr    Cdt    CMr    CMt    wd     ws
ELPROP ormpipe1 pipe    0.525 0.0341    0.8     0.1     2.0     0.2    1.291 0.161
ODp    ODw    rks
```

```
1.0841 1.0841   0.5

#              name      type   diam

ELPROP ormcontact roller   0.400

ELPROP ormcontact1 roller   0.400

#           name      type     ix   iy iz irx iry irz

ELPROP vessel1 genspring   1   1   1   1   1   1
```

The elements in SIMLA are organized into element groups each having a specific name, e.g. PIPE31 for pipe element. Each group is further defined by a reference to element type and material type. The element group, references to element and material types as well as the element connectivity is defined by the ELCON command.

```
#         group     elty   material     ID n1 n2 n3 n4

ELCON ormpipe1 pipe31 pipemat1   1   1   2

#           n     j   k

REPEAT 400   1   1

#           group   elty   material   ID   n1

ELCON seabed cont126 cosurf1   10001   1

#            n      j   k

REPEAT 400    1   1
```

The material properties must be defined for each element. This is done by the MATERIAL command. There are 15 material types available in SIMLA. Among

them, LINEAR, ELASTOPLASTIC, EPCURVE, HYCURVE, SEA, CONTACT, GENSPRING are applied in this model.

LINEAR represents linear material properties for the elastic pipe element. In the option, the poisson's ratio, axial stiffness, bending stiffness, torsion stiffness, young's modulus, shear modulus and so on are specified.

```
#              name      type poiss talfa     tecond   heatc   beta    ea

MATERIAL pipemat1 linear 0.3   1.17e-5    50       800      0     2.249e7

eiy          eiz       git       em    gm

3.10e6    3.10e6    2.39e6    2e8    8e7
```

ELASTOPLASTIC represents elastic strain-stress behavior with kinematic/isotropic hardening for the elastoplastic pipe elements. Any number of pairs of strain and stress can be given and linear interpolation is applied between the supplied data. Either kinematic hardening or isotropic hardening is applied.

```
#                name          type       ih poiss    ro       talfa    tec     hc        eps             sigma

MATERIAL pipemat2 elastoplastic   1     0.3   7.850   1.17e-5    50    800          0            0
                                                                                    1.691E-03       3.50E+05
                                                                                    0.005           4.50E+05
                                                                                    9.980E-02       8.35E+05
```

EPCURVE represents elastoplastic material behavior with kinematic/isotropic hardening. And HYCURVE represents hyperelastic (nonlinear elastic) material behavior.

In the model, the seabed is considered made up of 3D elastoplastic spring elements. In the x,y direction, EPCURVE model is used and HYCURVE model is applied in z direction.

```
# seabed soil

# name type rmyx rmyy xname yname zname

MATERIAL soil1 contact 0.5 1.0 soilx soily soilz

MATERIAL soil2 contact 0.5 1.0 soilx soily soilz2


#          name   type     alfa   eps     sig

MATERIAL soilx   epcurve  1      0       0

                                 0.005   1

                                 100.00  10


#          name type         eps         sig

MATERIAL soilz hycurve   -10000    -10000000

                          10000     10000000


# Tensioner

#          name     type       apr1     spr2     spr3      spr4   spr5   spr6

MATERIAL vessel1 genspring surgesp1 yawsp heavesp rollsp pitchsp swaysp
```

MATERIAL yawsp hycurve -1000 0

1000 0

In the following tables give some model information.

Table 6.1 Element Properties for PIPE in the model

RAD	**0.525**
TH	0.341
RCD	0.8
TCD	0.1
RMADD	2.0
TMADD	0.2
MD	1.291
MS	0.161
ODP	1.096
ODW	1.096

RKS	0.5

where in the table:

RAD: Structural radius i.e. the mean radius of the pipe wall (unit: m).

TH: Structural thickness, i.e. the wall thickness (unit: m).

RCD: Radial drag coefficient (unit: -).

TCD: Tangential drag coefficient (unit: -).

RMADD: Radial added mass coefficient (unit: -).

TMADD: Tangential added mass coefficient (unit: -).

MD: Dry mass (unit: ton/m).

MS: Submerged mass = dry mass - buoyancy mass (unit: ton/m)

ODP: Outer diameter D_{op} (unit: m)

ODW: External wrapping outer diameter Dow (unit: m)

RKS: External wrapping fraction η(0,1). Hence the diameter that will be applied to calculate drag and mass forces will be: $D = (1 - \eta)D_{op} + \eta D_{ow}$.

Table 6.2 Material properties of pipe element with LINEAR material

POISS	**0.3**
TALFA	1.17e-5
TECOND	50

HEATC	800
BETA	0
EA	2.2497e7
EIY	3.10e6
EIZ	3.10e6
GIT	2.39e6
EM	2e8
GM	8e7

where in the table:

POISS: Poisson's ratio (unit: -).

TALFA: Temperature elongation coefficient (unit: -)

TECOND: Thermal conductivity (dummy) (unit: W/mC^0)

HEATC: Heat capacity (dummy) (unit: unit: J/kgC^0)

BETA: Tension/torsion coupling parameter. Normally zero, but can be specified to capture torsion effect if the relation between tension/torsion is known (unit: m).

EA: Axial stiffness (unit: kN)

EIY: Bending stiffness about y axis (unit: kNm^2)

EIZ: Bending stiffness about z axis (unit: kNm^2)

GIT: Torsion stiffness (unit: kNm^2)

EM: Young's modulus (unit: kNm^{-2})

GM: Shear modulus (unit: kNm^{-2})

More information about the input code refers to (Svein, 2010). The model is shown in Figure 6.3.

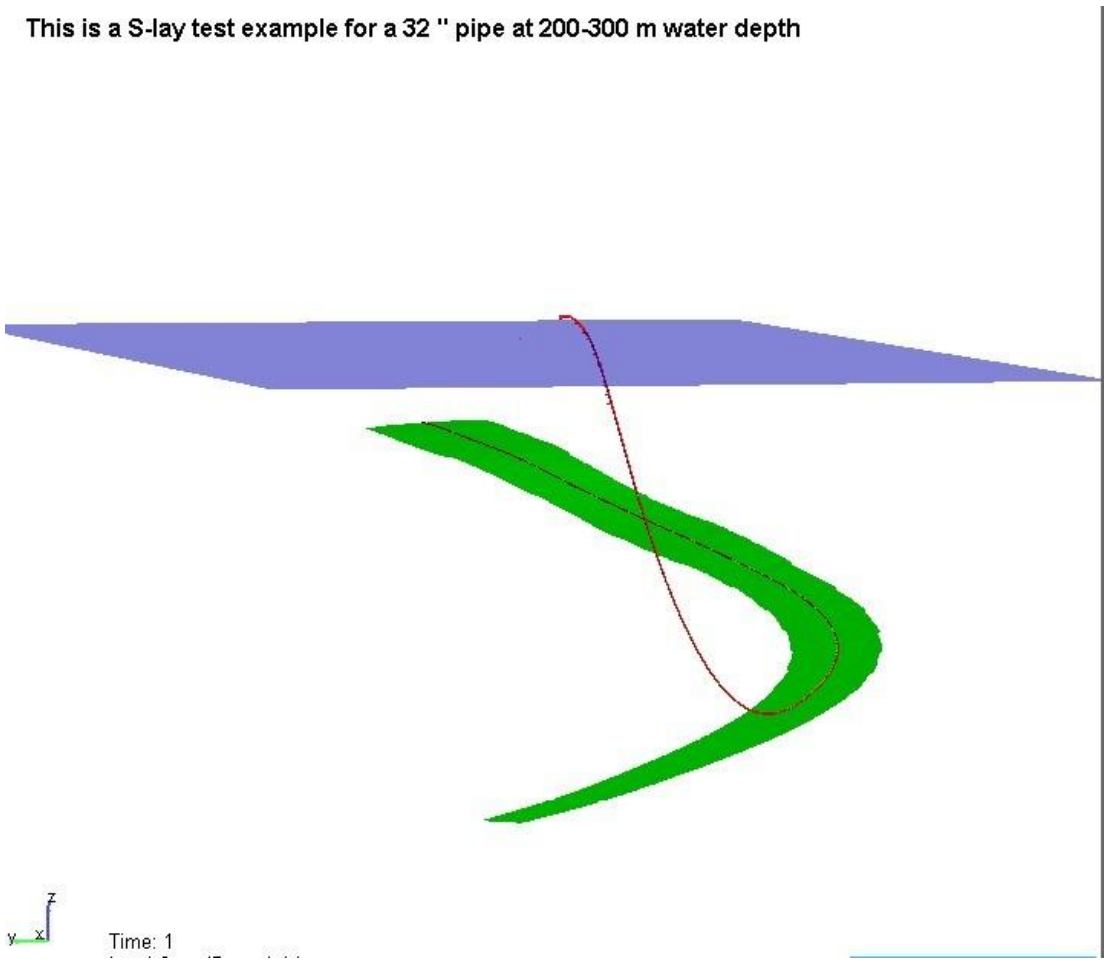

Figure 6.3 The S-Lay Model in XPOST

6.2 Analysis setup

Both static analysis and dynamic are performed. The static analysis provides the initial static configuration for the subsequent dynamic analysis.

The static analysis is done in one load step using the AUTOSTART feature that enables initiation of S-lay. The static and dynamic analysis is defined in two sequences using the TIMECO card, steps 0-1 with step length 1 s for static analysis and then steps 1.1 s-3600 s with 0.1 s step length for dynamic analysis. In order to get enough results to observe the dynamic behaviors of the touchdown point (TDP), the simulation time is set to 3600 s. For each case, the total running time is more or less 6 hours. In our case, two TIMECO cards are used for dynamic analysis to avoid too large .raf file. The first card for dynamic analysis sets the time increment between each restart and visual storage to the .raf file is 1 sec. And for the second one, it is set to be 10 sec.

```
-------------------------------------------------------------------------------------------------

#          t       dt   dtvi    dtdy   dto    type         hla?    Steptype iter itcrit

TIMECO   1.0       1.0   1.0     1.0   201.0  STATIC     NOHLA

TIMECO   360.0     0.10  1.0     1.0   201.0  DYNAMIC    NOHLA auto none    all 20 5   1.0e-4

TIMECO   3600.0    0.10  10.0    1.0   201.0  DYNAMIC    NOHLA auto none all 20 5   1.0e-4

-------------------------------------------------------------------------------------------------
```

For the static analysis gravity loading is applied in one step to the full value. Note that in this case, the material properties for the SPRING137 vessel element have set to zero as the displacement of node 501 is kinematically fully described by using the CONSTR PDISP SPECIAL option for node 501 using the eccentricities between node ID 3001 and node ID 501and the CONSTR PDISP RAO for node 3001 which is the vessel. For the dynamic analysis, the full value of tension is applied in element ID 500 as a concentrated load in node 501 by the CLOAD command. The concentrated nodal loads are defined in the global coordinate system.

```
-------------------------------------------------------------------------------------------------
#                          sn dof mn   fi1   fi2   fi3   ex        ey     ez

CONSTR PDISP SPECIAL 501 1   3001   0   0.0   0   -89.469   0     5.000

CONSTR PDISP SPECIAL 501 2   3001   0   0.0   0   -89.469   0     5.000

CONSTR PDISP SPECIAL 501 3   3001   0   0.0   0   -89.469     0   5.000
```

```
CONSTR PDISP SPECIAL 501 4   3001   0   0.0   0   -89.469    0   5.000

#                        sn   dof head     waveno function name

CONSTR PDISP RAO 3001   1   2.437945 100      surge

CONSTR PDISP RAO 3001   2   2.437945 100      sway

CONSTR PDISP RAO 3001   3   2.437945 100      heave

CONSTR PDISP RAO 3001   4   2.437945 100      roll

CONSTR PDISP RAO 3001   5   2.437945 100      pitch

CONSTR PDISP RAO 3001   6   2.437945 100      yaw


#       hist dir   no      r1

CLOAD 50    1   501 0.166195E+04
```

In this model, the pipeline is subjected to the hydrodynamic forces arising from the irregular waves and current.

The influence of various parameters viz wave height, wave period and wave direction are investigated in this thesis.

Four sea states are considered with four sets of significant wave height and the peak period (Hs，Tp) = （1 m, 7.5 s）, (8.4s, 2m), (3m, 9.2s), (4m, 10s).

And the propagation directions of the waves are 0 deg, 45 deg, 90 deg. 12 cases with different combinations of the sea states and the propagation directions are investigated.

In SIMLA, the wave loading is assumed to occur as a result of a wave generator positioned at a point x_o, y_o in the XYZ global coordinate frame. In the wave generator, surface elevation, wave-induced water particle velocity and acceleration, dynamical pressure and pressure gradient, of an arbitrary point in space and time is defined mathematically.

#	seagrp	type	waveno	hist	xo	yo	beta	T	H	D
WAVELO	sea1	IRREGULAR	100	250	0.0	0.0	0	7.5	1.0	2200

Dt	Tsim	Tstart	Kdepth	seed	spec
0.1	3600	1.1	125	0	1

In general, in this analysis model, two-parameter Pierson Moskowitz spectrum is applied at a water depth of 2200. The duration of irregular wave is 3600s equal to the duration of dynamic analysis.

Kinematic water depth is set to be 125m. The calculations below show it is reasonable to use this quantity.

First order wave forces are usually assumed to have significant energy of interest for marine structures in the period range 3-24 sec.

When the wave period is T=10s, the corresponding wave length λ is

$$\lambda = \frac{gT^2}{2\pi} = 156.13\text{m}$$

Assume that the limit for breaking waves is given by:

$$H_{max} = \frac{\lambda}{7} = 22.3\text{m}$$

The maximum wave height is 22.3m (double amplitude). The wave particle speed at the sea surface can be found according to the linear theory for deep water:

$$v_{max} = \pi H_{max}/T = 7\text{m/s}$$

According to linear theory, the amplitude of wave effects will decrease as an exponential function of the vertical location of the water particle, determined by the factor $e^{-2\pi d/\lambda}$.

So at a water depth of 125 m, the wave effect has died out with the particle velocity reduced to 0.05m/s. Thus the waves won't have any contact with the seabed at the depth of 200-300 m.

The current loading is specified along a route the curvilinear coordinate of the route as basis for interpolating an arbitrary number of current profiles.

Example:

```
#              no          depth curr     fi

CURLOAD 100 global 0          1.0    0.93

                        -200          0.1    0.93

                        -5000         0.1    0.93
```

In order to allow visual representation of the model including the sea surface in XPOST, the VISRES option has been applied.

Example:

```
#              mode     factor     result

VISRES   integration      1        sigma-xx
```

By the DYNRES cars, user selected results will be stored on the .dyn file on a format that enable direct use of the XPOST time history plot functionality. Elements, nodal and integration results can be stored.

```
#    nodal    type node direction
```

DYNRES_N 1 3001 1

DYNRES_N 1 3001 2

The preceding information above is a brief description about the dynamic analysis model and some of the input code. For more information, reference goes to (Svein, 2010) and Appendix B.

Chapter 7 Dynamic Analysis Results

In this chapter, the dynamic analysis results are illustrated. The dynamic analysis results are obtained from.raf files and can be shown visually in XPOST.

With regards to our interest, the time series of the pipe–interaction force and displacement are obtained. From seabed contact element 10213 the seabed has contact with the pipeline. We studied the time series of the transverse displacement, transverse force and vertical force for seabed contact element 10213, 10212, 10211, 10210 end 1 for 12 cases, see in the following figures.

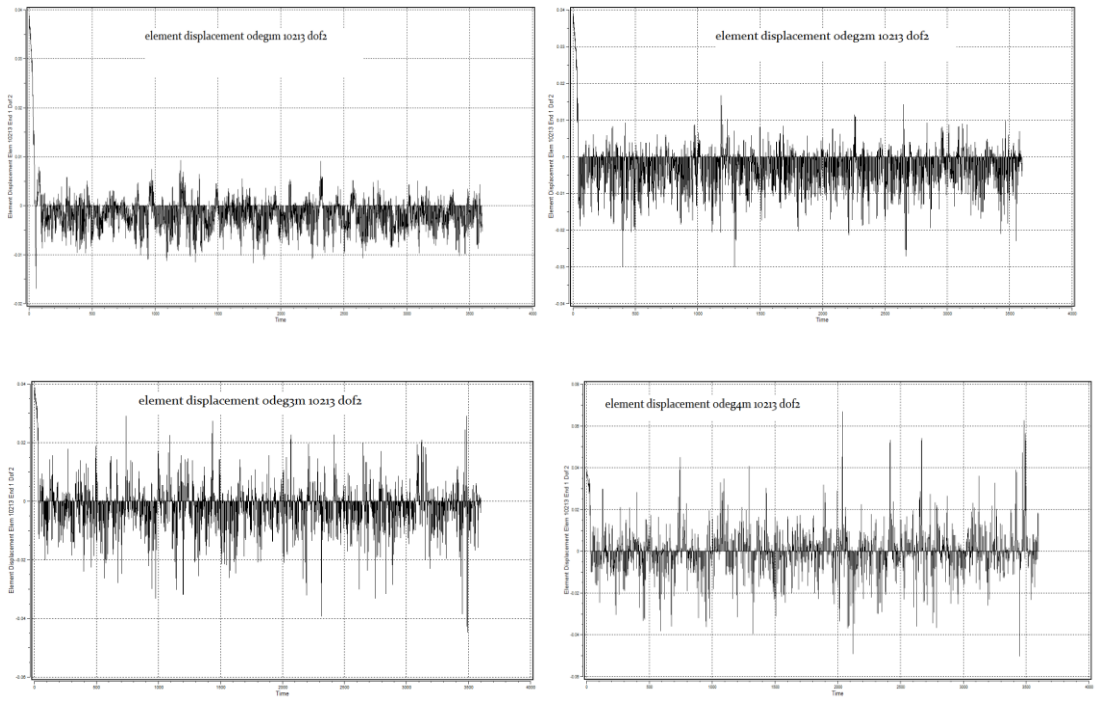

Figure 7.1 Element Displacement Element 10213 End 1 Dof2 with 0 deg Wave Direction

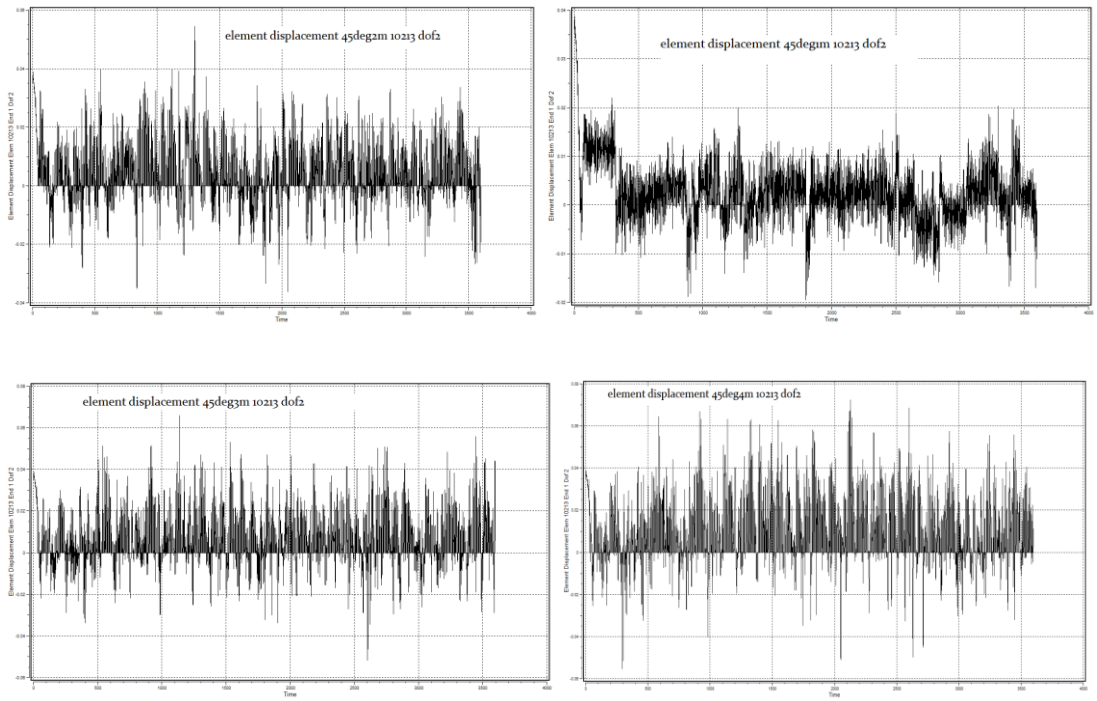

Figure 7.2 Element Displacement Element 10213 End 1 Dof2 for 45 deg Wave Direction

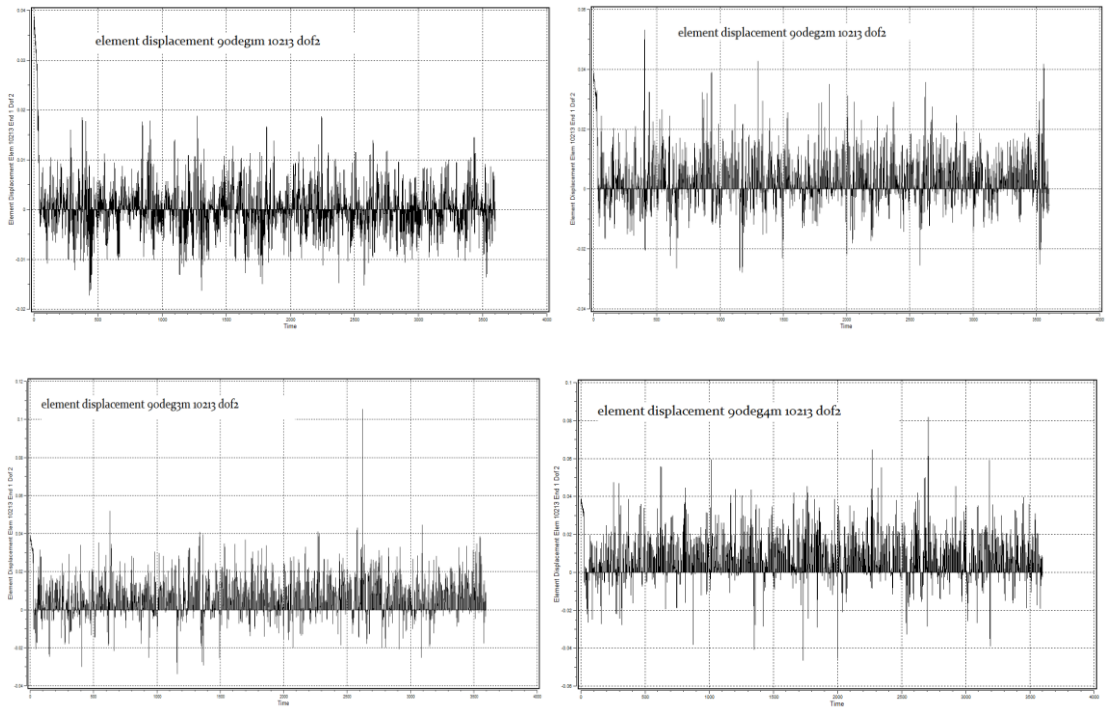

Figure 7.3 Element Displacement Element 10213 End 1 Dof2 for 90 deg Wave Direction

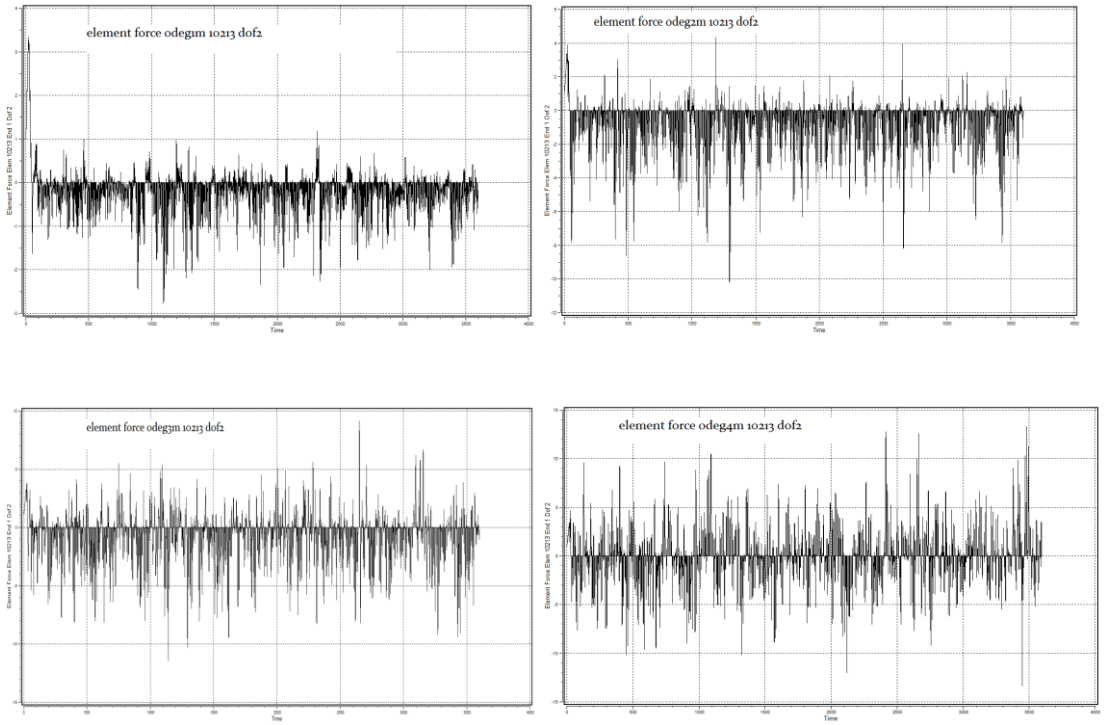

Figure 7.4 Element Force Element 10213 End 1 Dof 2 for 0 deg Wave Direction

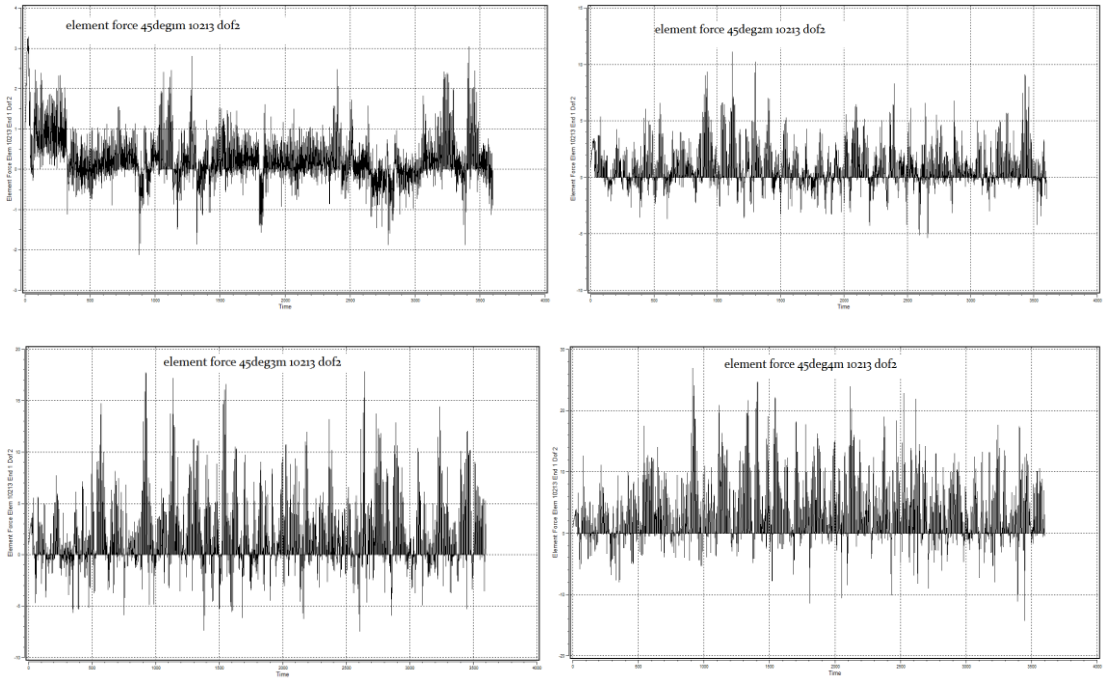

Figure 7.5 Element Force Element 10213 End 1 Dof 2 for 45 deg Wave Direction

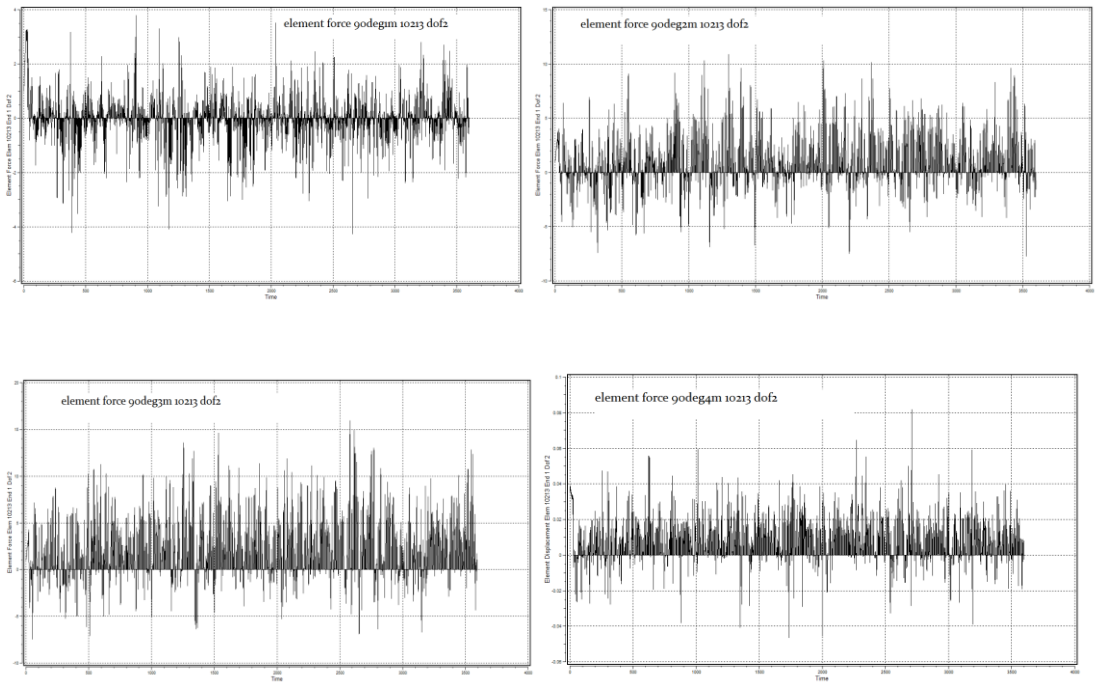

Figure 7.6 Element Force Element 10213 End 1 Dof 2 for 90 deg Wave Direction

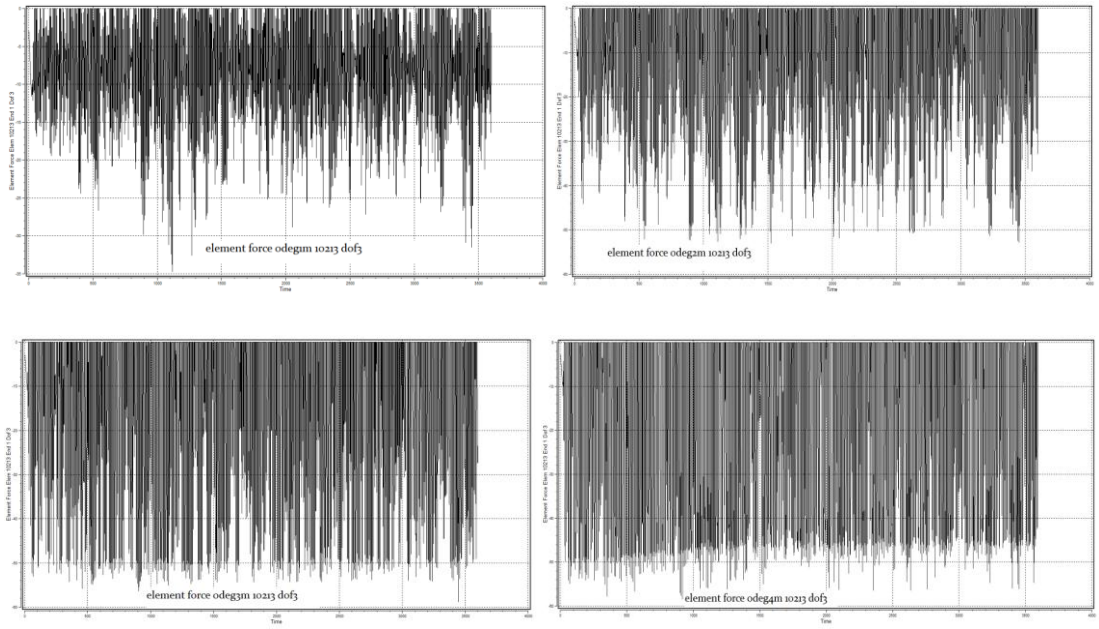

Figure 7.7 Element Force Element 10213 End 1 Dof 3 for 0 deg Wave Direction

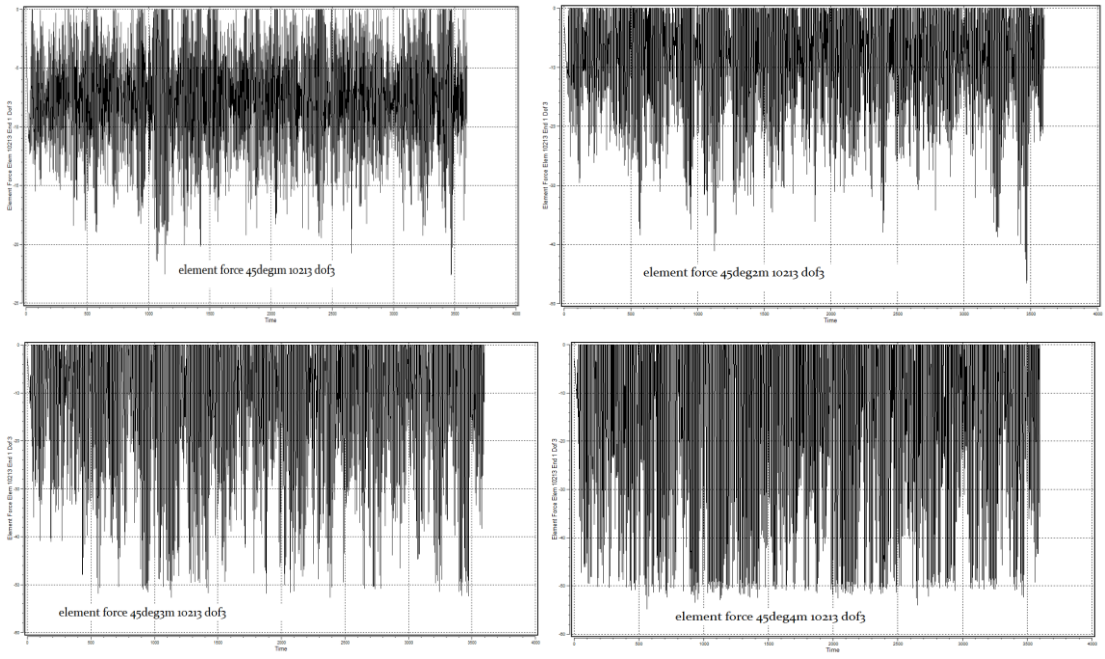

Figure 7.8 Element Force Element 10213 End 1 Dof 3 for 45 deg Wave Direction

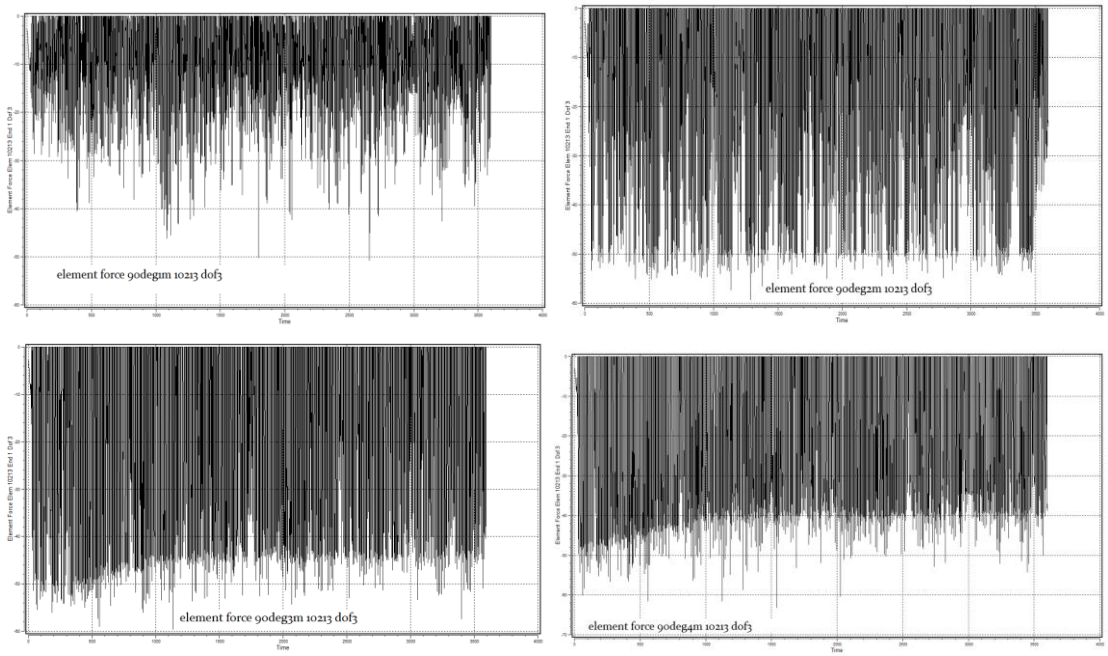

Figure 7.9 Element Force Element 10213 End 1 Dof 3 for 90 deg Wave Direction

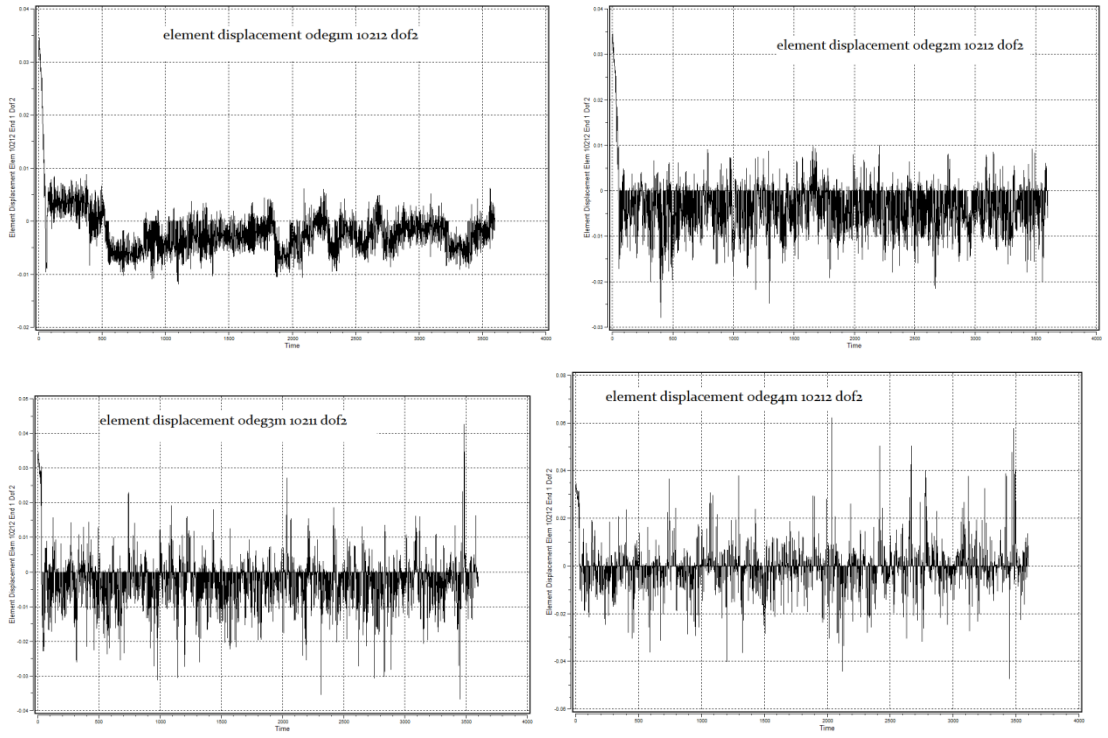

Figure 7.10 Element Displacement Element 10212 End 1 Dof2 with 0 deg Wave Direction

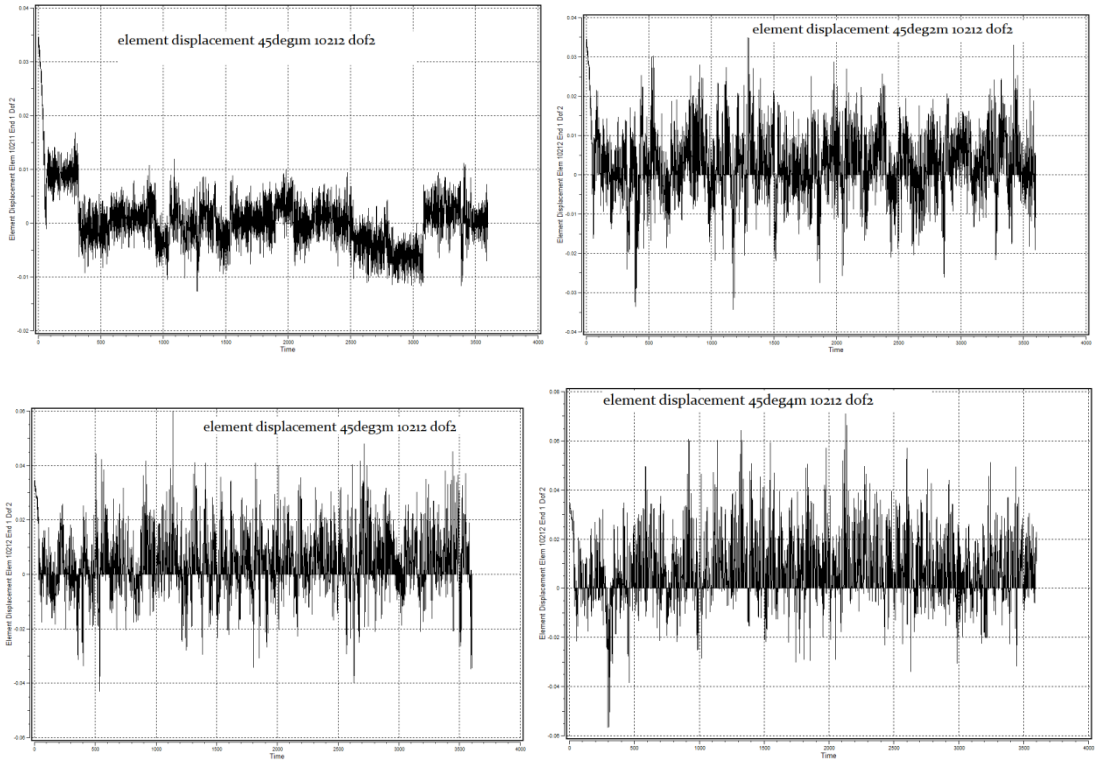

Figure 7.11 Element Displacement Element 10212 End 1 Dof2 for 45 deg Wave Direction

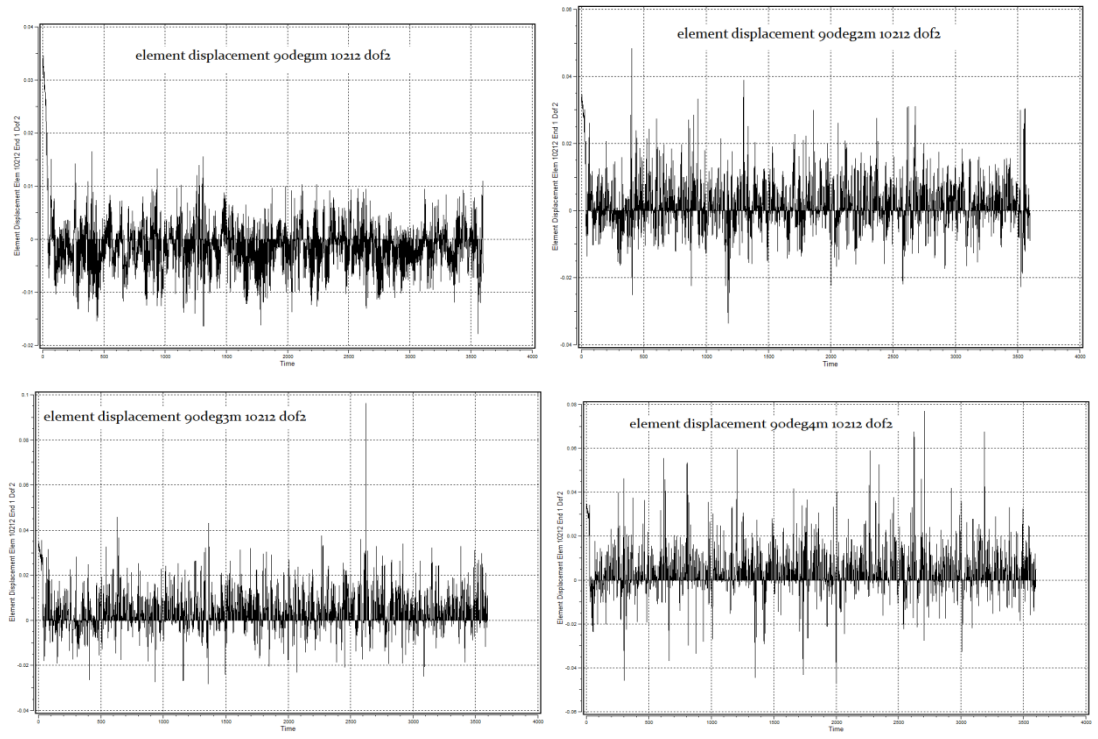

Figure 7.12 Element Displacement Element 10212 End 1 Dof2 for 90 deg Wave Direction

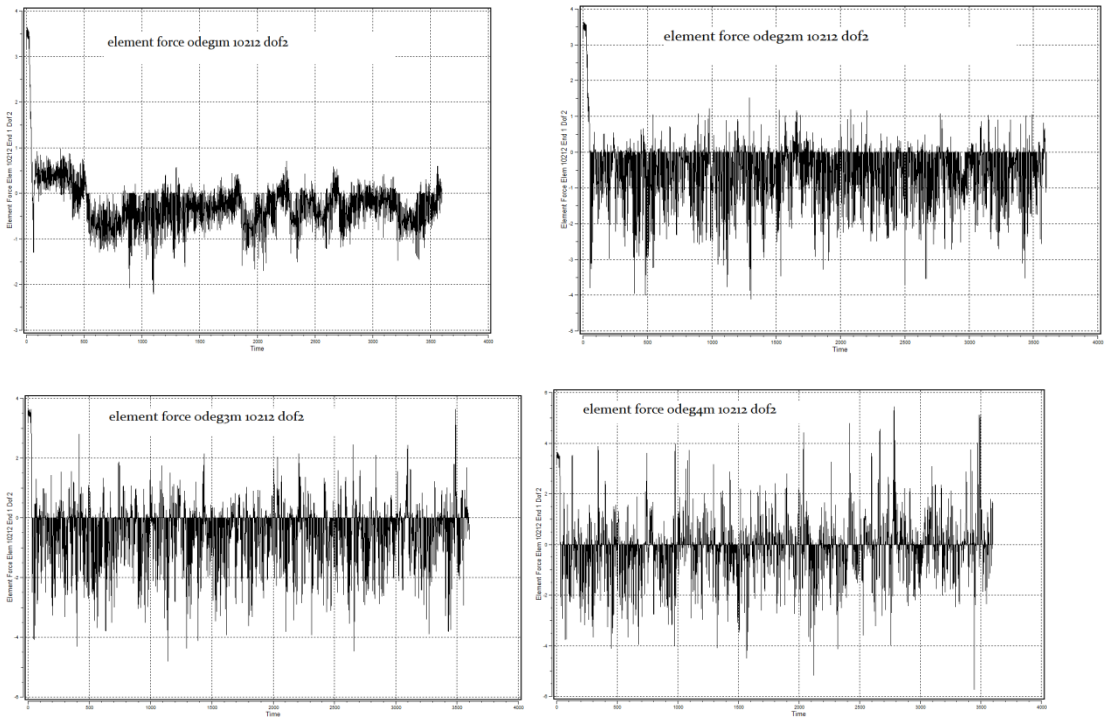

Figure 7.13 Element Force Element 10212 End 1 Dof2 for 0 deg Wave Direction

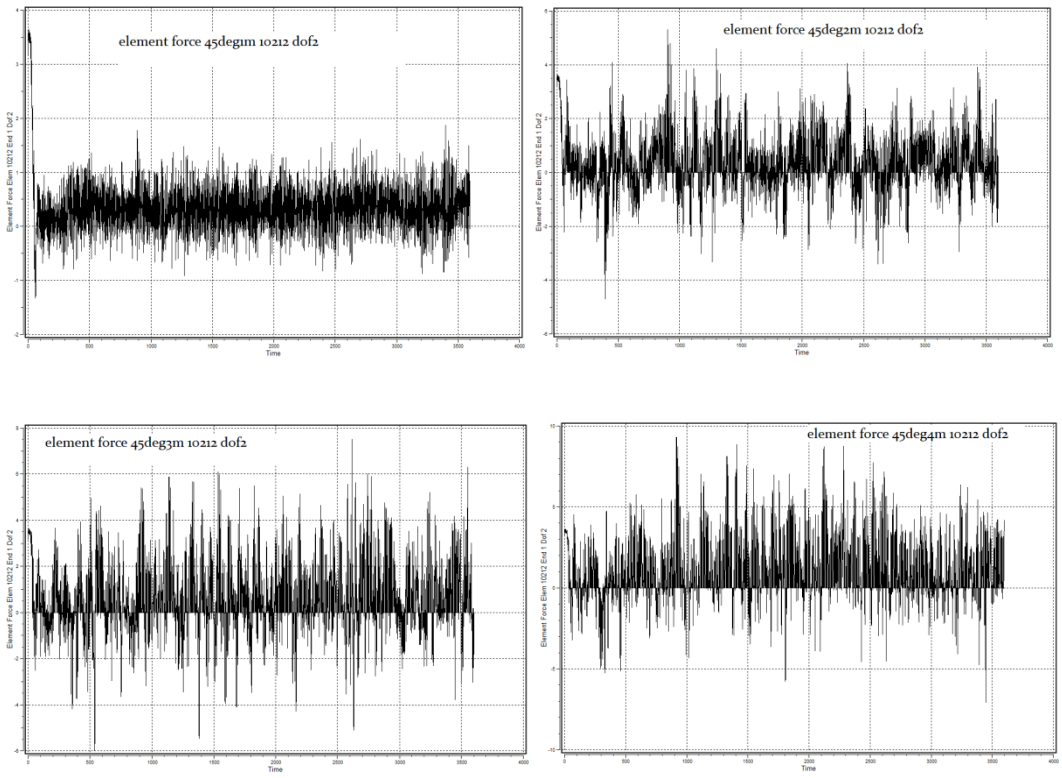

Figure 7.14 Element Force Element 10212 End 1 Dof2 for 0 deg Wave Direction

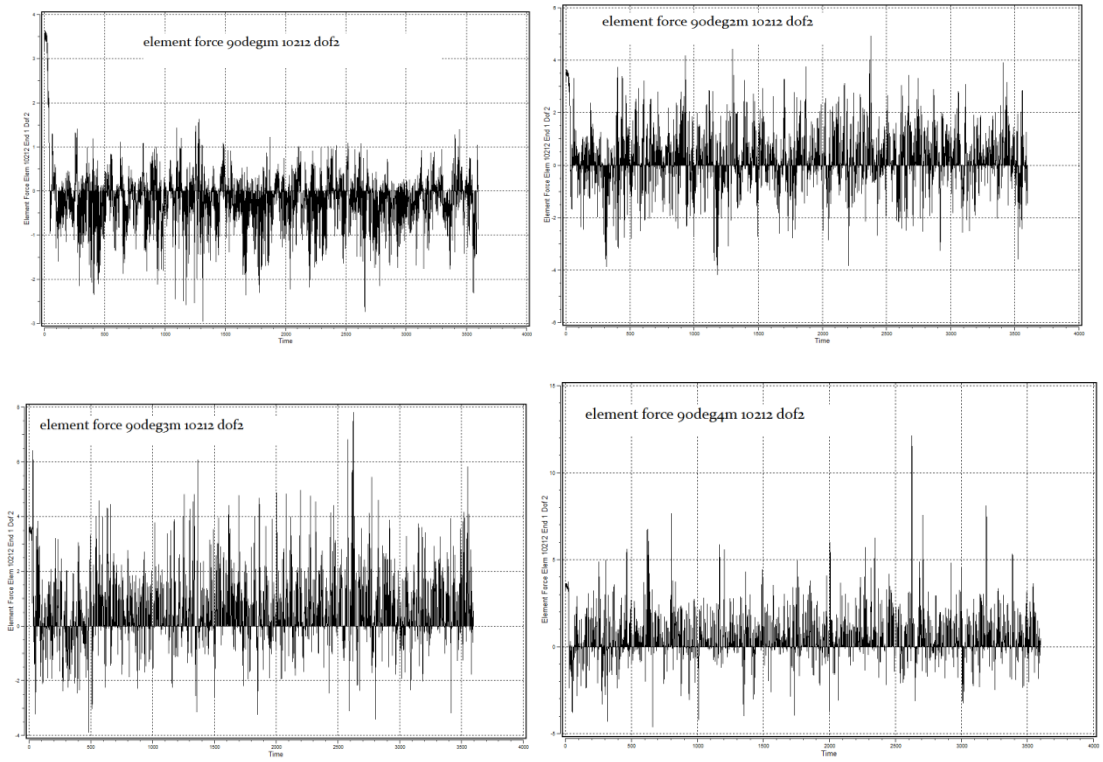

Figure 7.15 Element Force Element 10212 End 1 Dof2 for 90 deg Wave Direction

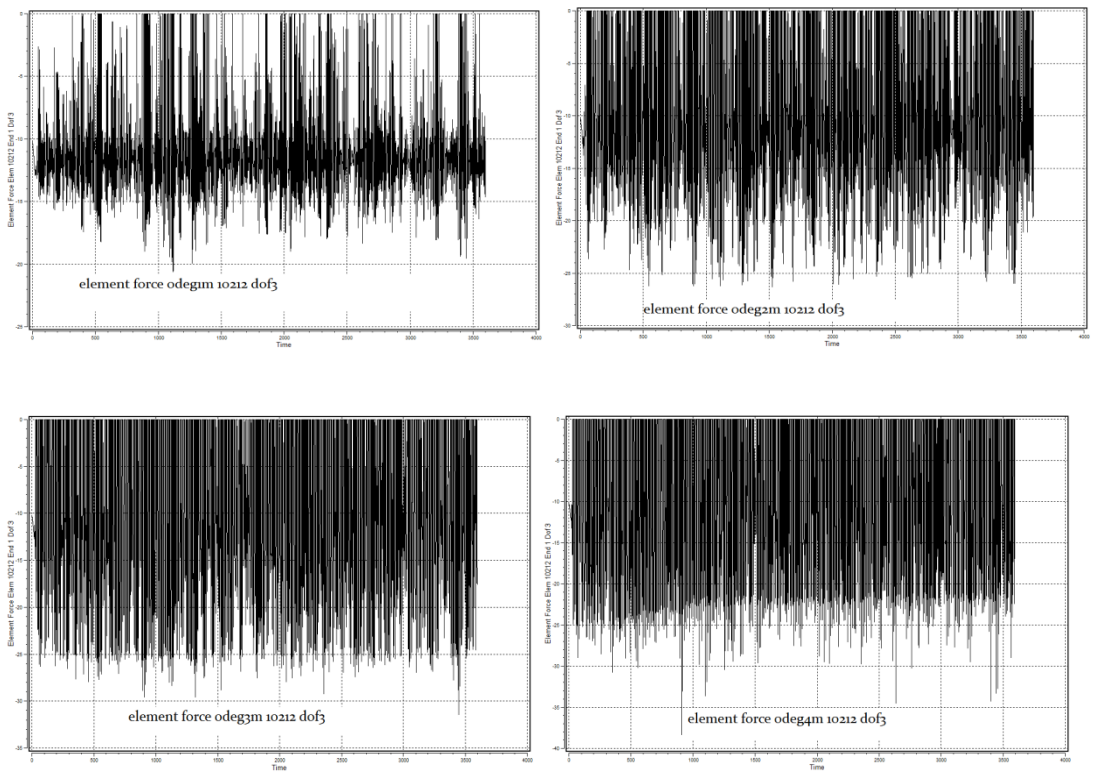

Figure 7.16 Element Force Element 10212 End 1 Dof3 for 0 deg Wave Direction

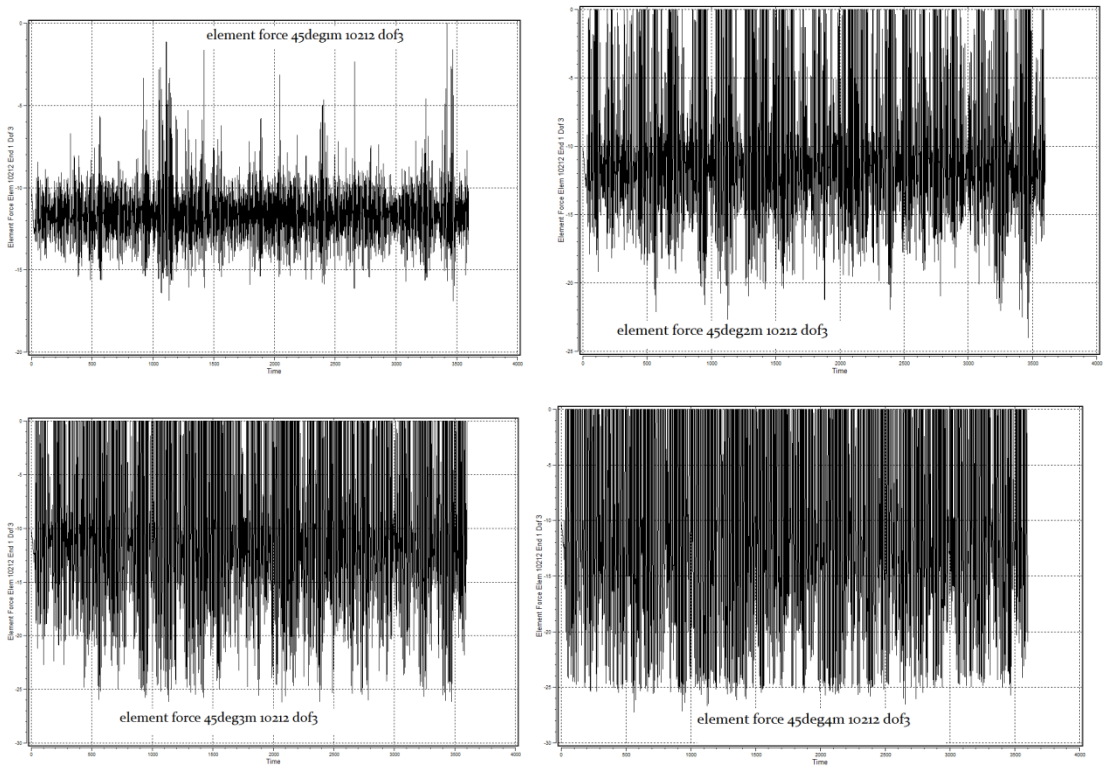

Figure 7.17 Element Force Element 10212 End 1 Dof3 for 45 deg Wave Direction

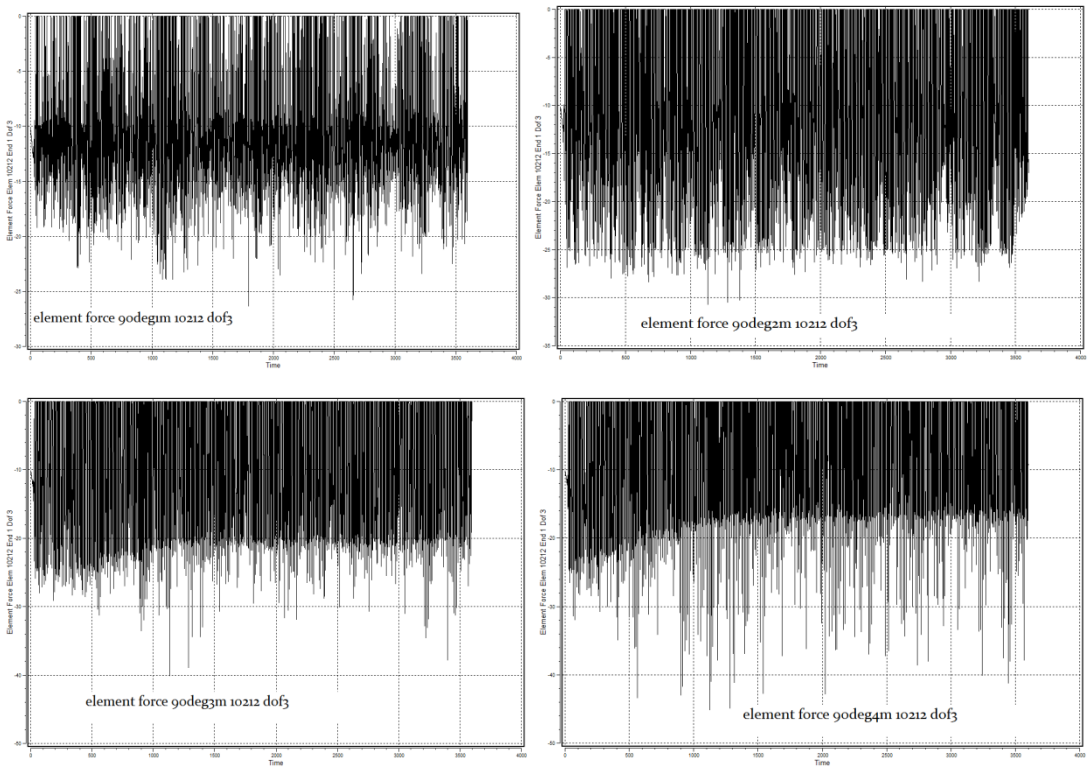

Figure 7.18 Element Force Element 10212 End 1 Dof3 for 90 deg Wave Direction

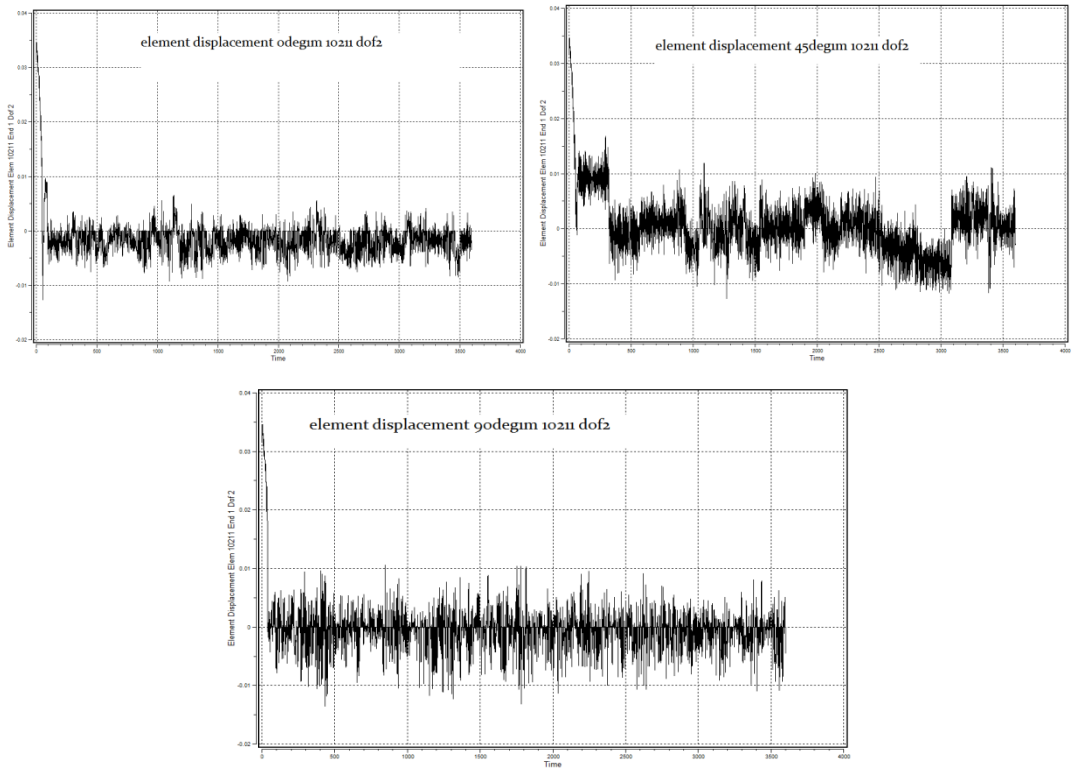

Figure 7.19 Element Displacement Element 10211 End 1 Dof2 for H_s=1m

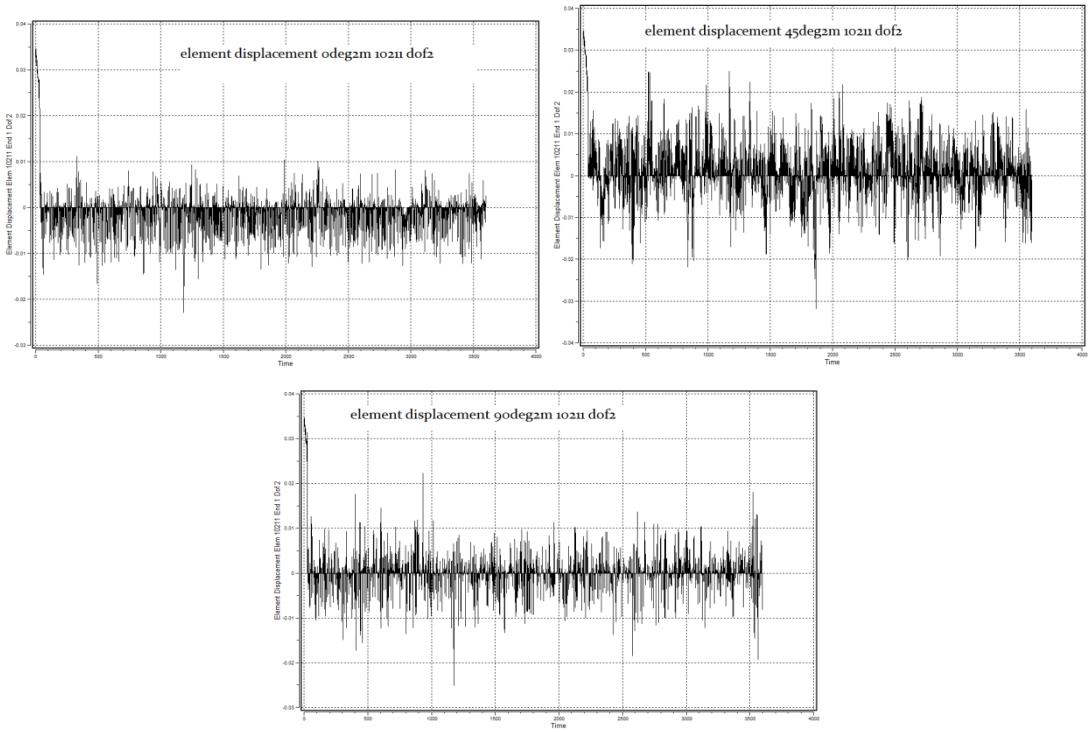

Figure 7.20 Element Displacement Element 10211 End 1 Dof2 for H_s=2m

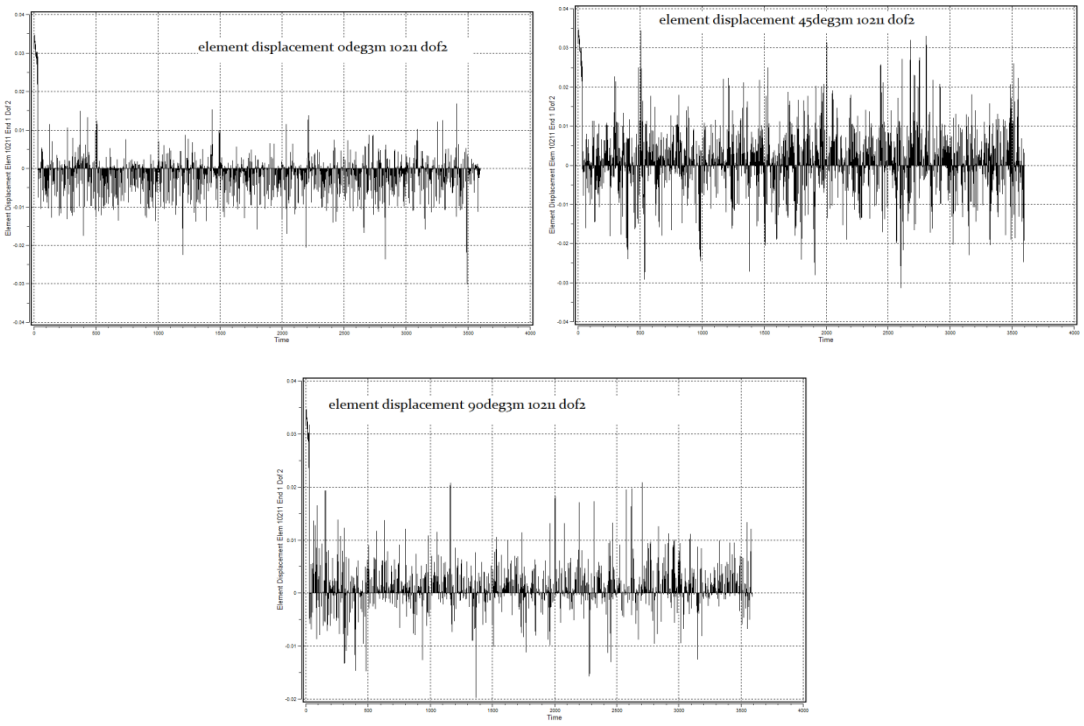

Figure 7.21 Element Displacement Element 10211 End 1 Dof2 for H_s=3m

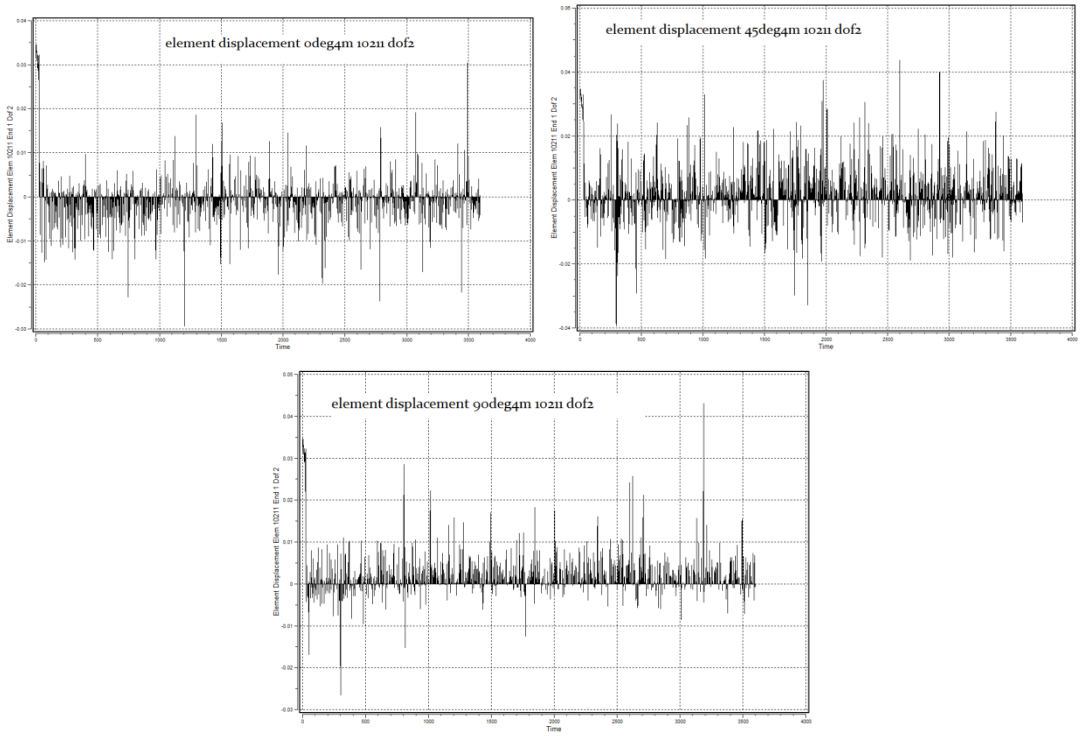

Figure 7.22 Element Displacement Element 10211 End 1 Dof2 for H_s=4m

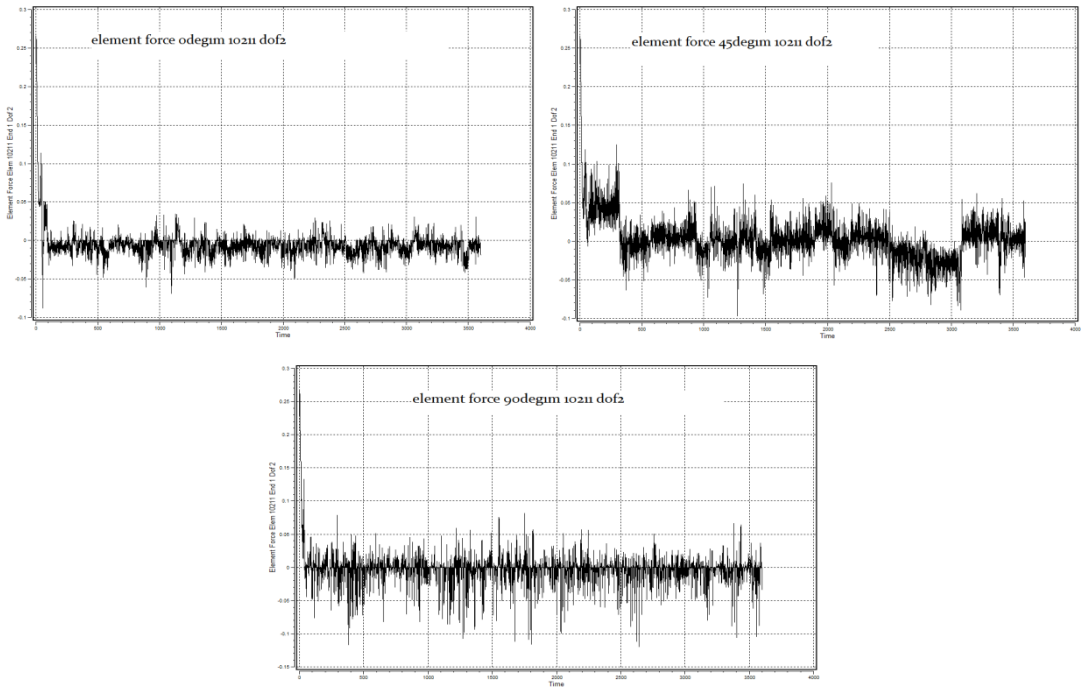

Figure 7.23 Element Force Element 10211 End 1 Dof2 for Hs=1m

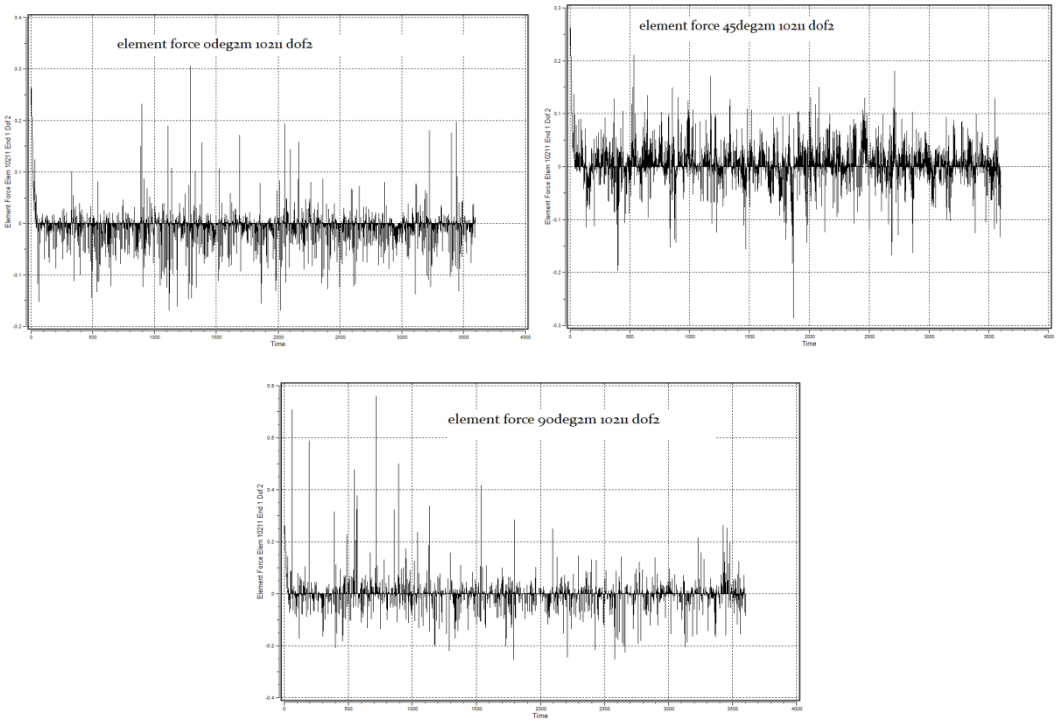

Figure 7.24 Element Force Element 10211 End 1 Dof2 for H_s=2m

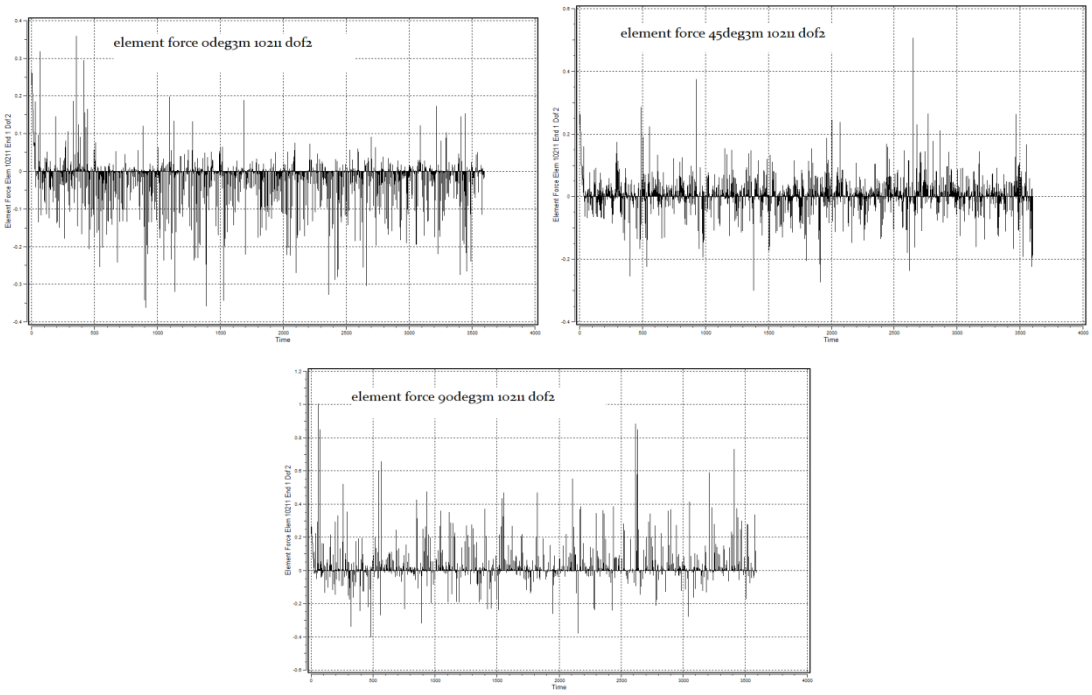

Figure 7.25 Element Force Element 10211 End 1 Dof2 for H_s=3m

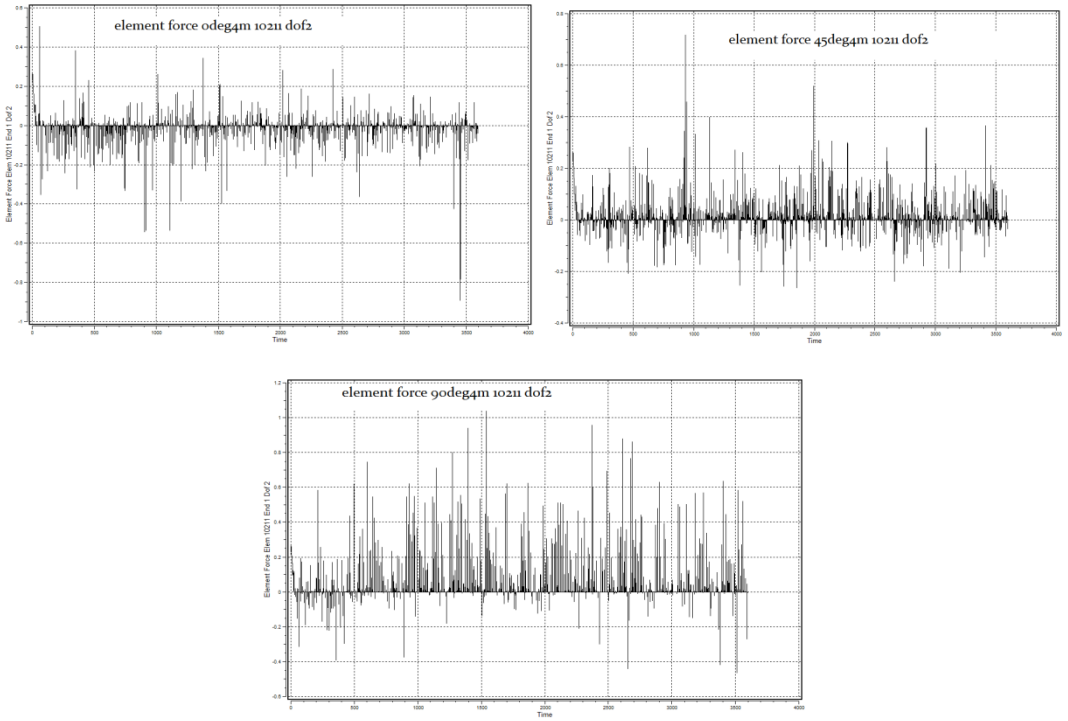

Figure 7.26 Element Force Element 10211 End 1 Dof2 for H_s=4m

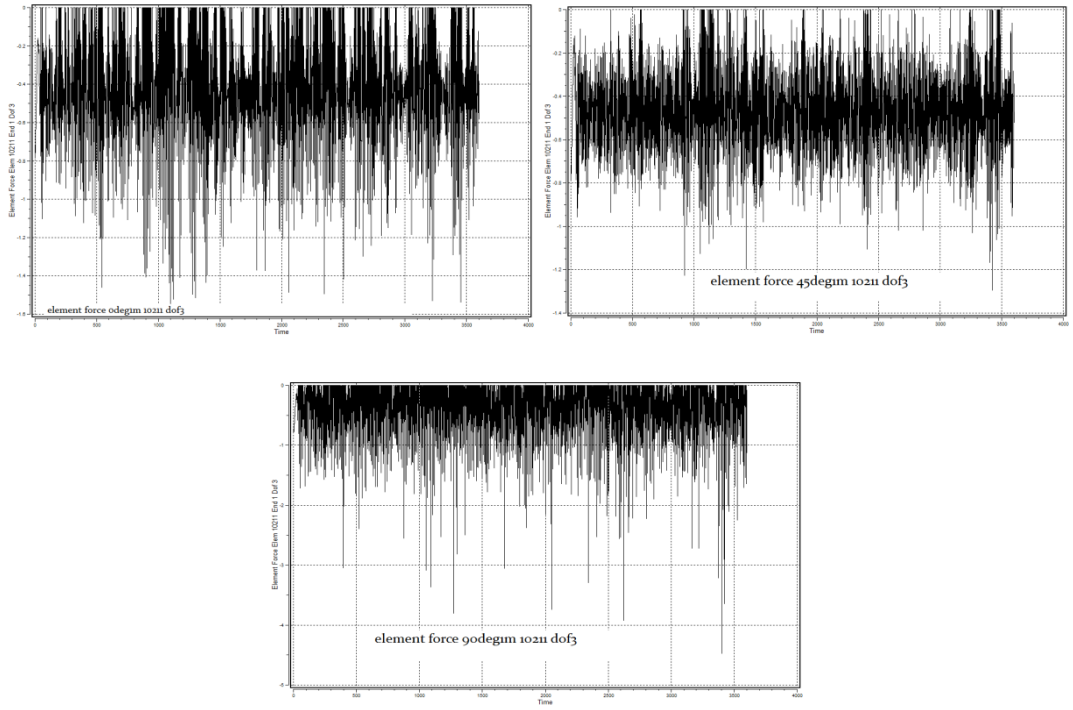

Figure 7.27 Element Force Element 10211 End 1 Dof3 for H_s=1m

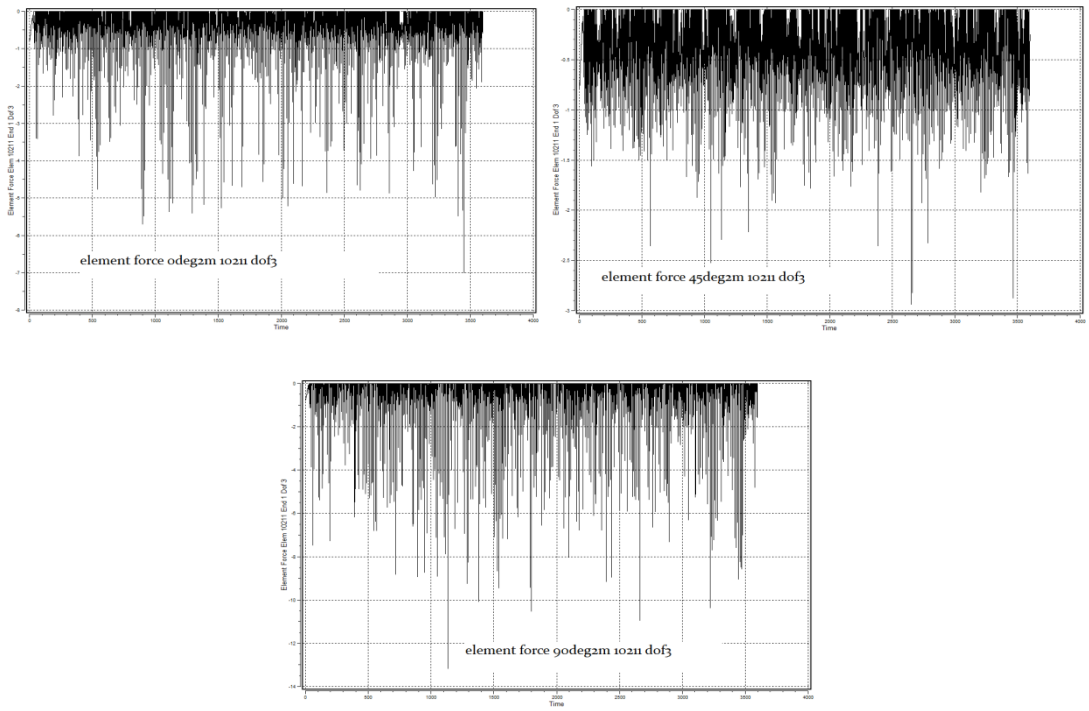

Figure 7.28 Element Force Element 10211 End 1 Dof3 for H_s=2m

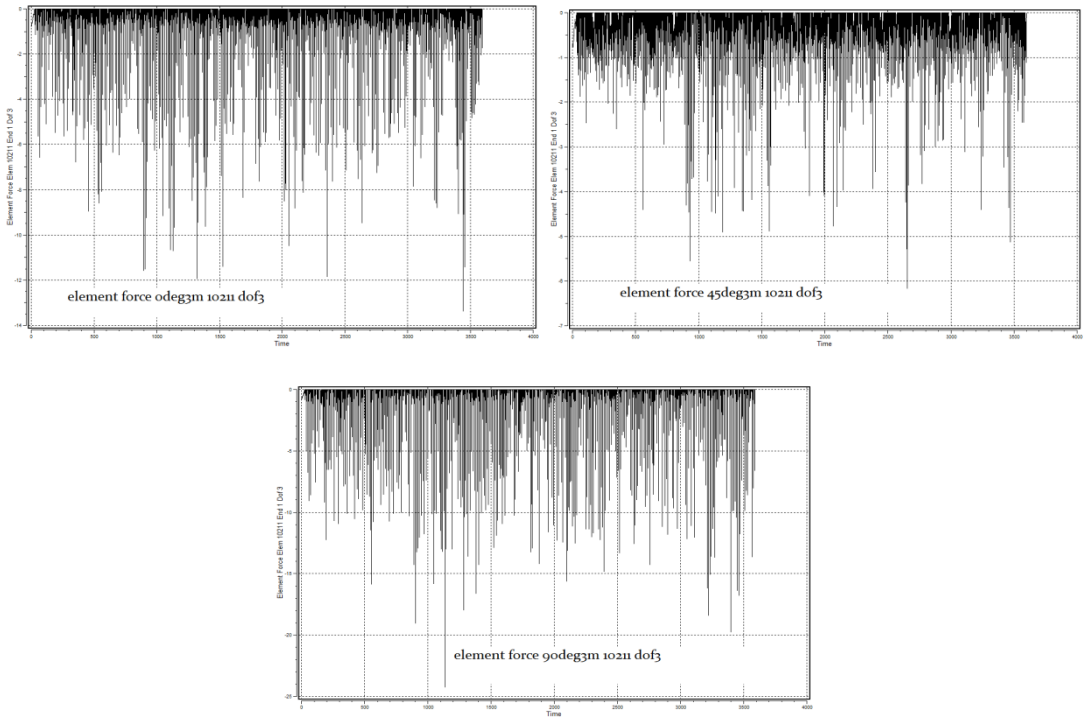

Figure 7.29 Element Force Element 10211 End 1 Dof3 for H_s=3m

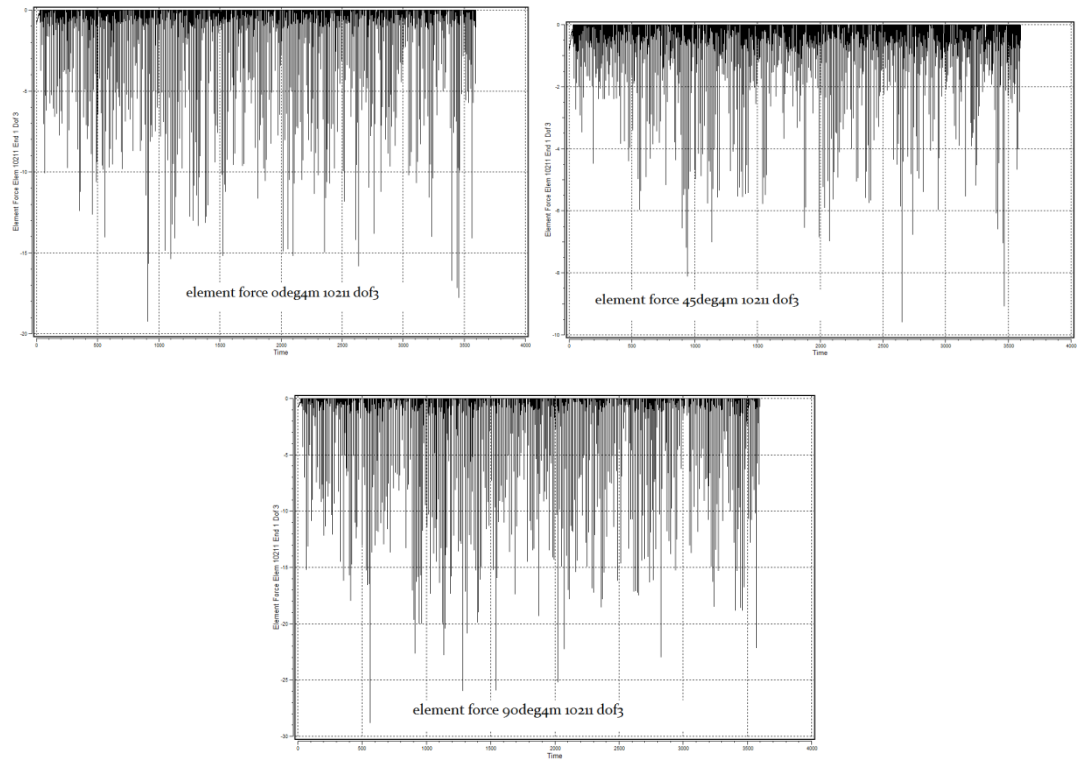

Figure 7.30 Element Force Element 10211 End 1 Dof3 for H_s=4m

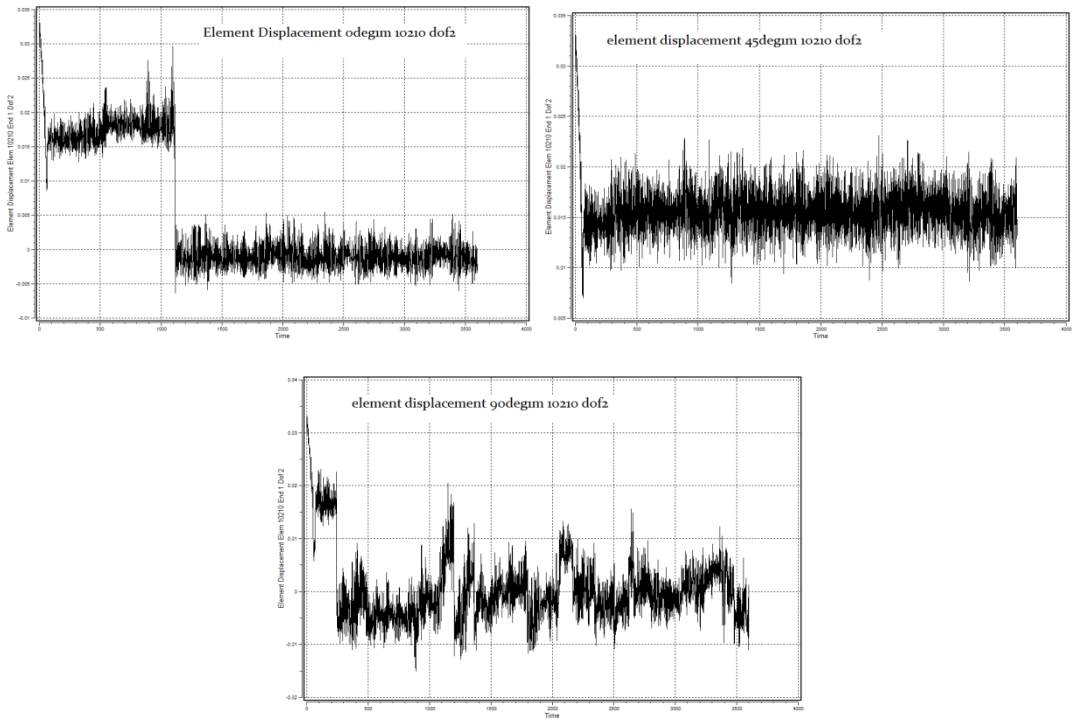

Figure 7.31 Element Displacement Element 10210 End 1 Dof2 for H_s=1m

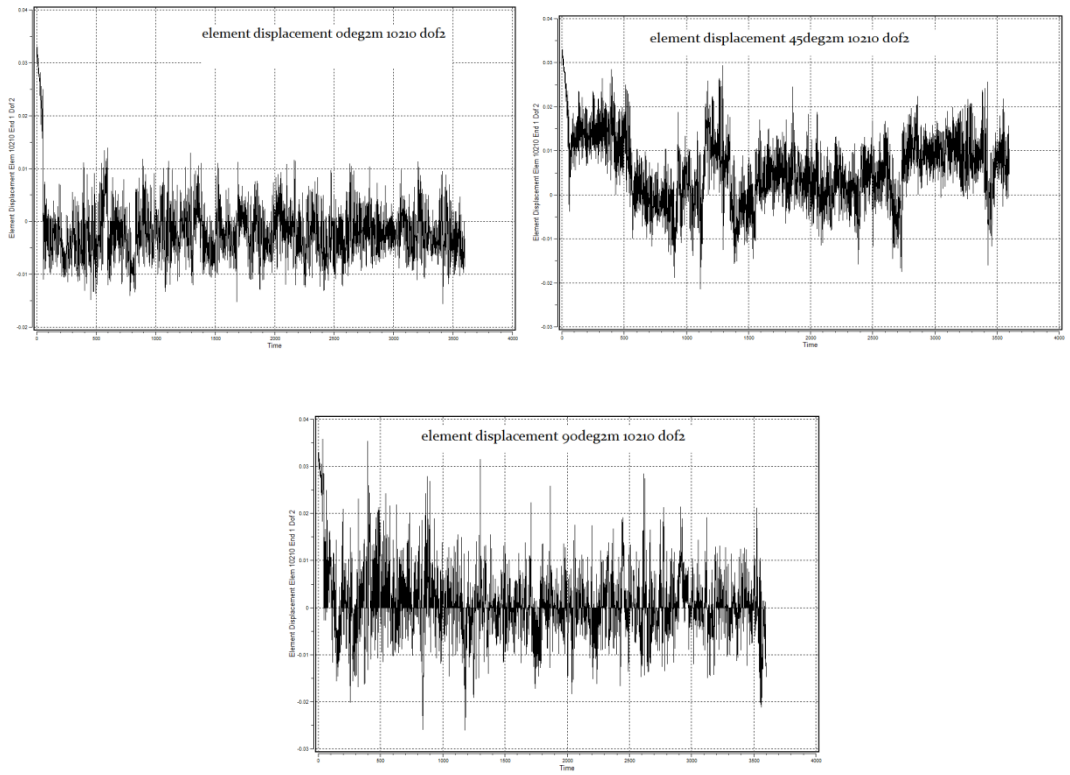

Figure 7.32 Element Displacement Element 10210 End 1 Dof2 for H_s=2m

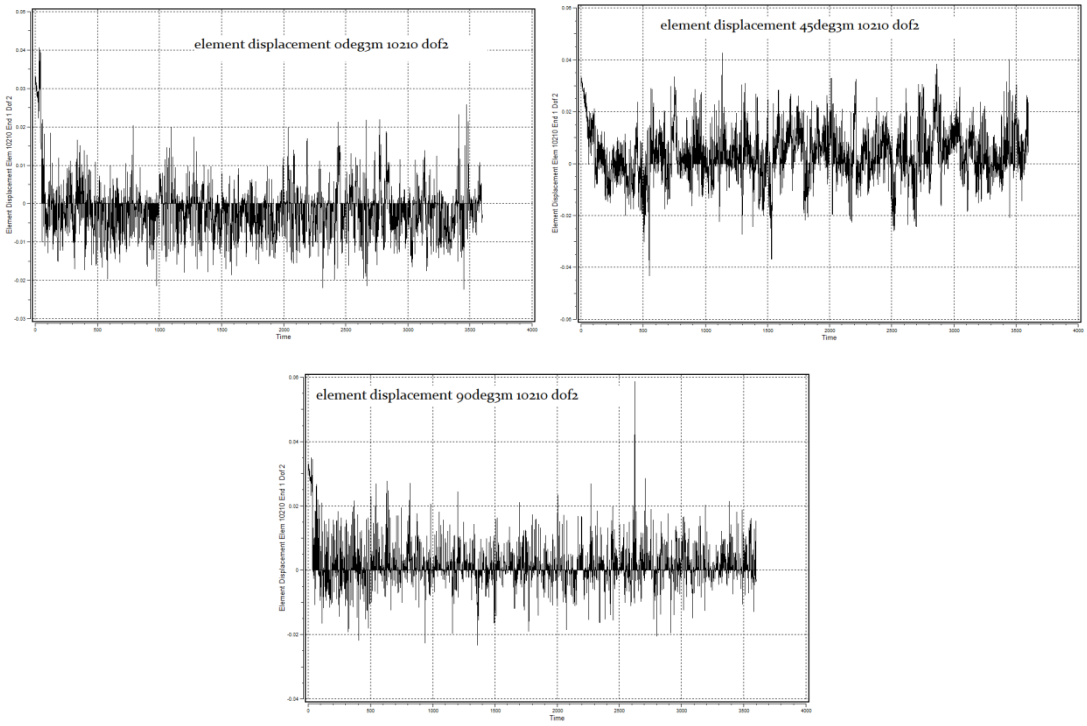

Figure 7.33 Element Displacement Element 10210 End 1 Dof2 for H_s=3m

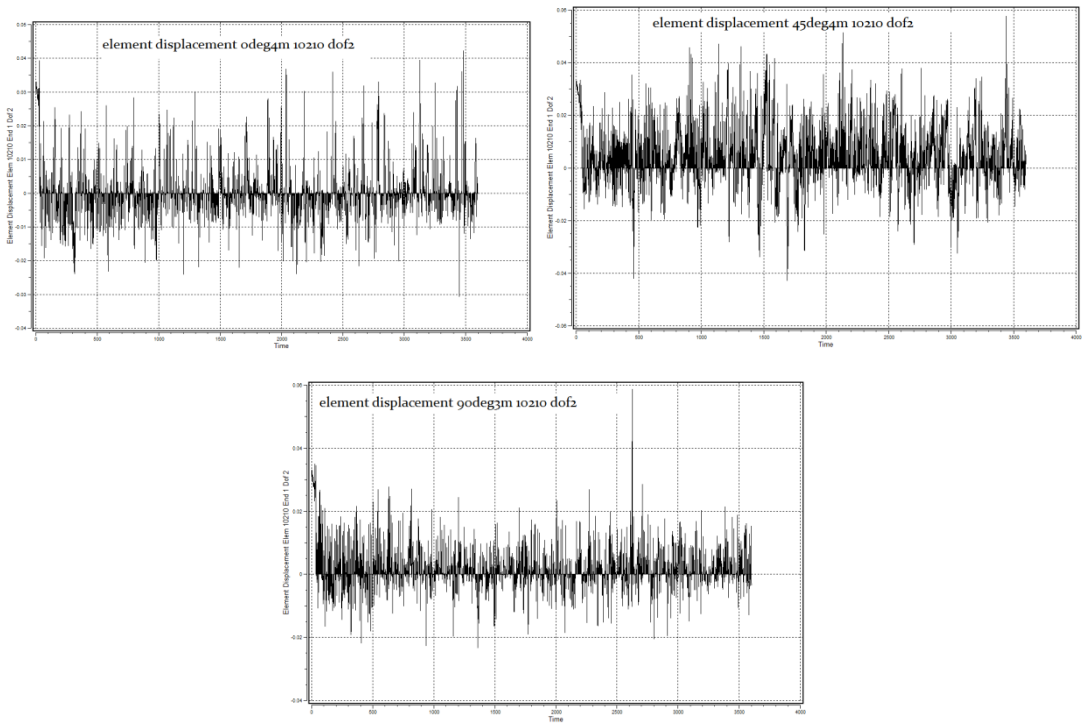

Figure 7.34 Element Displacement Element 10210 End 1 Dof2 for H_s=4m

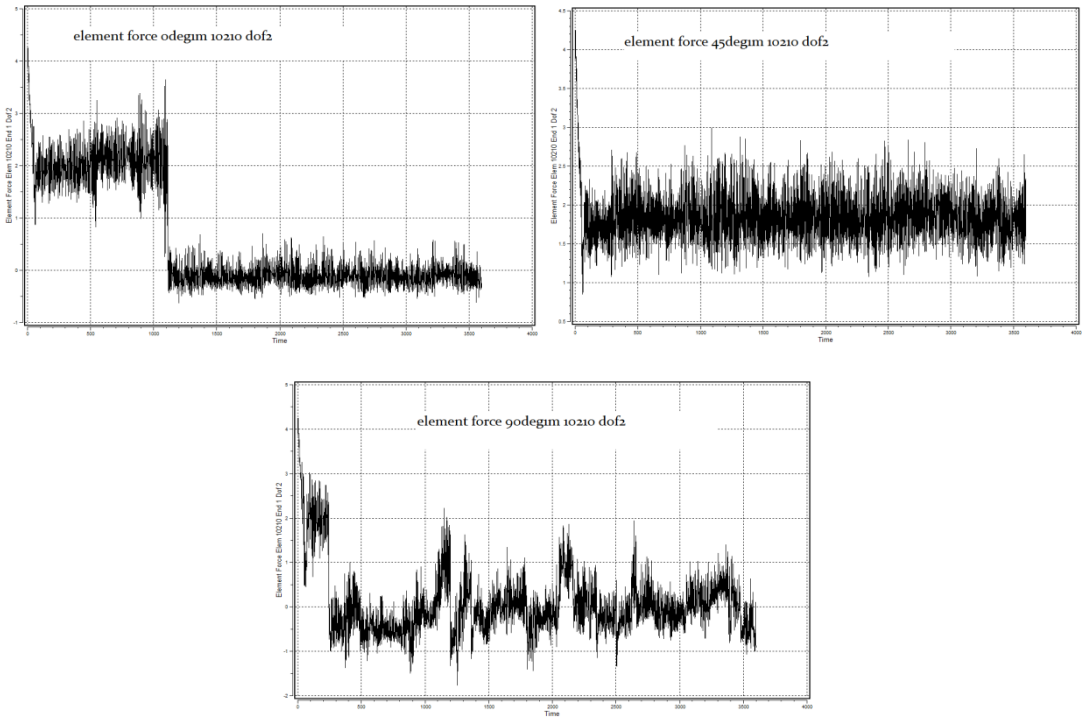

Figure 7.35 Element Force Element 10210 End 1 Dof2 for H_s=1m

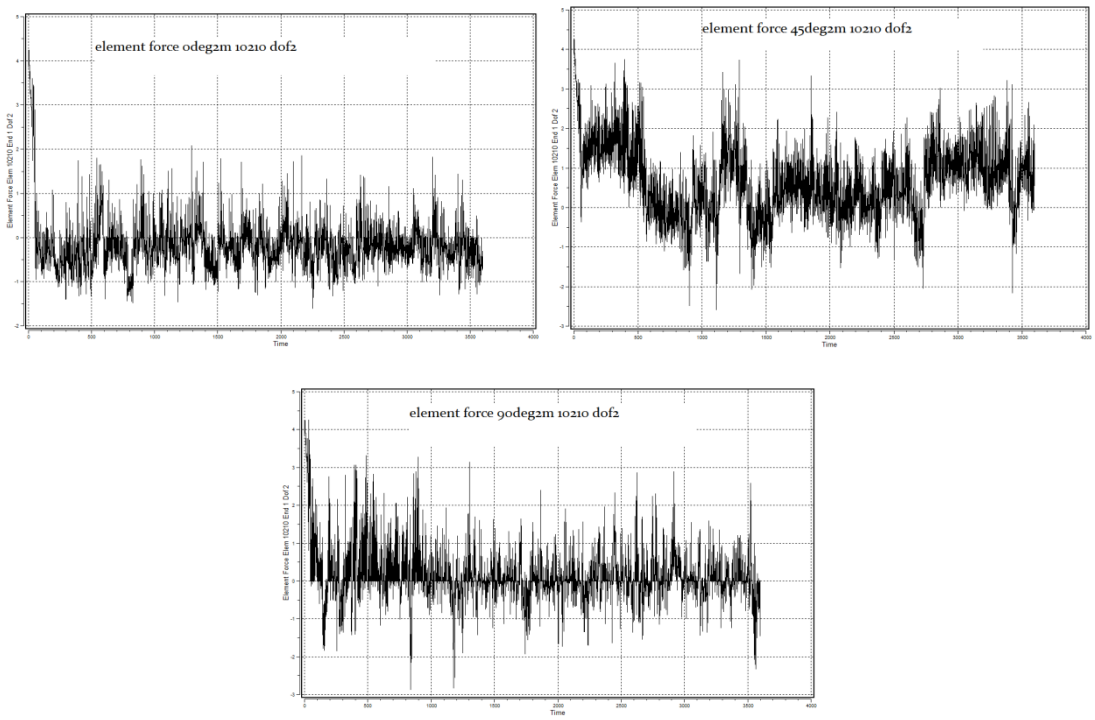

Figure 7.36 Element Force Element 10210 End 1 Dof2 for H_s=2m

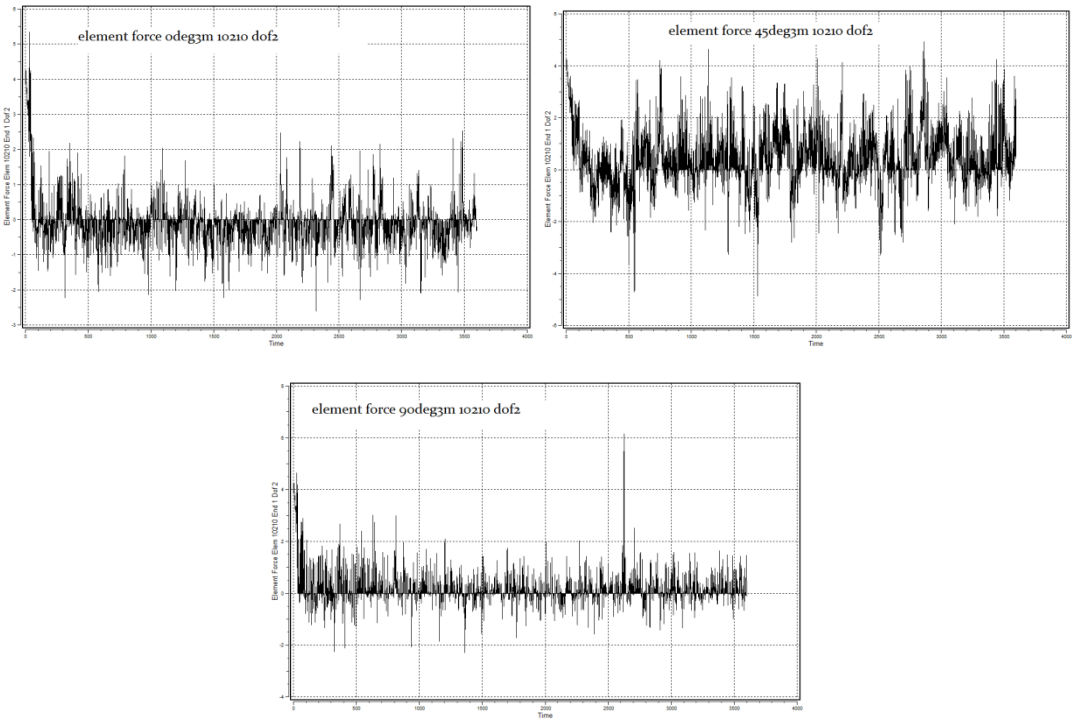

Figure 7.37 Element Force Element 10210 End 1 Dof2 for H_s=3m

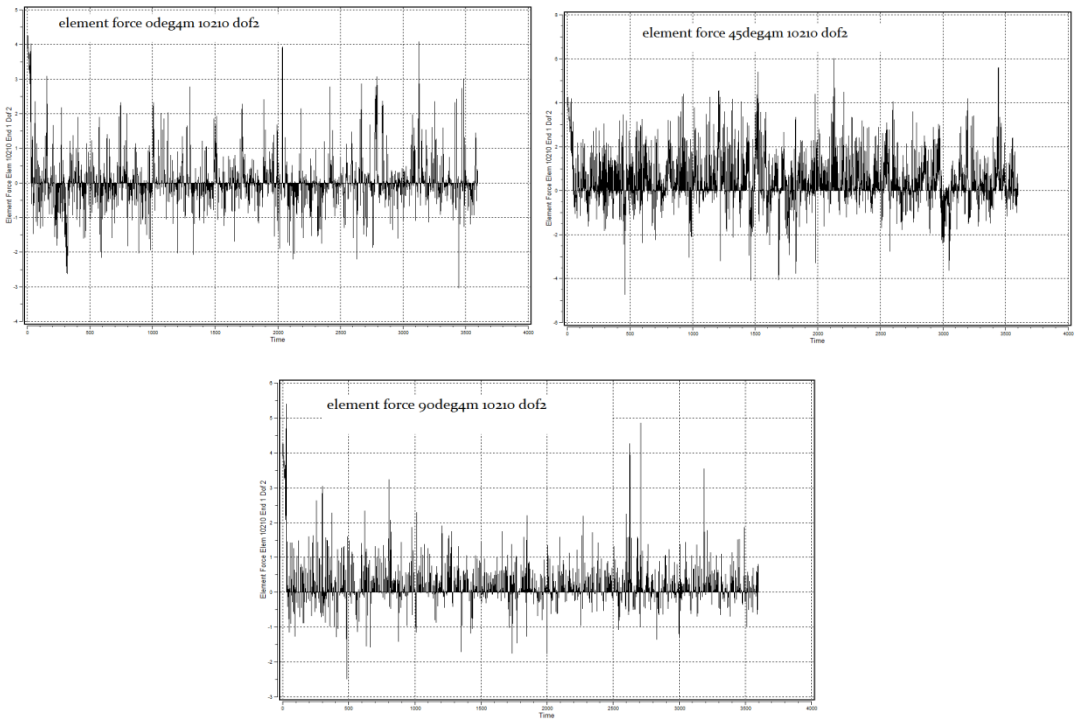

Figure 7.38 Element Force Element 10210 End 1 Dof2 for H_s=4m

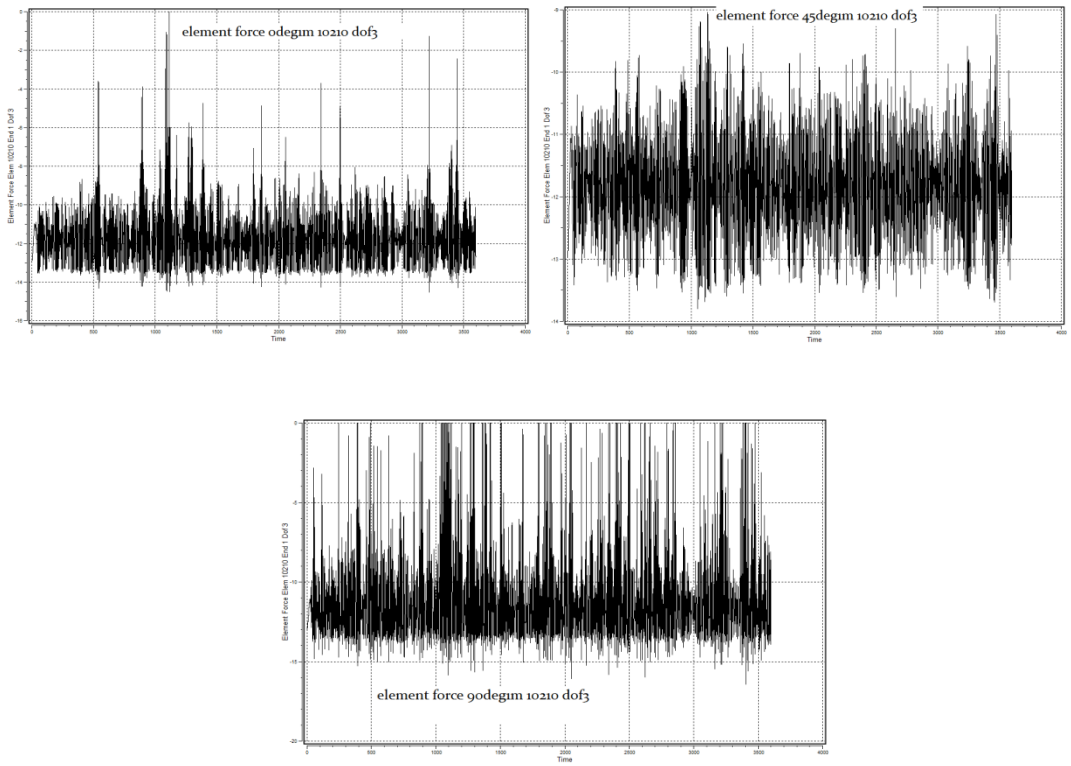

Figure 7.39 Element Force Element 10210 End 1 Dof3 for H_s=1m

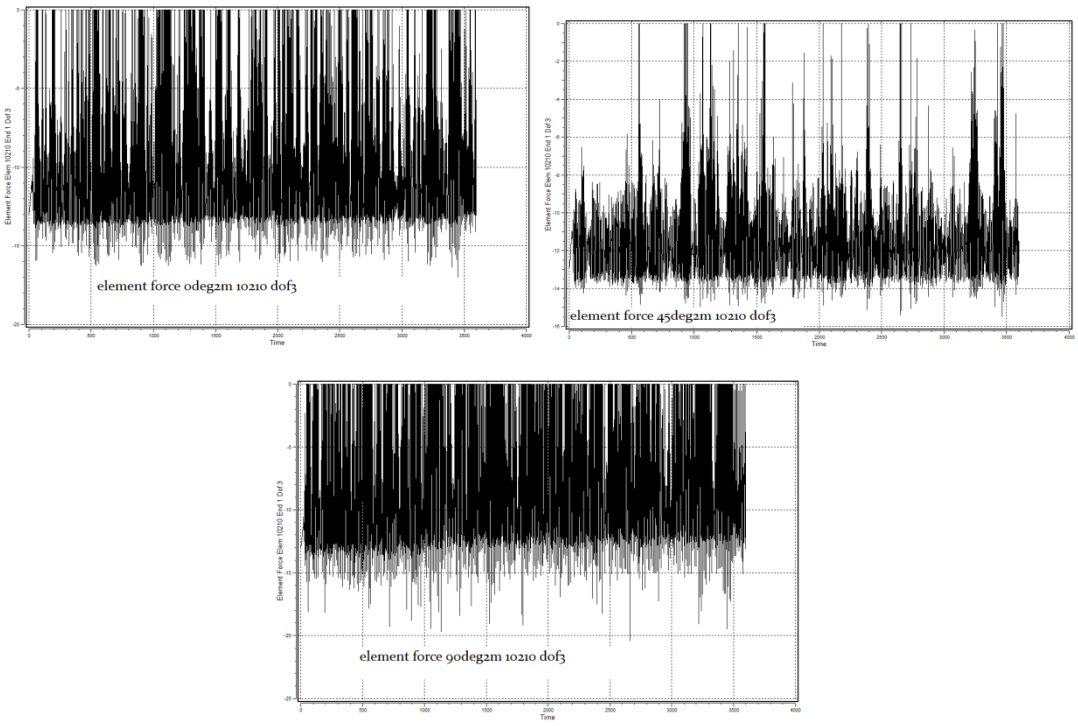

Figure 7.40 Element Force Element 10210 End 1 Dof3 for H_s=2m

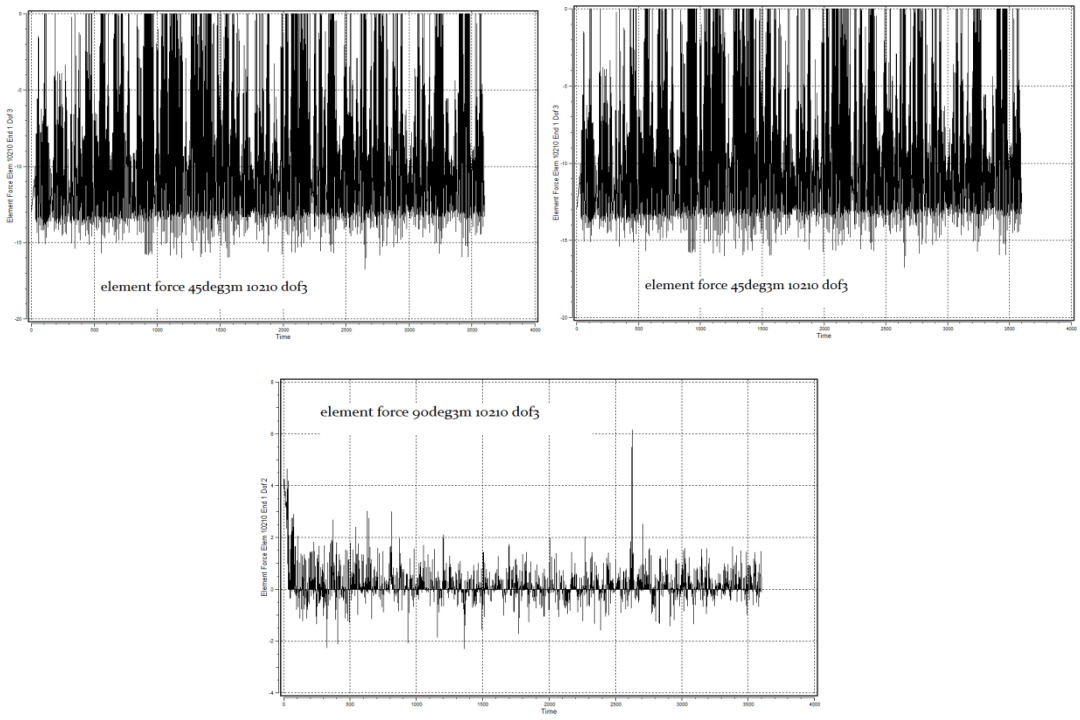

Figure 7.41 Element Force Element 10210 End 1 Dof3 for H_s=3m

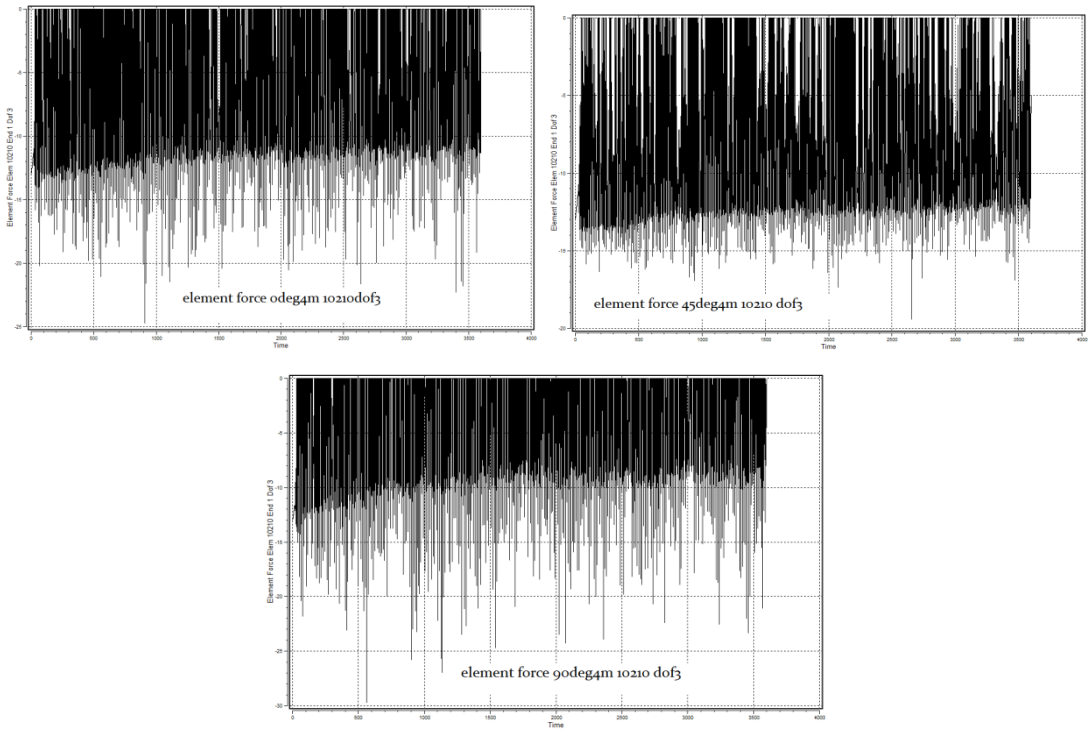

Figure 7.42 Element Force Element 10210 End 1 Dof3 for H_s=4m

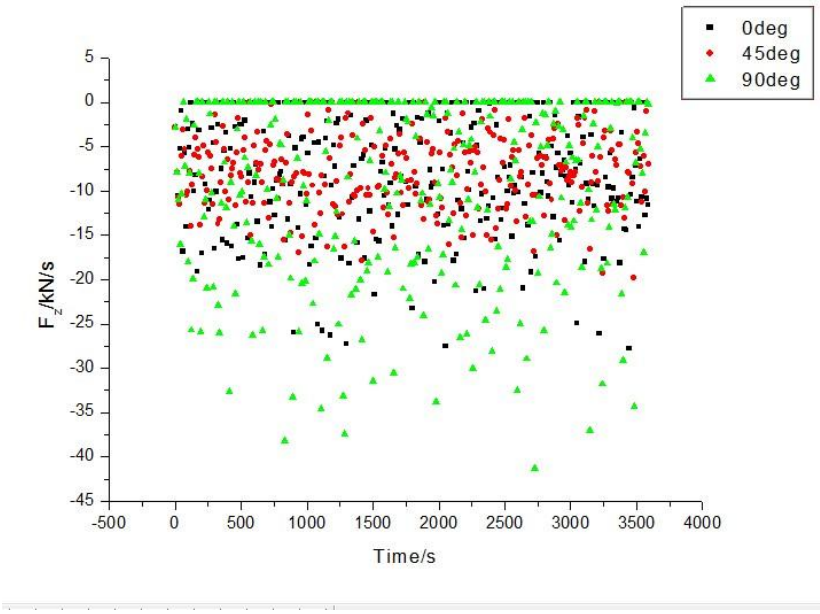

Figure 7.43 Element Force Element 10213 End 1 Dof3 for H_s=1m

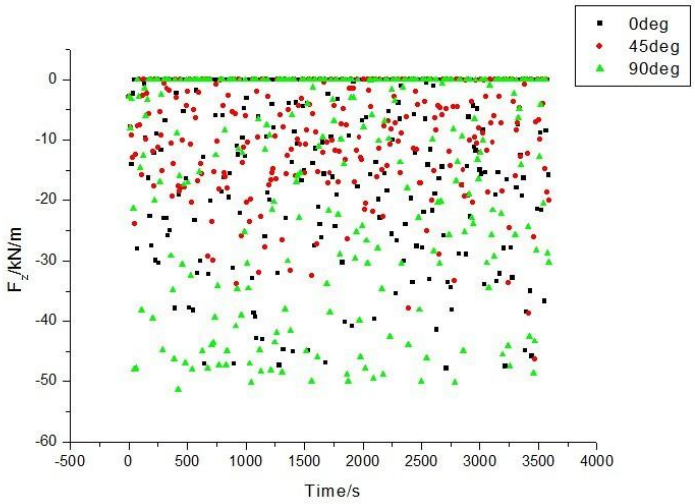

Figure 7.44 Element Force Element 10213 End 1 Dof3 for H_s=2m

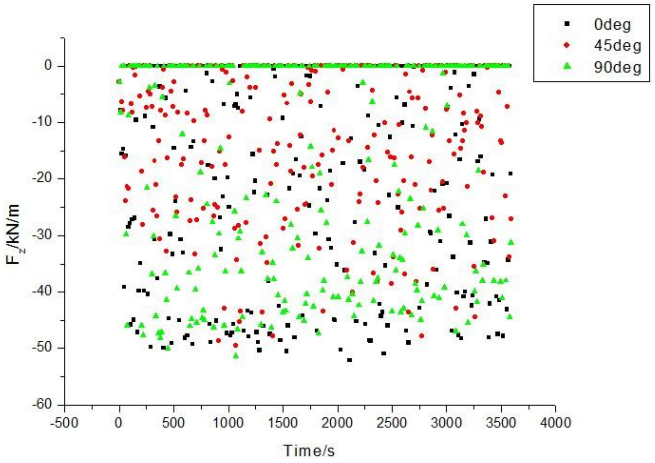

Figure 7.45 Element Force Element 10213 End 1 Dof3 for H_s=3m

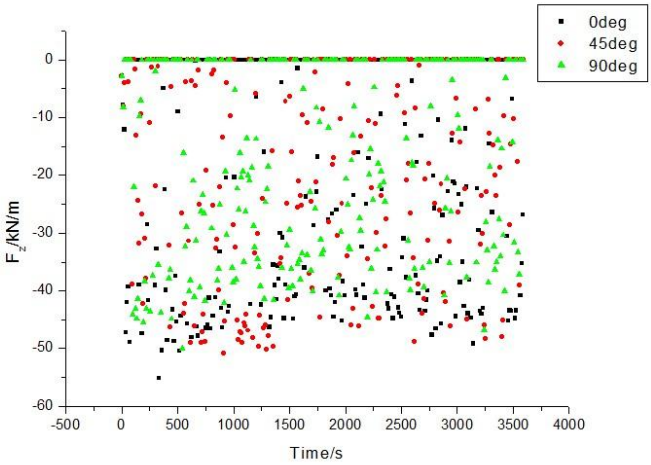

Figure 7.46 Element Force Element 10213 End 1 Dof3 for H_s=4m

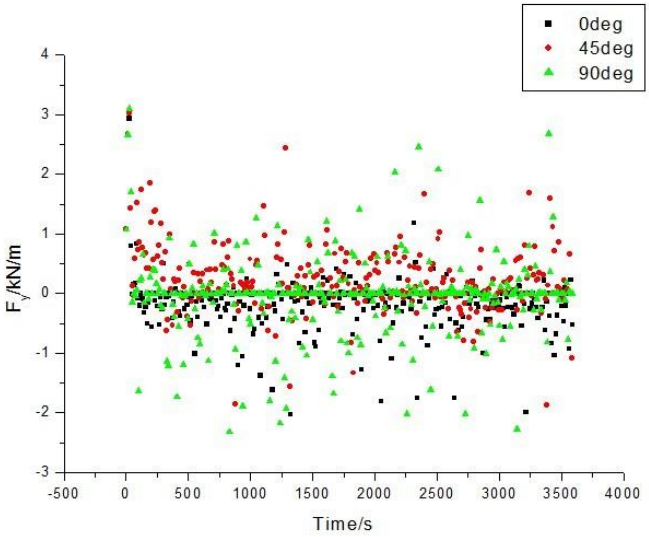

Figure 7.47 Element Force Element 10213 End 1 Dof2 for H_s=1m

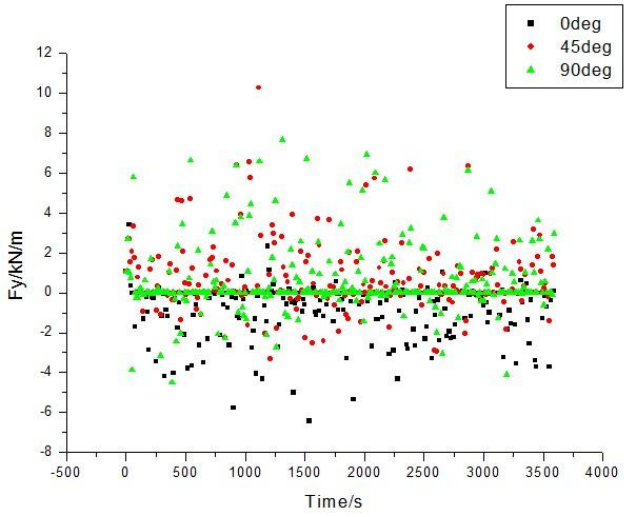

Figure 7.48 Element Force Element 10213 End 1 Dof2 for H_s=2m

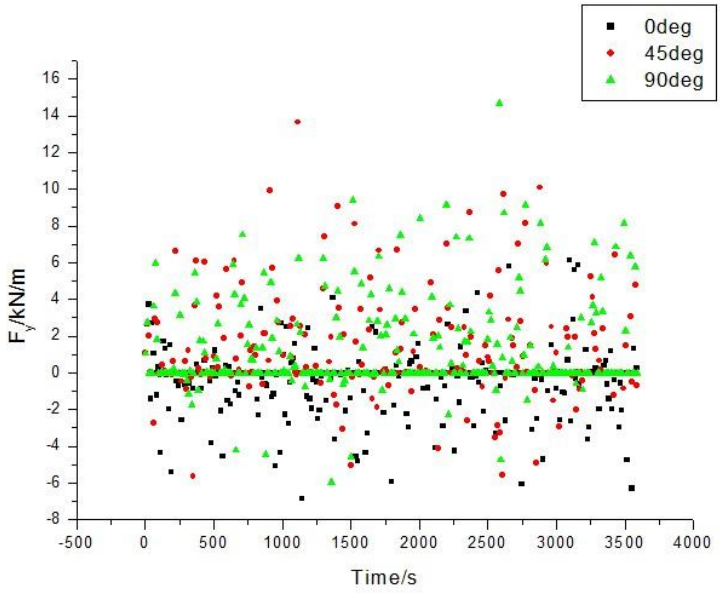

Figure 7.49 Element Force Element 10213 End 1 Dof2 for H_s=3m

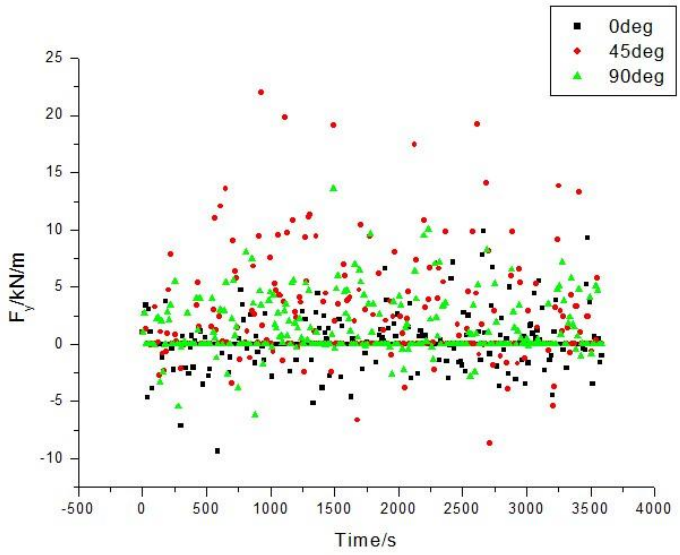

Figure 7.50 Element Force Element 10213 End 1 Dof2 for H_s=4m

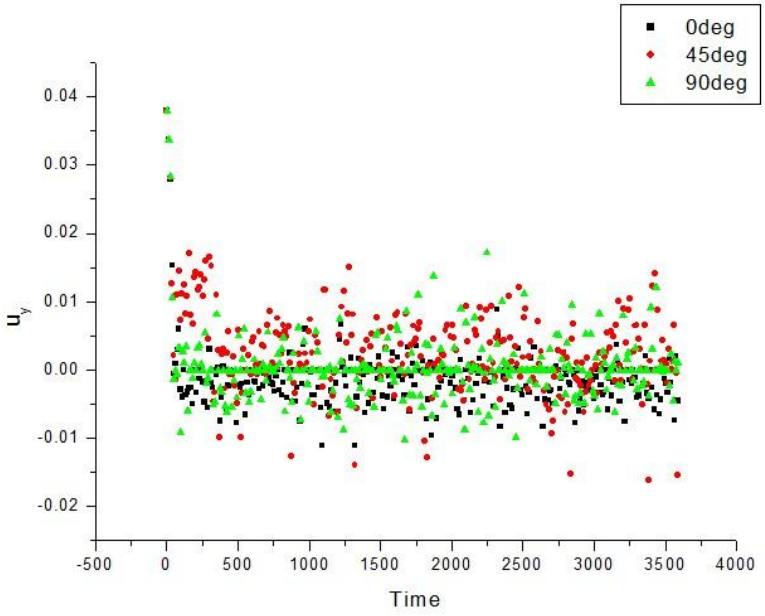

Figure 7.51 Element Force Element 10213 End 1 Dof2 for H_s=1m

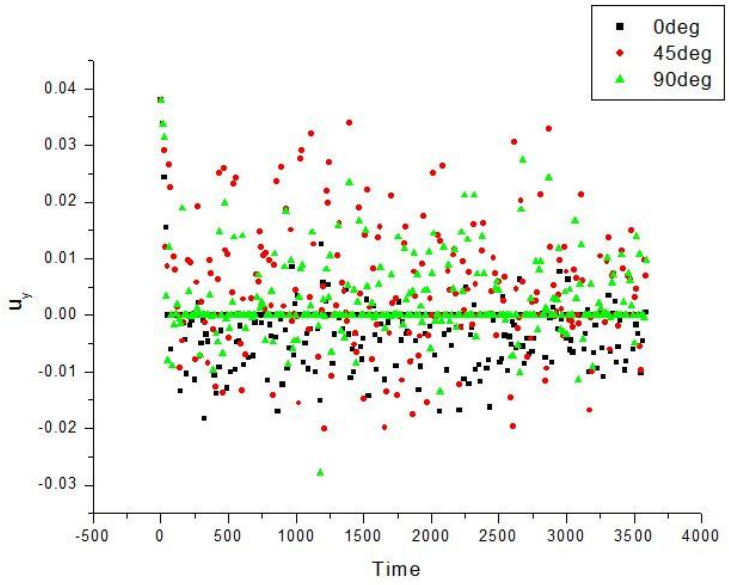

Figure 7.52 Element Displacement Element 10213 End 1 Dof2 for H_s=2m

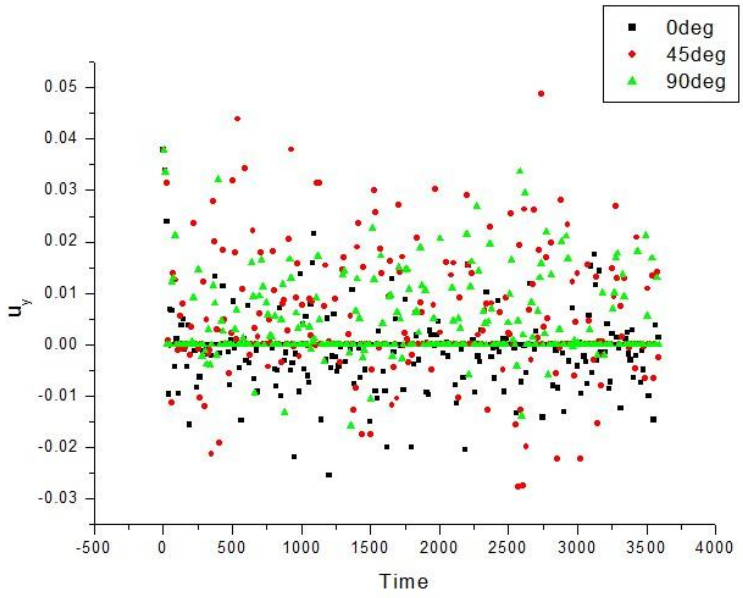

Figure 7.53 Element Displacement Element 10213 End 1 Dof2 for H_s=3m

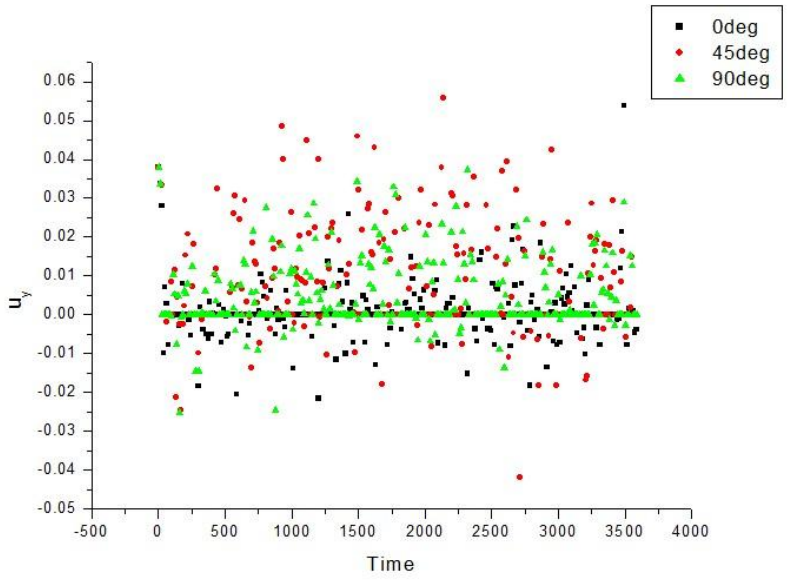

Figure 7.54 Element Displacement Element 10213 End 1 Dof2 for H_s=4m

Chapter 8 Conclusion

The purpose of the thesis is to try to give some information about the penetration of the pipeline during installation which may have large effect on the intervention work and cost impact. Thus, the dynamics at the touch down point (TDP) induced by 1st order motions from wave is of interest. It can perhaps explain the larger penetration than predicted behavior.

The thesis work focus on dynamic simulation of pipelines using the computer code. In order to get a comprehensive understanding of the problem, 4 sea states combined with 3 wave direction angles which in total, 12 different scenarios are studied in the thesis.

The wave direction angles have large effect on the vertical forces. It is very obvious that the vertical force is the largest for wave direction 90 deg, second for the 45 deg. As for 90 deg wave, the water particle velocity perpendicular to the pipeline is the largest compared to the other two cases. Then the lift force to the pipeline will be the largest. Thus the vertical force acts on the seabed will smallest as it equals the submerged weight of the pipeline minus the lift force.

The wave direction angles have small effect on the transverse force and displacement.

During the pipeline installation process, the pipeline keeps hitting and lifting off the seabed, which gives the seabed cyclic loading to the seabed resulting in larger penetration in the soil.

It is easy to understand that the more severe sea state, the more large response of the pipelines which therefore larger response on the seabed.

Recommendation for future work

This study is meant as an introduction investigation of the dynamics at the touch down point induced by 1st order motions from waves. A lot of simplifications have been made to easy the problem.

First, only the case for the installation using S-laying is studied here. It is also of interest to studying more cases using different pipeline installation methods to get a more overall understanding of the dynamics at the touch down point.

Second, a simple pipe-soil interaction model is used in this thesis. A pipeline moving cyclically accumulates penetration, which therefore results in an increased lateral soil resistance. So using the PONDUS pipe-soil interaction model will give a more robust result.

Reference

Bai, Yong and Bai, Qiang (2005): Subsea Pipelines and Risers.

Brennodden, H. (1991): Troll phase I- Verification of Expansion Curve Analysis and Consolidation Effects.

Brennodden, H., Sveggen, O., Wagner, D.A., Murff, J.D. (1986): Full Scale Pipe-Soil Interaction Tests.

Boyun Guo, Shanhong Song, Jacob Chacko, Ali Ghalambor (2005): Offshore Pipelines.

DNV (1998): Guideline No. 14- Free-Spanning Pipelines.

Egil Mollestad and Pål G. Bergan (1985): Nonlinear Dynamic Analysis of Submerged pipelines.

Fredsøe, B and Sumer,B.M. (1997): Hydrodynamics around Cylindrical Structures.

Gilbert Gedeon,P.E (2001): Brief Overview of Gulf of Mexico OCS Oil and Gas Pipelines: Installation, Potential Impacts, and Mitigation Measures.

H. Brennodden, J.T. Lieng, and T. Sotberg, SINTEF, and R.L.P. Verley, Statoil A/S (1989): An Energy-Based Pipe-Soil Interaction Model.

Hibbit, H. D., Marcal,P.V., and Rice, J.R. (1970): A Finite Element Formulation for Problems of Large Strain and Large Displacements.

Karal, K. (1977): Lateral Stability of Submarine Pipelines.

Lambe, W. and Whitman, R. (1969): Soil Mechanics.

Lambrakos, K. F. (1985): Marine Pipeline-Soil Friction Coefficients from In-Situ Testing.

Langen, I. and Sigbjørnsson, R. (1979): Dynamisk Analyse av Konstruksjoner. Lennon, G.P. (1985): Wave-induced Forces on Pipelines buried in permeable seabed.

Levold, E. (1990): Solid Mechanics and Material Models including Large Deformations, PhD thesis, NTH.

Lyons, C.G., (1973): Soil Resistance to Lateral Sliding of Marine Pipeline.

Magda, W. (1999): Wave-induced Cyclic Pore-pressure Perturbation Effects in Hydrodynamic Uplift Force Acting on Submarine Pipeline Buried on Seabed Sediments.

Mattiason,K. (1983): On the Co-rotational Finite Element Formulation for Large Deformation Problems. Technical Report Publication 83:1, Department of Structural Mechanics, Chalmers University of Technology.

McMeeking, R.M., Marcal, P.V., and Rice, J.R. (1975): Finite Element Formulations for Problems of Large Elastic-plastic deformation.

Morris, D.V., Webb, R.E., Dunlap, W.A. (1988): Self-Burial of Laterally Loaded Offshore Pipelines in Weak Sediments.

Ole, H. and Torsten, S. (2008): A 3D Elasto-Plastic Spring Element for Pipe-Soil Interaction Analysis.

Palmer, A.C., Steenfelt, J.S., Steensen Bach, J.O., and Jacobsen, V., (1988): Lateral Resistance of Marine Pipelines on Sand.

Spierenburg, S.E.J. (1986): Wave-induced Pore Pressures around Submarine Pipeline.

Svein Sævik (2008): SIMLA-Theory Manual. Marintek Report.

Svein Sævik, Ole David Økland, Gro Sagli Baarholm and Janne K.Ø. Gjøsteen (2010): SIMLA Version 3.13.0 User manual.

Søreide, T.H (1989): Lecture Notes on Analysis of Non-Linear Structures. Technical report, Norwegian Institute of Technology.

T.Moan (2003): Finite Element Modeling and Analysis of Marine Structures.

T.Moan and Svein Sævik (2009): Lecture Notes for Advanced Static analysis

Wagner, D.A., Murff, J.D., Brennodden, H., Sveggen, O. (1987): Pipe-Soil Interaction Model.

Appendix A

7.4 PONDUS Pipe-soil Interaction Model

The pipe soil interaction model implemented in the SIMLA also includes the model developed in the PONDUS program.

7.4.1 Definition of Forces

Fig. 7.2 shows the positive direction of the dynamic external forces per unit length acting on the submerged pipe.

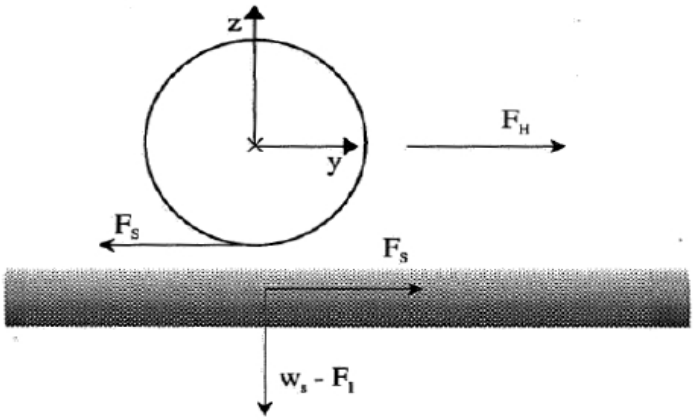

Figure 7.2: External forces per unit length.

Forces per unit length:

- lift force
- horizontal hydrodynamic force
- submerged weight
- soil force

Elastic or Plastic Soil Force

The pipe displacement may be expressed as a sum of the elastic and plastic displacement of soil material:

$$v = v_e + v_p, \tag{7.23}$$

where e_p is elastic displacement and e_p is plastic displacement. In the elastic range the soil force is expressed as:

$$F_s = k_s v_e + \alpha_s k_s \dot{v}, \tag{7.24}$$

where k_s is elastic soil stiffness (per unit length) and α_s is a soil damping constant. The damping force is included only in the linear range to damp out transient oscillations in the elastic soil displacement.

The inclusion of this damping force is because there will be some material damping even in the linear range the transient oscillations may otherwise in some cases dominate in the linear range

In the plastic range the soil force is expressed as a sum of a friction type force and a soil remaining force as follows:

$$\begin{aligned} F_s &= F_f + F_r \\ F_f &= \mu \left(w_s - \hat{F}_l \right) \frac{\dot{v}}{|\dot{v}|} \\ F_r &= D_s \frac{\dot{v}}{|\dot{v}|} \end{aligned} \tag{7.25}$$

where *min* is a function selecting the smallesr of its arguments, μ is the constant friction coefficient and D_s is the remaining force function.

$$\hat{F}_l = \begin{cases} F_l & \text{when } F_l < w_s \\ w_s & \text{when } F_l \geq w_s \end{cases} \tag{7.26}$$

Moreover we limit the range of the formulas, in the sense that $F_s = 0$ whenever:

$$\mu \left(w_s - \hat{F}_l \right) + D_s \leq 0 \tag{7.27}$$

The remaining force function may be a function of the plastic displacement and the number of oscillations and is also a function of the lift force.

The transition from elastic to plastic range is defined to take place when (damping force neglected):

$$|k_s v_e| = \left[\mu\left(w_s - \hat{F}_l\right) + D_s\right] \tag{7.28}$$

and the transition from plastic to elastic range is defined to occur when the pipe velocity changes sign, that is when $\dot{v} = 0$.

The elastic displacement corresponding to the total soil force is found as

$$v_e|_{\text{at } \dot{v}=0} = \frac{1}{k_e} F_s \text{ (plastic)} \tag{7.29}$$

Incremental Soil Force

In the elastic range the incremental form of the soil force is equal to

$$\Delta F_s = k_s \Delta v_e \alpha_s k_s \Delta \dot{v}, \tag{7.30}$$

and in the plastic range

$$\Delta F_s = \left[\mu\left(\Delta w_s - \Delta \hat{F}_l\right) + \Delta D_s\right] \frac{\dot{v}}{|\dot{v}|} \tag{7.31}$$

The remaining force function, D_s is defined to be a time dependent function of the plastic soil displacement only and the increment of the remaining force may then be expressed by the increment of the plastic displacement.

$$\Delta D_s = \frac{\partial D_s}{\partial v_p} v_p \tag{7.32}$$

The incremental plastic displacement may be expressed as the difference between the total displacement and the elastic contribution

$$\Delta v_p = \Delta v - \frac{1}{k_s} \Delta F_s \tag{7.33}$$

where the elastic term correspond to a change in the elastic displacement from any change in the magnitude of the soil force.

Inserting Eq. (7.33) and Eq. (7.32) into Eq. (7.31) gives the following result for the incremental soil force in the plastic range:

$$\Delta F_s = \frac{f}{1+f}\left(k_s \Delta v + \mu\left(\Delta w_s - \Delta \hat{F}_l\right) \frac{\dot{v}}{|\dot{v}|}\right) \tag{7.34}$$

where

$$f = \frac{\partial D_s}{\partial v_p}\frac{1}{k_s} \qquad (|f| > 1 \tag{7.35}$$

The slope of the remaining force function may be both positive and negative.

7.4.2 Pipe-Sand Model

The recommended model specifically developed for sand soils , is based on empirical equations which are fitted to large scale laboratory data from several sources. The development of penetration is described considering the work done by the pipe on the soil. The model applicability is limited to outer diameter of tube, $d_h > 0.1$ m, which applies for most cases.

The total soil force in the plastic range is expressed as (see Section 7.4.1):

$$\begin{aligned} |F_s| &= \mu\,(w_s - f_l) + F_r \qquad & w_s \geq F_l \\ |F_s| &= F_r & w_s < F_l \end{aligned} \tag{7.36}$$

The first term is related to pure friction resistance, whereas f_r is resistance due to pipe penetration. In the following, the penetration dependent function, F_r, is considered.

The soil force in the plastic range is computed in two steps; first the pipe penetration due to pipeline movement, and then the corresponding force-displacement curve.

Fig. 7.3 shows the shape chosen for the force-displacement curve for the penetration dependent force defined through the force levels F_{r1}, F_{r2} and F_{r3} and corresponding displacements y_1, y_2 and y_3.

For movements within 0 and y_1, the resistance is linearly elastic and no work is done. The pipe penetration does not change nor does the origin move. The distance y_1 is determined from the elastic stiffness of the soil and the force level F_{r1} which is taken as 30% of F_{r2}.

Initial penetration z_i for the pipe due to weight, w_s, is given by:

$$\frac{z_i}{d_h} = 0.037\kappa_0^{-\frac{2}{3}} \tag{7.37}$$

where

$$\kappa_0 = \frac{\gamma_s d_h^2}{w_s} \tag{7.38}$$

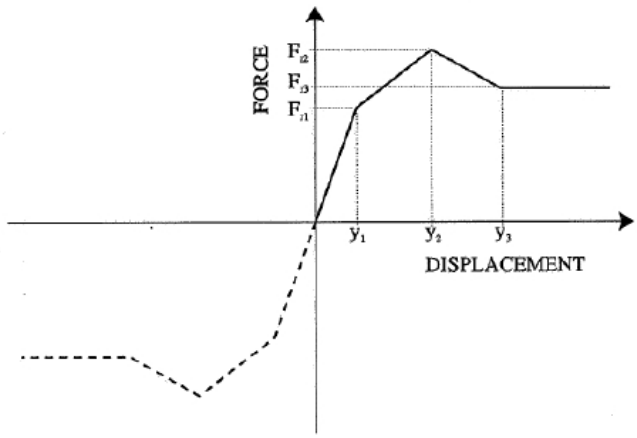

Figure 7.3: Force-displacement model.

where γ_s is submerged unit weight of soil and d_h is hydrodynamic diameter (outer diameter of coating).

The model is based on an empirical relation between the development of pipe penetration as a function of the work done by pipe-soil interaction. This relation is given as:

$$\frac{z_2 - z_i}{d_h} = 0.23 \left(\xi \kappa_i^{-1} \left(\frac{y}{d_h} \right)^{-\frac{1}{2}} \right)^{0.31} \tag{7.39}$$

$$\left(\frac{z_2 - z_i}{d_h} \right)_{max} = 1.0 \left(\frac{y}{d_h} \right)^{-\frac{1}{2}} \kappa_i^{-\frac{1}{2}} \tag{7.40}$$

where

$$\xi = \frac{E}{\gamma_s d_h^3}, \qquad E(t) = \int_0^t F_r ds \qquad \text{and} \qquad \kappa_i = \frac{\gamma_s d_h^2}{F_{ci}}$$

where y is the instantaneous distance of pipe from the origin (defined in the model, see later and F_{ci} is the value of the vertical soil contact force at the instant of maximum horizontal soil resistance, F_{r2}

Between y_1 and y_2, the displacement corresponds to the maximum resistance F_{r2} which is given as:

$$\frac{F_{r2}}{\gamma_s d_h^2} = (5.0 - 0.15\kappa_i)\left(\frac{z_2}{d_h}\right)^{1.25} \qquad \kappa_i \leq 20 \tag{7.41}$$

$$\frac{F_{r2}}{\gamma_s d_h^2} = 2.0\kappa_i\left(\frac{z_2}{d_h}\right)^{1.25} \qquad \kappa_i > 20$$

Where z_2 is the reference penetration for break-out (maximum pre-break-out penetration) The increasing penetration causes the force level F_{r2} to increase.

For displacements $y > y_2$, the origin is translated a distance $(y - y_2)$ and the penetration decreases until $y = y_3$, after which it remains constant.

If the pipe section continues to move in the same direction after break-out, there is a horizontal resistance (in addition to the friction) due to a mount of soil being pushed ahead of the pipe. The residual force, F_{r3}, will have an effect on how far a pipe section will move after break-out whilst pipe motion is still in the same direction.

Through the expression for F_{r2}, F_{r3} is expressed as an equivalent penetration after break-out, z_3, which is given as:

$$\frac{z_3}{\overset{*}{z_2}} = 0.82 - 3.2\left(\frac{\overset{*}{z_3}}{d_h}\right) \qquad \left(\frac{\overset{*}{z_2}}{d_h}\right) \leq 0.1 \tag{7.42}$$

$$\frac{z_3}{\overset{*}{z_2}} = 0.5 \qquad \left(\frac{\overset{*}{z_2}}{d_h}\right) > 0.1 \tag{7.43}$$

where $\overset{*}{z_2}$ is the maximum value of $z_2$found in simulation up to the instant time considered.

The model modifies the nominal penetration, z_2, as the pipe moves from the position associated with z_2 to that associated with z_3. Therefore, z_2 in the above expression is replaced by $\overset{*}{z_2}$, the maximum penetration z_2 realised in the simulation up to the instant of time considered.

During simulation, the model may go through many force-displacement cycles of different amplitude. Fig. 7.4 indicates a cycle of amplitude greater than y_2 causing both the force level F_{r2} (and therefore F_{r1} and F_{r3}) to decrease and the origin to move.

The displacement y_2, for which maximum break-out force F_{r2} occurs, is set to $0.5d_h$. The value of y_3, i.e. where the resistance force becomes stable after break-out is taken as:

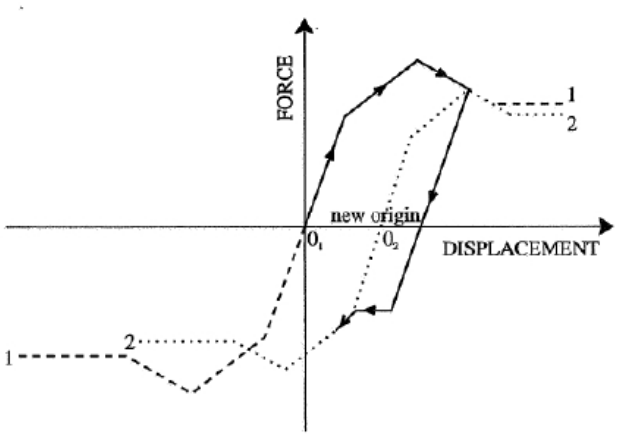

Figure 7.4: Force-displacement cycle with amplitude $> y_2$.

$$\frac{y_3}{d_h} = \frac{y2}{d_h} + 0.1 + 3.3\frac{\overset{*}{z}_2}{d_h} \qquad \frac{\overset{*}{z}_2}{d_h} \leq 0.15 \tag{7.44}$$

$$\frac{y_3}{d_h} = \frac{y2}{d_h} + 0.1 + 0.6 \qquad \frac{\overset{*}{z}_2}{d_h} > 0.15 \tag{7.45}$$

$$\tag{7.46}$$

Pipe-Clay Model

As for sand model, the total soil force in the plastic range is expressed as, see Eq. (7.36):

$$|F_s| = \mu\,(w_s - f_l) + F_r \qquad w_s \geq F_l$$
$$|F_s| = F_r \qquad w_s < F_l$$

The first term is related to pure friction resistance, whereas f_r is resistance due to pipe penetration. In the following, the penetration dependent function, F_r, is considered.

The soil force in the plastic range is computed in two steps; first the pipe penetration due to pipeline movement, and then the corresponding force-displacement curve.

Fig. 7.3 shows the shape chosen for the force-displacement curve for the penetration dependent force defined through the force levels F_{r1}, F_{r2} and F_{r3} and corresponding displacements y_1, y_2 and y_3.

For movements within 0 and y_1, the resistance is linearly elastic and no work is done.

The pipe penetration does not change nor does the origin move. The distance y_1 is determined as a function of pipe outer diameter:

$$y_1 = 0.02 d_h \tag{7.47}$$

Initial penetration z_i for the pipe due to self weight, w_s, is given by:

$$\frac{z_i}{d_h} = 0.0071 \left(S\, G^{0.3}\right)^{3.2} + 0.062 \left(S\, G^{0.3}\right)^{0.7} \tag{7.48}$$

where

$$G = \frac{S_u}{d_h \gamma_s} \qquad S = \frac{w_s}{d_h\, S_u}$$

where w_s is submerged weight of pipe, S_u is remoulded undrained shear strength of soil, γ_s is submerged unit weight of soil and d_h is the hydrodynamic diameter (outer diameter of coating)

The maximum break-out force corresponding to a given pipe penetration z is taken as:

$$F_{r2} = 4.13 d_h\, S_u\, G^{-0.392} \left(\frac{z}{d_h}\right)^{1.31} \tag{7.49}$$

where z is penetration of pipe into soil. The displacement y_2, for which maximum break-out force F_{r2} occurs, is set to $0.5 d_h$.

The relation between pipe penetration and the work (energy) is given by:

$$\frac{z2}{d_h} = 0.012 \xi^{0.32}\, S^{0.637} \left(\frac{a}{d_h}\right)^{-0.25} \qquad \frac{a}{d_h} \geq 0.05 \tag{7.50}$$

If the factor $\frac{a}{d_h}$ is less than 0.05, it is adjusted to have the value 0.05.

$$\xi = \frac{E}{S_u\, d_h^2}$$

a is pipe oscillation amplitude (1/2 cycle) and E is energy (work) done by pipe on soil:

$$E(t) = \int_0^t F_r\, ds \tag{7.51}$$

$$\begin{aligned} \left(\frac{z_2}{d_h}\right)_{max} &= S\, G^{0.4} \left(\frac{a}{d_h}\right)^{0.2} && \frac{z_2}{d_h} \leq 0.5 \quad \frac{a}{d_h} \geq 0.05 \\ \left(\frac{z_2}{d_h}\right)_{max} &= 0.5 && \frac{z_2}{d_h} > 0.5 \end{aligned} \tag{7.52}$$

The increasing penetration causes the force level F_{r2} to increase.

For displacements $y > y_2$, the origin is translated a distance $y - y_2$ and the penetration decreases until $y = y_3$, after which it remains constant.

If the pipe section continues to move in the same direction after break-out, there is a horizontal resistance (in addition to the friction) due to a mount of soil being pushed ahead of the pipe. The residual force, F_{r3}, will have an effect on how far a pipe section will move after break-out whilst pipe motion is still in the same direction.

Through the expression for ůF_{r2}, F_{r3} is expressed as an equivalent penetration after break-out, z_3, which is obtained using equation , using the actual vertical force F_v as the submerged weight w_s.

The model modifies the nominal penetration, z_2, as the pipe moves from the position associated with z_2 to that associated with z_3. Therefore z_2 in the above expression is replaced by z_2^*, the maximum penetration z_2 realised in the simulation up to the instant of time considered.

The point y_3 is determined through the expression:

$$\frac{y_3}{d_h} = 0.6\left(\frac{5.5}{k} + 1\right) + \frac{y_2}{d_h} \tag{7.53}$$

7.5 Material model for concrete coating element

Two material models are required for the finite element:

- A non-linear shear interaction model capturing cyclic material model effects for the corrosion coating applied between the pipe and the concrete coating.
- A model capturing the cyclic non-linear material behaviour for the concrete coating.

Both material models have been based on adopting the concepts described by (Levold, 1990). The stick-slip behaviour governing the corrosion coating is handled by applying an elastoplastic model. The concrete coating is treated by modifying the elastoplastic model so that it behaves elastoplastic on the compressive side, but hyper-elastic in tension. This requires one extra parameter, ϵ_0, to keep track of when tensile stresses are to occur, see Fig. 7.5. It is well known that concrete looses its tensile strength for small loads. This behaviour is simulated by applying a very small stiffness on the tensile side, sufficient to improve numerical stability, but without influencing the results which is primarily governed by the compressive capacity of the concrete.

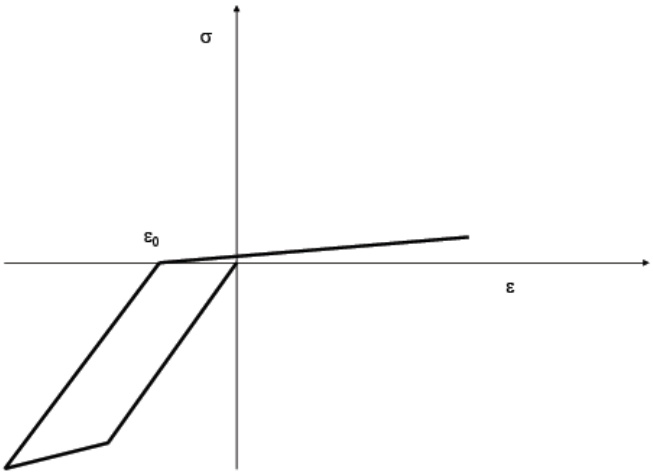

Figure 7.5: Applied material model for concrete coating element

7.6 2D Iso-Friction Material

7.6.1 Normal direction

The stiffness in the $\mathbf{n}_3$ direction during contact is governed by application of the penalty parameter k taken to be constant or variable according to a hyper-elastic material law.

7.6.2 Tangential direction

With respect to the tangential directions a model including isotropic friction and visco-elasticity has been developed based on the same principles as described by (Shyu et al., 1988), (Michalowski and Mroz, 1978) and (Meyer et al., 1992) and as described below.

Friction model

The constitutive relation used to model the components of friction is established based on the same principles as applied for material plasticity, see (Levold, 1990). It consists of two major ingredients:

- A friction surface
- A slip rule

The constitutive model used is established based on including material hardening to improve numerical stability. The friction surface is assumed to be a function of the contact normal force F_3, the bi-directional force components F_1, F_2 and the friction coefficient μ:

$$f_s = f_s\left(F_3, F_2, F_1, \mu\right) \tag{7.54}$$

Assuming a linear surface, we have:

$$f_s = \sqrt{F_1^2 + F_2^2} - \mu F_3 = \bar{F} - F_f = 0 \tag{7.55}$$

The slip increment is divided into two parts:

$$\Delta\gamma = \Delta\gamma_e + \Delta\gamma_p \tag{7.56}$$

where $\Delta\gamma_e$ is the 2-dimensional increment of elastic slip and $\Delta\gamma_p$ is the corresponding increment of plastic slip. Assuming symmetry, i.e. an associative slip rule, the following slip rule is postulated:

$$\Delta\gamma_p = \Delta\lambda\nabla_F\bar{F} \tag{7.57}$$

and also:

$$\Delta\bar{\gamma}_p = \Delta\lambda\sqrt{\nabla_F\bar{F}\nabla_F\bar{F}} \tag{7.58}$$

where λ is a still unknown proportional constant. The proportional constant is determined from the consistency condition:

$$d\mathbf{f}_s = \nabla_F\bar{F} : \Delta\mathbf{F} - \mu\Delta F_3 - \Delta\lambda F_3\frac{\partial\mu}{\partial\bar{\gamma}_p}\sqrt{\nabla_F\bar{F} : \nabla_F\bar{F}} = 0 \tag{7.59}$$

where the last term is associated with the variable friction coefficient. The expressions are further developed by defining the hardening parameter ψ as:

$$\frac{\partial\mu}{\partial\bar{\gamma}_p} = \psi \tag{7.60}$$

and introducing the elastic incremental material law:

$$\Delta\mathbf{F} = \mathbf{C}_e : \Delta\gamma_e = \mathbf{C}_e : (\Delta\gamma - \Delta\gamma_p) \tag{7.61}$$

where $\mathbf{C}_e$ is the elastic material law governing prior to plastic slip. By combining the above equations, the following incremental constitutive relation is obtained for the isotropic friction effect:

$$\begin{bmatrix} \Delta F_1 \\ \Delta F_2 \end{bmatrix} = E\begin{bmatrix} 1 - \frac{F_1^2}{F^2(1+\psi F_3/E)} & -\frac{F_1F_2}{F^2(1+\psi F_3/E)} \\ -\frac{F_1F_2}{F^2(1+\psi F_3/E)} & 1 - \frac{F_2^2}{F^2(1+\psi F_3/E)} \end{bmatrix}\begin{bmatrix} \Delta\gamma_1 \\ \Delta\gamma_2 \end{bmatrix} + k\mu\begin{bmatrix} \frac{F_1}{F(1+\psi F_3/E)} \\ \frac{F_2}{F(1+\psi F_3/E)} \end{bmatrix}\Delta g \tag{7.62}$$

where it is noted that the classical Coulomb friction model is obtained by setting ψ equal to zero.

Visco-elastic model

In addition visco-elastic surface interaction is allowed for by including the following velocity dependent terms in the dynamic equilibrium equation:

$$\begin{bmatrix} F_1 \\ F_2 \end{bmatrix}_i = \begin{bmatrix} |\dot{\bar{\gamma}}|^{p-1}\dot{\bar{\gamma}}\frac{\gamma_1}{|\bar{\gamma}|} & |\dot{\bar{\gamma}}|^{p-1}\dot{\bar{\gamma}}\frac{\gamma_2}{|\bar{\gamma}|} \\ |\dot{\bar{\gamma}}|^{p-1}\dot{\bar{\gamma}}\frac{-\gamma_1}{|\bar{\gamma}|} & |\dot{\bar{\gamma}}|^{p-1}\dot{\bar{\gamma}}\frac{\gamma_2}{|\bar{\gamma}|} \end{bmatrix} \tag{7.63}$$

where c is the visco-elastic damping coefficient, p is the exponent starting at 1 and:

$$\bar{\gamma} = \sqrt{\gamma_1^2 + \gamma_2^2} \tag{7.64}$$

Appendix B

```
# Dynamical Analysis Model
HEAD This is a S-lay test example for a 32 " pipe at 200-300 m water depth
HEAD Irregular wave H=4m T = 10s - Elastic & elastoplastic material model - 500 pipe element
#
#-------------------------------------------------------------------------
--------
# Control data:
#-------------------------------------------------------------------------
--------
#              maxit   ndim  isolvr  npoint  ipri   conr    gacc      iproc
CONTROL        50       3      1        16     1     1e-5      9.81      restart  1
#             imass    alpha1   alpha2       alfa
DYNCONT     1          0.0      0.095       -0.05
#
# visual results
#
VISRES   integration  1  sigma-xx
# Dynamic Plots
DYNRES_N      1  3001  1
DYNRES_N      1  3001  2
DYNRES_N      1  3001  3
DYNRES_N      1  3001  4
DYNRES_N      1  3001  5
DYNRES_N      1  3001  6
DYNRES_N      1  224  1
DYNRES_N      1  224  2
DYNRES_E      2  2303    1   3
DYNRES_E      2  2304    1   3
DYNRES_E      2  2305    1   3
DYNRES_E      2  2306    1   3
DYNRES_E      2  2307    1   3
DYNRES_E      2  2308    1   3
```

Hong, Wei

```
DYNRES_E      2  2309     1   3
DYNRES_E      2  2310     1   3
DYNRES_E      2  2311     1   3
DYNRES_E      2  2401     1   3
DYNRES_E      2  2402     1   3
DYNRES_E      2  2403     1   3
DYNRES_E      2  2404     1   3
DYNRES_E      1  3000     1   1
DYNRES_E      2  3000     1   1
DYNRES_E      2  500      2   1
DYNRES_I      1  449      1  9
#
DYNRES_E      1  10201    1   2
DYNRES_E      1  10202    1   2
DYNRES_E      1  10203    1   2
DYNRES_E      1  10204    1   2
DYNRES_E      1  10205    1   2
DYNRES_E      1  10206    1   2
DYNRES_E      1  10207    1   2
DYNRES_E      1  10208    1   2
DYNRES_E      1  10209    1   2
DYNRES_E      1  10210    1   2
DYNRES_E      1  10211    1   2
DYNRES_E      1  10212    1   2
DYNRES_E      1  10213    1   2
DYNRES_E      1  10214    1   2
DYNRES_E      1  10215    1   2
DYNRES_E      1  10216    1   2
DYNRES_E      1  10217    1   2
DYNRES_E      1  10218    1   2
DYNRES_E      1  10219    1   2
DYNRES_E      1  10220    1   2
DYNRES_E      1  10221    1   2
DYNRES_E      1  10222    1   2
DYNRES_E      1  10223    1   2
DYNRES_E      1  10224    1   2
##
DYNRES_E      2  10201    1   2
DYNRES_E      2  10202    1   2
DYNRES_E      2  10203    1   2
DYNRES_E      2  10204    1   2
DYNRES_E      2  10205    1   2
```

Hong, Wei

```
DYNRES_E      2  10206    1   2
DYNRES_E      2  10207    1   2
DYNRES_E      2  10208    1   2
DYNRES_E      2  10209    1   2
DYNRES_E      2  10210    1   2
DYNRES_E      2  10211    1   2
DYNRES_E      2  10212    1   2
DYNRES_E      2  10213    1   2
DYNRES_E      2  10214    1   2
DYNRES_E      2  10215    1   2
DYNRES_E      2  10216    1   2
DYNRES_E      2  10217    1   2
DYNRES_E      2  10218    1   2
DYNRES_E      2  10219    1   2
DYNRES_E      2  10220    1   2
DYNRES_E      2  10221    1   2
DYNRES_E      2  10222    1   2
DYNRES_E      2  10223    1   2
DYNRES_E      2  10224    1   2
##
DYNRES_E      2  10201    1   3
DYNRES_E      2  10202    1   3
DYNRES_E      2  10203    1   3
DYNRES_E      2  10204    1   3
DYNRES_E      2  10205    1   3
DYNRES_E      2  10206    1   3
DYNRES_E      2  10207    1   3
DYNRES_E      2  10208    1   3
DYNRES_E      2  10209    1   3
DYNRES_E      2  10210    1   3
DYNRES_E      2  10211    1   3
DYNRES_E      2  10212    1   3
DYNRES_E      2  10213    1   3
DYNRES_E      2  10214    1   3
DYNRES_E      2  10215    1   3
DYNRES_E      2  10216    1   3
DYNRES_E      2  10217    1   3
DYNRES_E      2  10218    1   3
DYNRES_E      2  10219    1   3
DYNRES_E      2  10220    1   3
DYNRES_E      2  10221    1   3
DYNRES_E      2  10222    1   3
```

```
DYNRES_E     2  10223    1   3
DYNRES_E     2  10224    1   3
##
ENVRES_N  1   1    501  1  1
ENVRES_N  1   1    501  2  1
ENVRES_N  1   1    501  3  1
ENVRES_E  2   2301  2314  1  3  1
ENVRES_E  2   10001  10400  1  3  1
ENVRES_E  2   10001  10400  1  2  1
ENVRES_E  2   10001  10400  1  1  1
ENVRES_E  2   1    500  2  1  1
ENVRES_E  2   1    500  2  5  1
ENVRES_E  3   1    500  1  2  1
#
#-------------------------------------------------------------------------
--------
#  Units  used  (for  correct  display  in  plots)
#
#          mass      length    time
UNITS     1.0e-3   1.0       1.0
#-----------------------------------------------------------------
#  Analysis  time  control:
#-----------------------------------------------------------------
#           t     dt    dtvi  dtdy      dt0    type      hla?
TIMECO     1.0   1.0   1.0     1.0    201.0   STATIC    NOHLA
TIMECO   360.0   0.10  1.0   1.0     201.0   DYNAMIC  NOHLA  auto     none     all      20       5
1.0e-4
TIMECO     3600.0    0.10  10.0   1.0     201.0   DYNAMIC  NOHLA  auto     none     all      20
5          1.0e-4
#
#-------------------------------------------------------------------------
--------
#  Nocoor  input
#-------------------------------------------------------------------------
--------
#
#         no         x      y          z
NOCOOR  coordinates   1      0     0     10
21    192.5983199    0    10
41    370.3978694 0     10
61    534.5357488 0     10
81    686.0616864 0     10
```

101	825.9447521	0	10
121	955.0795549	0	10
141	1074.291964	0	10
161	1184.344392	0	10
181	1285.940668	0	10
201	1379.730542	0	10
202	1384.226079	0	10
203	1388.703682	0	10
204	1393.163421	0	10
205	1397.605367	0	10
206	1402.029593	0	10
207	1406.436168	0	10
208	1410.825163	0	10
209	1415.196647	0	10
210	1419.550692	0	10
211	1423.887366	0	10
212	1428.206739	0	10
213	1432.50888	0	10
214	1436.793857	0	10
215	1441.061739	0	10
216	1445.312595	0	10
217	1449.546491	0	10
218	1453.763497	0	10
219	1457.963678	0	10
220	1462.147103	0	10
221	1466.313838	0	10
222	1470.463949	0	10
223	1474.597504	0	10
224	1478.714568	0	10
225	1482.815207	0	10
226	1486.899486	0	10
227	1490.96747	0	10
228	1495.019226	0	10
229	1499.054817	0	10
230	1503.074308	0	10
231	1507.077763	0	10
232	1511.065246	0	10
233	1515.036821	0	10
234	1518.992551	0	10
235	1522.9325	0	10
236	1526.85673	0	10
237	1530.765305	0	10

238	1534.658286	0	10
239	1538.535736	0	10
240	1542.397717	0	10
241	1546.244291	0	10
242	1550.075518	0	10
243	1553.891461	0	10
244	1557.69218	0	10
245	1561.477736	0	10
246	1565.248189	0	10
247	1569.0036	0	10
248	1572.744029	0	10
249	1576.469536	0	10
250	1580.180179	0	10
251	1583.876018	0	10
252	1587.557113	0	10
253	1591.223523	0	10
254	1594.875305	0	10
255	1598.512518	0	10
256	1602.13522	0	10
257	1605.74347	0	10
258	1609.337324	0	10
259	1612.916841	0	10
260	1616.482077	0	10
261	1620.033089	0	10
262	1623.569935	0	10
263	1627.09267	0	10
264	1630.601351	0	10
265	1634.096035	0	10
266	1637.576776	0	10
267	1641.043631	0	10
268	1644.496654	0	10
269	1647.935902	0	10
270	1651.361429	0	10
271	1654.773289	0	10
272	1658.171538	0	10
273	1661.55623	0	10
274	1664.927418	0	10
275	1668.285157	0	10
276	1671.6295	0	10
277	1674.960501	0	10
278	1678.278212	0	10
279	1681.582688	0	10

280	1684.87398	0	10
281	1688.152142	0	10
282	1691.417225	0	10
283	1694.669282	0	10
284	1697.908365	0	10
285	1701.134526	0	10
286	1704.347816	0	10
287	1707.548286	0	10
288	1710.735988	0	10
289	1713.910973	0	10
290	1717.07329	0	10
291	1720.222992	0	10
292	1723.360128	0	10
293	1726.484749	0	10
294	1729.596903	0	10
295	1732.696642	0	10
296	1735.784014	0	10
297	1738.859069	0	10
298	1741.921856	0	10
299	1744.972424	0	10
300	1748.010822	0	10
301	1751.037097	0	10
302	1754.0513	0	10
303	1757.053477	0	10
304	1760.043677	0	10
305	1763.021948	0	10
306	1765.988337	0	10
307	1768.942891	0	10
308	1771.885658	0	10
309	1774.816685	0	10
310	1777.736018	0	10
311	1780.643705	0	10
312	1783.539791	0	10
313	1786.424323	0	10
314	1789.297348	0	10
315	1792.15891	0	10
316	1795.009057	0	10
317	1797.847832	0	10
318	1800.675282	0	10
319	1803.491452	0	10
320	1806.296387	0	10
321	1809.090132	0	10

322	1811.87273	0	10
323	1814.644228	0	10
324	1817.404668	0	10
325	1820.154096	0	10
326	1822.892555	0	10
327	1825.620089	0	10
328	1828.336741	0	10
329	1831.042555	0	10
330	1833.737574	0	10
331	1836.421842	0	10
332	1839.0954	0	10
333	1841.758292	0	10
334	1844.410561	0	10
335	1847.052248	0	10
336	1849.683396	0	10
337	1852.304047	0	10
338	1854.914243	0	10
339	1857.514026	0	10
340	1860.103436	0	10
341	1862.682517	0	10
342	1865.251307	0	10
343	1867.80985	0	10
344	1870.358185	0	10
345	1872.896354	0	10
346	1875.424397	0	10
347	1877.942353	0	10
348	1880.450265	0	10
349	1882.948171	0	10
350	1885.436112	0	10
351	1887.914127	0	10
352	1890.382256	0	10
353	1892.840538	0	10
354	1895.289013	0	10
355	1897.727719	0	10
356	1900.156697	0	10
357	1902.575984	0	10
358	1904.985619	0	10
359	1907.38564	0	10
360	1909.776087	0	10
361	1912.156997	0	10
362	1914.528409	0	10
363	1916.89036	0	10

```
364 1919.242887  0    10
365 1921.586029  0    10
366 1923.919824  0    10
367 1926.244307  0    10
368 1928.559517  0    10
369 1930.86549   0    10
370 1933.162264  0    10
371 1935.449874  0    10
372 1937.728358  0    10
373 1939.997752  0    10
374 1942.258092  0    10
375 1944.509415  0    10
376 1946.751756  0    10
377 1948.985151  0    10
378 1951.209636  0    10
379 1953.425246  0    10
380 1955.632017  0    10
381 1957.829984  0    10
382 1960.019182  0    10
383 1962.199646  0    10
384 1964.371412  0    10
385 1966.534513  0    10
386 1968.688984  0    10
387 1970.83486   0    10
388 1972.972175  0    10
389 1975.100963  0    10
390 1977.221258  0    10
391 1979.333094  0    10
392 1981.436505  0    10
393 1983.531525  0    10
394 1985.618186  0    10
395 1987.696523  0    10
396 1989.766568  0    10
397 1991.828354  0    10
398 1993.881915  0    10
399 1995.927284  0    10
400 1997.964492  0    10
401 1999.993573  0    10
501  2200.000000      0       10.0000
#
NOCOOR  coordinates   3001   2289.469      0     5.0
NOCOOR  coordinates   2101    16357   10385      0
```

```
                          2111    16757   10385      0
NOCOOR  coordinates   2112    16357   10425      0
                          2122    16757   10425      0
NOCOOR  coordinates   2123    16357   10465      0
                          2133    16757   10465      0
NOCOOR  coordinates   2134    16357   10505      0
                          2144    16757   10505      0
NOCOOR  coordinates   2145    16357   10545      0
                          2155    16757   10545      0
NOCOOR  coordinates   2156    16357   10585      0
                          2166    16757   10585      0
NOCOOR  coordinates   2167    16357   10625      0
                          2177    16757   10625      0
NOCOOR  coordinates   2178    16357   10665      0
                          2188    16757   10665      0
NOCOOR  coordinates   2189    16357   10705      0
                          2199    16757   10705      0
NOCOOR  coordinates   2200    16357   10745      0
                          2210    16757   10745      0
NOCOOR  coordinates   2211    16357   10785      0
                          2221    16757   10785      0
#
#  Orient  input
#-------------------------------------------
#                                 no          x       y          z
ELORIENT  COORDINATES      1           0      10000     10
                                 500        2200      10000     10
ELORIENT  EULERANGLE      3000         0         0         0
ELORIENT  EULERANGLE      10001        0         0         0
                                10400         0         0         0
ELORIENT  EULERANGLE       2301         0         0         0
                                  2314        0         0         0
ELORIENT  EULERANGLE        2401        0         0         0
                                  2404        0         0         0
#
#
#
#  Elcon   input:
#-------------------------------------------
#          group          elty          material   ID   n1       n2   n3     n4
ELCON   ormpipe1     pipe31       pipemat1   1    1        2
#              n   j  k
```

```
REPEAT   400  1  1
#
#              group          elty          material   ID     n1       n2    n3     n4
ELCON    ormpipe2     pipe33       pipemat2   401   401      402
#              n    j   k
REPEAT   100  1    1
#  Lay-vessel
#          group          elty          material   ID    n1       n2
ELCON    vessel1      spring137   vessel1   3000  3001  501
#
#                                  name  of  surface          ID     n1
ELCON    seabed       cont126      cosurf1            10001   1
#           n    j   k
REPEAT  400  1  1
#
#
#  The  stinger  section
ELCON    ormcontact     cont164      roller1   2301   3001
ELCON    ormcontact1   cont164      roller2   2302   3001
ELCON    ormcontact2   cont164      roller3   2303   3001
ELCON    ormcontact3   cont164      roller4   2304   3001
ELCON    ormcontact4   cont164      roller5   2305   3001
ELCON    ormcontact5   cont164      roller6   2306   3001
ELCON    ormcontact6   cont164      roller7   2307   3001
ELCON    ormcontact7   cont164      roller8   2308   3001
ELCON    ormcontact8   cont164      roller9   2309   3001
ELCON    ormcontact9   cont164      roller10  2310   3001
ELCON    ormcontact10  cont164      roller11  2311   3001
ELCON    ormcontact11  cont164      roller12  2312   3001
#          n    j
REPEAT  3  1  0
#
ELCON    ormcontact12  cont164      roller13  2401   3001
#          n    j
REPEAT  4  1  0
#
ELCON    sea1           sea150       seamat     2101  2101  2102   2113   2112
REPEAT  10  1  1
repeat  10  10  11
#
#  Elecc  data:
#-----------------------------------------------------------------
```

```
#
#        type       elno   end      ex              ey          ez                fi                dx1   dy1
dz1  dx2  dy2       dz2
ELECC   stinger    2301   1    -89.469          0       4.252             0                 0
     -1          0    0    1          0
ELECC   stinger    2302   1    -110.410041      0       3.058111827      -0.1139004670     -1
          0    0    1          0
ELECC   stinger    2303   1    -130.4379832     0      -0.360522377      -0.224227216      0
     -1          0    0    1          0
ELECC   stinger    2304   1    -139.2163505     0      -2.590866573      -0.273389145      0
     -1          0    0    1          0
ELECC   stinger    2305   1    -149.7034056     0      -5.871840641      -0.333035425      0
     -1          0    0    1          0
ELECC   stinger    2306   1    -159.634299      0      -9.630899746      -0.390673873      0
     -1          0    0    1          0
ELECC   stinger    2307   1    -168.4635771     0     -13.54082696       -0.443087862      0
     -1          0    0    1          0
ELECC   stinger    2308   1    -177.329431      0     -18.04524037       -0.497066699      0
     -1          0    0    1          0
ELECC   stinger    2309   1    -187.1788443     0     -23.78993046       -0.558960837      0
     -1          0    0    1          0
ELECC   stinger    2310   1    -195.3690509     0     -29.22208808       -0.612306666      0
     -1          0    0    1          0
ELECC   stinger    2311   1    -202.1900777     0     -34.25104409       -0.658304683      0
     -1          0    0    1          0
ELECC   stinger    2312   1    -208.0500466     0     -38.97753767       -0.699167567      0
     -1          0    0    1          0
ELECC   stinger    2313   1    -213.7204751     0     -43.94717772       -0.740092451      0
     -1          0    0    1          0
ELECC   stinger    2314   1    -219.2000795     0     -49.16175439 -0.781149162 0     -1
0    0    1          0
ELECC   stinger    2401   1    -110.410041      0       3.058111827      -0.1139004670
     -0.75048  0    0    -0.75048  1.5
ELECC   stinger    2402   1    -110.410041      0       3.058111827      -0.1139004670
     0.75048   0    0    0.75048   1.5
ELECC   stinger    2403   1    -187.1788443     0     -23.78993046       -0.558960837       0
     -0.75048  0    0    -0.75048  1.5
ELECC   stinger    2404   1    -187.1788443     0     -23.78993046       -0.558960837       0
     0.75048   0    0    0.75048   1.5
ELECC   beam       3000   1    -89.469          0       4.999
#-----------------------------------------------------------------
#
```

```
# Cosurfpr data
#-----------------------------------------------------------------
#
#            name      data file                          nlines   kp0   x0          y0       fi    id
COSURFPR cosurf1 "OLT_revF_numeric_route.txt"  1         0    0           0        0      100
COSUPR 100  -100000  10000000      soil1
#
#
# Contact interface data:
#-----------------------------------------------------------------
---------
#          groupn       mname              name       is1 isn  istx   isty   istz    gt1 gt2
CONTINT seabed          ormpipe1        cosurf1     1 401       3       1 1       50   1.0
CONTINT ormcontact    ormcontact     ormpipe2 401 501  10000  10000 1      50   1.0
CONTINT ormcontact1   ormcontact1    ormpipe2 401 501  10000  10000 1      50   1.0
CONTINT ormcontact2   ormcontact2    ormpipe2 401 501  10000  10000 1      50   1.0
CONTINT ormcontact3   ormcontact3    ormpipe2 401 501  10000  10000 1      50   1.0
CONTINT ormcontact4   ormcontact4    ormpipe2 401 501  10000  10000 1      50   1.0
CONTINT ormcontact5   ormcontact5    ormpipe2 401 501  10000  10000 1      50   1.0
CONTINT ormcontact6   ormcontact6    ormpipe2 401 501  10000  10000 1      50   1.0
CONTINT ormcontact7   ormcontact7    ormpipe2 401 501  10000  10000 1      50   1.0
CONTINT ormcontact8   ormcontact8    ormpipe2 401 501  10000  10000 1      50   1.0
CONTINT ormcontact9   ormcontact9    ormpipe2 401 501  10000  10000 1      50   1.0
CONTINT ormcontact10  ormcontact10   ormpipe2 401 501  10000  10000 1      50   1.0
CONTINT ormcontact11  ormcontact11   ormpipe2 401 501  10000  10000 1      50   1.0
CONTINT ormcontact12  ormcontact12   ormpipe2 401 501  10000  10000 1      50   1.0
CONTINT sea1            sea1            ormpipe1
CONTINT sea1            sea1            ormpipe2
#
#
# Element property input:
#-----------------------------------------------------------------
#            name      type      rad       th      CDr   Cdt   CMr   CMt    wd         ws        ODp
ODw      rks
ELPROP ormpipe1 pipe   0.525 0.0341     0.8   0.1   2.0   0.2    1.291   0.161    1.0841
1.0841   0.5
ELPROP ormpipe2 pipe   0.525 0.0341     0.8   0.1   2.0   0.2    1.291   0.161    1.0841
1.0841   0.5
#            name           type      diam
ELPROP ormcontact    roller   0.400
ELPROP ormcontact1   roller   0.400
ELPROP ormcontact2   roller   0.400
```

```
ELPROP  ormcontact3   roller   0.400
ELPROP  ormcontact4   roller   0.400
ELPROP  ormcontact5   roller   0.400
ELPROP  ormcontact6   roller   0.400
ELPROP  ormcontact7   roller   0.400
ELPROP  ormcontact8   roller   0.400
ELPROP  ormcontact9   roller   0.400
ELPROP  ormcontact10  roller   0.400
ELPROP  ormcontact11  roller   0.400
ELPROP  ormcontact12  roller   0.400
#
#          name           type              ix    iy    iz    irx    iry    irz
ELPROP  vessel1       genspring        1     1     1      1      1      1
#
#
#-------------------------------------------------------------------
---
#  LOAD  INPUT:
#-------------------------------------------------------------------
---
#
#  Concentrated  nodal  loads:
#-----------------------------------------------
#       hist   dir   no1  r1   no2  r2           n  m
CLOAD    50      1   501  0.166195E+04
#
#  External  pressure  and  gravity:
#-----------------------------------------------
PELOAD  100  100
#
#TLOAD   200  100  100  200  100
#
#PILOAD   200  100  20  200  20
#
#  Current  and  wave  loads:
#-------------------------------------------------
#          name      x1     y1       x2     y2       icur  ihist
SEALO    sea1  -400000      0        0     0         100    400
                    0      0   2400000     0        200    500
#
#
#          no       depth      curr       fi
```

```
CURLOAD  100  global     0          1.0     0.93
                 -200        0.1     0.93
                -5000        0.1     0.93
#          no      depth     curr      fi
CURLOAD  200  global     0          1.0     0.93
                 -200        0.1     0.93
                -5000        0.1     0.93
#
#
#         seagrp        type     wav  hist     x0      y0     phi         T         H      D     Phase
#WAVELO     sea1    REGULAR     100    250  1667.270  0     2.437    10       2.0    2200    0
WAVELO    sea1    IRREGULAR     100    250     0.0               0.0      1.570796     10      4.0
2200  0.1    3600      1.1      125     0    1
#
#
#
#-------------------------------------------------------------------------
----
#  Boundary  condition  data
#-------------------------------------------------------------------------
----
#
#         Loc       node    dir
BONCON  GLOBAL   1         1
BONCON  GLOBAL   1         2
#BONCON  GLOBAL   1         3
#BONCON  GLOBAL   1         4
#BONCON  GLOBAL   1         5
#BONCON  GLOBAL   1         6
#
#
#
BONCON  GLOBAL  2101      1
REPEAT     121  1
BONCON  GLOBAL  2101      2
REPEAT     121  1
#-----------------------------------------------
#  CONSTRAINT  INPUT:
#-----------------------------------------------
#
#                              sn  dof  mn    fi1    fi2    fi3    ex      ey    ez
#CONSTR  PDISP  SPECIAL   501  1    3001  0     0.0      0    -89.469    0    5.000
```

```
CONSTR  PDISP  SPECIAL   501  2   3001  0    0.0     0   -89.469  0   5.000
CONSTR  PDISP  SPECIAL   501  3   3001  0    0.0     0   -89.469  0   5.000
CONSTR  PDISP  SPECIAL   501  4   3001  0    0.0     0   -89.469  0   5.000
#                        sn   df      head
CONSTR  PDISP  RAO      3001  1     2.530727  100    surge
CONSTR  PDISP  RAO      3001  2     2.530727  100    sway
CONSTR  PDISP  RAO      3001  3     2.530727  100    heave
CONSTR  PDISP  RAO      3001  4     2.530727  100    roll
CONSTR  PDISP  RAO      3001  5     2.530727  100    pitch
CONSTR  PDISP  RAO      3001  6     2.530727  100    yaw
#
#
#  Wave  elevation:
#-----------------------------------------------------
CONSTR  PDISP  WAVE  2101   3  100
REPEAT    121  1
#
#-------------------------------------------------------------
#  History  data
#
#       no   istp   fac
THIST   50     0   0.0
               1   1.0
             360   1.0
#
THIST  100     0   1.0
             360   1.0
#
#       no   istp   fac
THIST  250
               0   0.0
              10   0.0
              40  1.0
              120   1.0
             360   1.0
#
THIST  300     0   0.0
              40   1.0
             360   1.0
#
THIST  400     0   0.0
              40   1.0
```

```
            360   1.0
THIST  500    0   0.0
             40   1.0
            360   1.0
THIST  999    0   0.0
            360   0.0
#
#
#-----------------------------------------------------------------------
-----------
#   Material  data:
#-----------------------------------------------------------------------
-----------
#
#           name        type       poiss    talfa  tecond    heatc     beta           ea
MATERIAL  pipemat1  linear     0.3      1.17e-5     50        800     0         2.249e7
eiy      eiz          git       em      gm
3.10e6  3.10e6   2.39e6   2e8     8e7
#           name        type          alfa  poiss  ro        talfa  tecondheatc  eps  sigma
#
MATERIAL  pipemat2  elastoplastic   1   0.3   7.850   1.17e-5  50  800   0        0
                                                                                  1.691E-03
                                                                      3.50E+05
                                                                                  0.005  4.50E+05
                                                                                    9.980E-02
                                                                    8.35E+05
#           name          type     density
MATERIAL  seamat       sea        1000e-3
#           name          type  rmyx  rmyy  xname  yname    zname
MATERIAL  soil1       contact  0.5     1.0    soilx   soily     soilz
MATERIAL  soil2       contact  0.5     1.0    soilx   soily     soilz2
MATERIAL  roller1    contact  0.3     0.3    soilx   soily     soilz3
MATERIAL  roller2    contact  0.3     0.3    soilx   soily     soilz4
MATERIAL  roller3    contact  0.3     0.3    soilx   soily     soilz5
MATERIAL  roller4    contact  0.3     0.3    soilx   soily     soilz6
MATERIAL  roller5    contact  0.3     0.3    soilx   soily     soilz7
MATERIAL  roller6    contact  0.3     0.3    soilx   soily     soilz8
MATERIAL  roller7    contact  0.3     0.3    soilx   soily     soilz9
MATERIAL  roller8    contact  0.3     0.3    soilx   soily     soilz10
MATERIAL  roller9    contact  0.3     0.3    soilx   soily     soilz11
MATERIAL  roller10  contact  0.3     0.3    soilx   soily     soilz12
MATERIAL  roller11  contact  0.3     0.3    soilx   soily     soilz13
```

```
MATERIAL  roller12  contact  0.3     0.3    soilx   soily     soilz14
MATERIAL  roller13  contact  0.3     0.3    soilx   soily     soilz15
#           name        type     alfa     eps       sig
MATERIAL  soilx     epcurve  1        0          0
                                        0.005     1
                                      100.00      10
#           name        type              eps       sig
MATERIAL  soily     epcurve  1          0         0
                                        0.10      1
                                     100.00       2
#           name        type         eps       sig
MATERIAL  soilz     hycurve   -10000  -10000000
                                10000   10000000
#
#           name        type         eps       sig
MATERIAL  soilz2    hycurve   -10000  -10000000
                                10000   10000000
#
#           name        type         eps       sig
MATERIAL  soilz3    hycurve   -10000   -240000000
                                10000    240000000
MATERIAL  soilz4    hycurve   -10000   -220000000
                                10000    220000000
MATERIAL  soilz5    hycurve   -10000   -200000000
                                10000    200000000
MATERIAL  soilz6    hycurve   -10000   -170000000
                                10000    170000000
MATERIAL  soilz7    hycurve   -10000   -142000000
                                10000    142000000
MATERIAL  soilz8    hycurve   -10000   -116000000
                                10000    116000000
MATERIAL  soilz9    hycurve   -10000   -82000000
                                10000    82000000
MATERIAL  soilz10   hycurve   -10000   -58000000
                                10000    58000000
MATERIAL  soilz11   hycurve   -10000   -48000000
                                10000    48000000
MATERIAL  soilz12   hycurve   -10000   -40000000
                                10000    40000000
MATERIAL  soilz13   hycurve   -10000   -30000000
                                10000    30000000
MATERIAL  soilz14   hycurve   -10000   -20000000
```

```
                                10000     20000000
MATERIAL  soilz15   hycurve   -10000   -200000000
                                10000     200000000
#
#           name        type         apr1     spr2    spr3     spr4     spr5     spr6
MATERIAL  vessel1  genspring  surgesp1  yawsp  heavesp   rollsp   pitchsp  swaysp
#                                Tensioner
MATERIAL  surgesp   epcurve     1
                                 0.00      0.0
                                 1.00     50.0
                                23.00     200.0
MATERIAL  surgesp1  hycurve   -10000     -50000
                               -24.00     -40000
                               -23.00     -200
                                -1.00     -50
                                 1.00     50
                                23.00     200
                                24.00     40000
                                10000     50000
MATERIAL  surgesp2  hycurve  -1000  0
                               1000  0
MATERIAL  yawsp     hycurve  -1000  0
                               1000  0
MATERIAL  heavesp   hycurve  -1000  0
                               1000  0
MATERIAL  rollsp    hycurve  -1000   0
                               1000   0
MATERIAL  pitchsp   hycurve  -1000   0
                               1000   0
MATERIAL  swaysp    hycurve  -1000   0
                               1000   0
#-------------------------------------------------
#  RAO  definitions:
#-------------------------------------------------
#-------------------------------------------------
#  RAO  definitions:
#-------------------------------------------------
RAOPROP  surge  DEF   0  1.57  3.14  4.71  6.28   surge1  surge2  surge3  surge4  surge5
RAOPROP  sway   DEF   0  1.57  3.14  4.71  6.28   sway1  sway2  sway3   sway4   sway5
RAOPROP  heave  DEF   0  1.57  3.14  4.71  6.28   heave1  heave2  heave3  heave4  heave5
RAOPROP  roll   DEF   0  1.57  3.14  4.71  6.28   roll1  roll2  roll3  roll4  roll5
RAOPROP  pitch  DEF   0  1.57  3.14  4.71  6.28   pitch1  pitch2  pitch3  pitch4  pitch5
```

```
RAOPROP  yaw     DEF    0  1.57  3.14  4.71  6.28    yaw1  yaw2  yaw3  yaw4  yaw5
#
RAOPROP  surge1  CURVE  0          0          0.000000000
                 0.314159265       1.1908    3.129375349
                 0.34906585         1.0798    3.127630020
                 0.369599136       1.0253    3.127630020
                 0.392699082        0.9693    3.124139361
                 0.41887902         0.909     3.122394032
                 0.448798951        0.8391    3.125884690
                 0.483321947        0.7541    3.127630020
                 0.502654825        0.7029    3.132866007
                 0.523598776        0.6435    -3.136356666
                 0.54636394         0.5734    -3.111922056
                 0.571198664        0.4888    -3.061307508
                 0.598398601        0.3833    -2.954842424
                 0.628318531        0.2414    -2.696533694
                 0.661387927        0.0802    -1.642354826
                 0.698131701       0.1581    0.322885912
                 0.785398163        0.1889    0.895353906
                 0.897597901        0.1167    -1.162389282
                 1.047197551       0.0337    -1.956514091
                 1.256637061       0.0581    0.497418837
                 1.570796327        0.0143    -2.651155134

RAOPROP  surge2  CURVE  0          0          0.000000000
                       0.314159265        0          0.000000000
                       0.34906585          0          0.000000000
                       0.369599136        0          0.000000000
                       0.392699082         0          0.000000000
                       0.41887902          0          0.000000000
                       0.448798951         0          0.000000000
                       0.483321947         0          0.000000000
                       0.502654825         0          0.000000000
                       0.523598776         0          0.000000000
                       0.54636394          0          0.000000000
                       0.571198664         0          0.000000000
                       0.598398601         0          0.000000000
                       0.628318531         0          0.000000000
                       0.661387927         0          0.000000000
                       0.698131701        0          0.000000000
                       0.785398163         0          0.000000000
                       0.897597901         0          0.000000000
```

Hong, Wei

```
                    1.047197551        0          0.000000000
                    1.256637061        0          0.000000000
                    1.570796327        0          0.000000000

RAOPROP  surge3  CURVE   0          0          0.000000000
                  0.314159265      -1.1908    3.129375349
                  0.34906585       -1.0798    3.12763002
                  0.369599136      -1.0253    3.12763002
                  0.392699082      -0.9693    3.124139361
                  0.41887902       -0.909     3.122394032
                  0.448798951      -0.8391    3.12588469
                  0.483321947      -0.7541    3.12763002
                  0.502654825      -0.7029    3.132866007
                  0.523598776      -0.6435    -3.136356666
                  0.54636394       -0.5734    -3.111922056
                  0.571198664      -0.4888    -3.061307508
                  0.598398601      -0.3833    -2.954842424
                  0.628318531      -0.2414    -2.696533694
                  0.661387927      -0.0802    -1.642354826
                  0.698131701      -0.1581    0.322885912
                  0.785398163      -0.1889    0.895353906
                  0.897597901      -0.1167    -1.162389282
                  1.047197551      -0.0337    -1.956514091
                  1.256637061      -0.0581    0.497418837
                  1.570796327      -0.0143    -2.651155134

RAOPROP  surge4  CURVE  0          0          0.000000000
                    0.314159265        0          0.000000000
                    0.34906585         0          0.000000000
                    0.369599136        0          0.000000000
                    0.392699082        0          0.000000000
                    0.41887902         0          0.000000000
                    0.448798951        0          0.000000000
                    0.483321947        0          0.000000000
                    0.502654825        0          0.000000000
                    0.523598776        0          0.000000000
                    0.54636394         0          0.000000000
                    0.571198664        0          0.000000000
                    0.598398601        0          0.000000000
                    0.628318531        0          0.000000000
                    0.661387927        0          0.000000000
                    0.698131701        0          0.000000000
```

```
                0.785398163     0       0.000000000
                0.897597901     0       0.000000000
                1.047197551     0       0.000000000
                1.256637061     0       0.000000000
                1.570796327     0       0.000000000

RAOPROP  surge5  CURVE  0       0       0.000000000
                0.314159265     1.1908  3.129375349
                0.34906585      1.0798  3.127630020
                0.369599136     1.0253  3.127630020
                0.392699082     0.9693  3.124139361
                0.41887902      0.909   3.122394032
                0.448798951     0.8391  3.125884690
                0.483321947     0.7541  3.127630020
                0.502654825     0.7029  3.132866007
                0.523598776     0.6435  -3.136356666
                0.54636394      0.5734  -3.111922056
                0.571198664     0.4888  -3.061307508
                0.598398601     0.3833  -2.954842424
                0.628318531     0.2414  -2.696533694
                0.661387927     0.0802  -1.642354826
                0.698131701     0.1581  0.322885912
                0.785398163     0.1889  0.895353906
                0.897597901     0.1167  -1.162389282
                1.047197551     0.0337  -1.956514091
                1.256637061     0.0581  0.497418837
                1.570796327     0.0143  -2.651155134

RAOPROP  sway1   CURVE  0       0       0.000000000
                0.314159265     0       0.000000000
                0.34906585      0       0.000000000
                0.369599136     0       0.000000000
                0.392699082     0       0.000000000
                0.41887902      0       0.000000000
                0.448798951     0       0.000000000
                0.483321947     0       0.000000000
                0.502654825     0       0.000000000
                0.523598776     0       0.000000000
                0.54636394      0       0.000000000
                0.571198664     0       0.000000000
                0.598398601     0       0.000000000
```

```
                0.628318531     0       0.000000000
                0.661387927     0       0.000000000
                0.698131701     0       0.000000000
                0.785398163     0       0.000000000
                0.897597901     0       0.000000000
                1.047197551     0       0.000000000
                1.256637061     0       0.000000000
            1.570796327   0     0

RAOPROP  sway2   CURVE  0       0       0.000000000
                0.314159265     1.1908   3.129375349
                0.34906585      1.0798   3.127630020
                0.369599136     1.0253   3.127630020
                0.392699082     0.9693   3.124139361
                0.41887902      0.909    3.122394032
                0.448798951     0.8391   3.125884690
                0.483321947     0.7541   3.127630020
                0.502654825     0.7029   3.132866007
                0.523598776     0.6435   -3.136356666
                0.54636394      0.5734   -3.111922056
                0.571198664     0.4888   -3.061307508
                0.598398601     0.3833   -2.954842424
                0.628318531     0.2414   -2.696533694
                0.661387927     0.0802   -1.642354826
                0.698131701     0.1581   0.322885912
                0.785398163     0.1889   0.895353906
                0.897597901     0.1167   -1.162389282
                1.047197551     0.0337   -1.956514091
                1.256637061     0.0581   0.497418837
                1.570796327     0.0143   -2.651155134

RAOPROP  sway3   CURVE  0       0       0.000000000
                0.314159265     0       0.000000000
                0.34906585      0       0.000000000
                0.369599136     0       0.000000000
                0.392699082     0       0.000000000
                0.41887902      0       0.000000000
                0.448798951     0       0.000000000
                0.483321947     0       0.000000000
                0.502654825     0       0.000000000
                0.523598776     0       0.000000000
                0.54636394      0       0.000000000
```

Hong, Wei

```
                0.571198664     0       0.000000000
                0.598398601     0       0.000000000
                0.628318531     0       0.000000000
                0.661387927     0       0.000000000
                0.698131701     0       0.000000000
                0.785398163     0       0.000000000
                0.897597901     0       0.000000000
                1.047197551     0       0.000000000
                1.256637061     0       0.000000000
            1.570796327 0   0

RAOPROP  sway4  CURVE  0       0       0.000000000
                0.314159265     -1.1908 3.129375349
                0.34906585      -1.0798 3.12763002
                0.369599136     -1.0253 3.12763002
                0.392699082     -0.9693 3.124139361
                0.41887902      -0.909  3.122394032
                0.448798951     -0.8391 3.12588469
                0.483321947     -0.7541 3.12763002
                0.502654825     -0.7029 3.132866007
                0.523598776     -0.6435 -3.136356666
                0.54636394      -0.5734 -3.111922056
                0.571198664     -0.4888 -3.061307508
                0.598398601     -0.3833 -2.954842424
                0.628318531     -0.2414 -2.696533694
                0.661387927     -0.0802 -1.642354826
                0.698131701     -0.1581 0.322885912
                0.785398163     -0.1889 0.895353906
                0.897597901     -0.1167 -1.162389282
                1.047197551     -0.0337 -1.956514091
                1.256637061     -0.0581 0.497418837
                1.570796327     -0.0143 -2.651155134

RAOPROP  sway5  CURVE  0       0       0.000000000
                0.314159265     0       0.000000000
                0.34906585      0       0.000000000
                0.369599136     0       0.000000000
                0.392699082     0       0.000000000
                0.41887902      0       0.000000000
                0.448798951     0       0.000000000
                0.483321947     0       0.000000000
                0.502654825     0       0.000000000
```

```
                0.523598776         0          0.000000000
                0.54636394          0          0.000000000
                0.571198664         0          0.000000000
                0.598398601         0          0.000000000
                0.628318531         0          0.000000000
                0.661387927         0          0.000000000
                0.698131701         0          0.000000000
                0.785398163         0          0.000000000
                0.897597901         0          0.000000000
                1.047197551         0          0.000000000
                1.256637061         0          0.000000000
            1.570796327    0     0

RAOPROP  heave1  CURVE  0          0          0
                0.314159265       1.0639   0.829031395
                0.34906585        1.0692   0.753982237
                0.369599136       1.0767   0.706858347
                0.392699082       1.0844   0.654498469
                0.41887902        1.0906   0.596902604
                0.448798951       1.0907   0.53581608
                0.483321947       1.0688   0.464257581
                0.502654825       1.0455   0.424115008
                0.523598776       1.01     0.380481777
                0.54636394        0.963    0.333357887
                0.571198664       0.9081   0.277507351
                0.598398601       0.8551   0.240855437
                0.628318531       0.7643   0.298451302
                0.661387927       0.5216   0.521853446
                0.698131701       0.1095   0.773180859
                0.785398163       0.2618   -1.987930018
                0.897597901       0.0802   1.628392192
                1.047197551       0.1258   1.256637061
                1.256637061       0.1161   -2.605776573
                1.570796327       0.0291   -1.436405974

RAOPROP  heave2  CURVE  0          0          0
                0.314159265       1.0639   0.829031395
                0.34906585        1.0692   0.753982237
                0.369599136       1.0767   0.706858347
                0.392699082       1.0844   0.654498469
                0.41887902        1.0906   0.596902604
```

```
                0.448798951     1.0907   0.53581608
                0.483321947     1.0688   0.464257581
                0.502654825     1.0455   0.424115008
                0.523598776     1.01     0.380481777
                0.54636394      0.963    0.333357887
                0.571198664     0.9081   0.277507351
                0.598398601     0.8551   0.240855437
                0.628318531     0.7643   0.298451302
                0.661387927     0.5216   0.521853446
                0.698131701     0.1095   0.773180859
                0.785398163     0.2618   -1.987930018
                0.897597901     0.0802   1.628392192
                1.047197551     0.1258   1.256637061
                1.256637061     0.1161   -2.605776573
                1.570796327     0.0291   -1.436405974

RAOPROP  heave3  CURVE  0        0        0
                0.314159265     1.0639   0.829031395
                0.34906585      1.0692   0.753982237
                0.369599136     1.0767   0.706858347
                0.392699082     1.0844   0.654498469
                0.41887902      1.0906   0.596902604
                0.448798951     1.0907   0.53581608
                0.483321947     1.0688   0.464257581
                0.502654825     1.0455   0.424115008
                0.523598776     1.01     0.380481777
                0.54636394      0.963    0.333357887
                0.571198664     0.9081   0.277507351
                0.598398601     0.8551   0.240855437
                0.628318531     0.7643   0.298451302
                0.661387927     0.5216   0.521853446
                0.698131701     0.1095   0.773180859
                0.785398163     0.2618   -1.987930018
                0.897597901     0.0802   1.628392192
                1.047197551     0.1258   1.256637061
                1.256637061     0.1161   -2.605776573
                1.570796327     0.0291   -1.436405974

RAOPROP  heave4  CURVE  0        0        0
                0.314159265     1.0639   0.829031395
                0.34906585      1.0692   0.753982237
                0.369599136     1.0767   0.706858347
```

```
                0.392699082      1.0844   0.654498469
                0.41887902       1.0906   0.596902604
                0.448798951      1.0907   0.53581608
                0.483321947      1.0688   0.464257581
                0.502654825      1.0455   0.424115008
                0.523598776      1.01     0.380481777
                0.54636394       0.963    0.333357887
                0.571198664      0.9081   0.277507351
                0.598398601      0.8551   0.240855437
                0.628318531      0.7643   0.298451302
                0.661387927      0.5216   0.521853446
                0.698131701      0.1095   0.773180859
                0.785398163      0.2618   -1.987930018
                0.897597901      0.0802   1.628392192
                1.047197551      0.1258   1.256637061
                1.256637061      0.1161   -2.605776573
                1.570796327      0.0291   -1.436405974

RAOPROP  heave5  CURVE  0        0        0
                0.314159265      1.0639   0.829031395
                0.34906585       1.0692   0.753982237
                0.369599136      1.0767   0.706858347
                0.392699082      1.0844   0.654498469
                0.41887902       1.0906   0.596902604
                0.448798951      1.0907   0.53581608
                0.483321947      1.0688   0.464257581
                0.502654825      1.0455   0.424115008
                0.523598776      1.01     0.380481777
                0.54636394       0.963    0.333357887
                0.571198664      0.9081   0.277507351
                0.598398601      0.8551   0.240855437
                0.628318531      0.7643   0.298451302
                0.661387927      0.5216   0.521853446
                0.698131701      0.1095   0.773180859
                0.785398163      0.2618   -1.987930018
                0.897597901      0.0802   1.628392192
                1.047197551      0.1258   1.256637061
                1.256637061      0.1161   -2.605776573
                1.570796327      0.0291   -1.436405974


RAOPROP  roll1   CURVE  0        0        0.000000000
```

```
                0.314159265         0          0.000000000
                0.34906585          0          0.000000000
                0.369599136         0          0.000000000
                0.392699082         0          0.000000000
                0.41887902          0          0.000000000
                0.448798951         0          0.000000000
                0.483321947         0          0.000000000
                0.502654825         0          0.000000000
                0.523598776         0          0.000000000
                0.54636394          0          0.000000000
                0.571198664         0          0.000000000
                0.598398601         0          0.000000000
                0.628318531         0          0.000000000
                0.661387927         0          0.000000000
                0.698131701         0          0.000000000
                0.785398163         0          0.000000000
                0.897597901         0          0.000000000
                1.047197551         0          0.000000000
                1.256637061         0          0.000000000
            1.570796327    0     0

RAOPROP  roll2   CURVE  0          0          0.000000000
                0.314159265       0.00996583        -0.027925268
                0.34906585        0.0108926         -0.027925268
                0.369599136       0.011477285       -0.026179939
                0.392699082       0.012126548       -0.02443461
                0.41887902        0.012821189       -0.02443461
                0.448798951       0.013494886       -0.013962634
                0.483321947       0.014060372       -0.005235988
                0.502654825       0.014254104       0.003490659
                0.523598776       0.014327408       0.019198622
                0.54636394        0.014241887       0.04712389
                0.571198664       0.013894566       0.097738438
                0.598398601       0.013158037       0.193731547
                0.628318531       0.011445869       0.39618974
                0.661387927       0.007897615       0.799360797
                0.698131701       0.003136357       1.736602606
                0.785398163       0.004256858       -2.331759881
                0.897597901       0.000949459       1.123992038
                1.047197551       0.001469567       1.052433539
                1.256637061       0.001350885       -2.686061719
                1.570796327       0.000439823       -1.466076572
```

```
RAOPROP  roll3   CURVE  0          0          0.000000000
                        0.314159265        0          0.000000000
                        0.34906585         0          0.000000000
                        0.369599136        0          0.000000000
                        0.392699082        0          0.000000000
                        0.41887902         0          0.000000000
                        0.448798951        0          0.000000000
                        0.483321947        0          0.000000000
                        0.502654825        0          0.000000000
                        0.523598776        0          0.000000000
                        0.54636394         0          0.000000000
                        0.571198664        0          0.000000000
                        0.598398601        0          0.000000000
                        0.628318531        0          0.000000000
                        0.661387927        0          0.000000000
                        0.698131701        0          0.000000000
                        0.785398163        0          0.000000000
                        0.897597901        0          0.000000000
                        1.047197551        0          0.000000000
                        1.256637061        0          0.000000000
                    1.570796327   0     0

RAOPROP  roll4   CURVE  0          0          0.000000000
                    0.314159265      -0.00996583      -0.027925268
                    0.34906585       -0.0108926       -0.027925268
                    0.369599136      -0.011477285     -0.026179939
                    0.392699082      -0.012126548     -0.02443461
                    0.41887902       -0.012821189     -0.02443461
                    0.448798951      -0.013494886     -0.013962634
                    0.483321947      -0.014060372     -0.005235988
                    0.502654825      -0.014254104     0.003490659
                    0.523598776      -0.014327408     0.019198622
                    0.54636394       -0.014241887     0.04712389
                    0.571198664      -0.013894566     0.097738438
                    0.598398601      -0.013158037     0.193731547
                    0.628318531      -0.011445869     0.39618974
                    0.661387927      -0.007897615     0.799360797
                    0.698131701      -0.003136357     1.736602606
                    0.785398163      -0.004256858     -2.331759881
                    0.897597901      -0.000949459     1.123992038
                    1.047197551      -0.001469567     1.052433539
```

```
                1.256637061       -0.001350885      -2.686061719
                1.570796327       -0.000439823      -1.466076572

RAOPROP  roll5   CURVE  0          0          0.000000000
                       0.314159265        0          0.000000000
                       0.34906585         0          0.000000000
                       0.369599136        0          0.000000000
                       0.392699082        0          0.000000000
                       0.41887902         0          0.000000000
                       0.448798951        0          0.000000000
                       0.483321947        0          0.000000000
                       0.502654825        0          0.000000000
                       0.523598776        0          0.000000000
                       0.54636394         0          0.000000000
                       0.571198664        0          0.000000000
                       0.598398601        0          0.000000000
                       0.628318531        0          0.000000000
                       0.661387927        0          0.000000000
                       0.698131701        0          0.000000000
                       0.785398163        0          0.000000000
                       0.897597901        0          0.000000000
                       1.047197551        0          0.000000000
                       1.256637061        0          0.000000000
                1.570796327    0     0


RAOPROP  pitch1  CURVE  0          0          0.000000000
                 0.314159265       0.00996583        -0.027925268
                 0.34906585        0.0108926         -0.027925268
                 0.369599136       0.011477285       -0.026179939
                 0.392699082       0.012126548       -0.02443461
                 0.41887902        0.012821189       -0.02443461
                 0.448798951       0.013494886       -0.013962634
                 0.483321947       0.014060372       -0.005235988
                 0.502654825       0.014254104       0.003490659
                 0.523598776       0.014327408       0.019198622
                 0.54636394        0.014241887       0.04712389
                 0.571198664       0.013894566       0.097738438
                 0.598398601       0.013158037       0.193731547
                 0.628318531       0.011445869       0.39618974
                 0.661387927       0.007897615       0.799360797
                 0.698131701       0.003136357       1.736602606
```

```
                0.785398163     0.004256858     -2.331759881
                0.897597901     0.000949459     1.123992038
                1.047197551     0.001469567     1.052433539
                1.256637061     0.001350885     -2.686061719
                1.570796327     0.000439823     -1.466076572

RAOPROP  pitch2  CURVE  0        0        0.000000000
                        0.314159265     0       0.000000000
                        0.34906585      0       0.000000000
                        0.369599136     0       0.000000000
                        0.392699082     0       0.000000000
                        0.41887902      0       0.000000000
                        0.448798951     0       0.000000000
                        0.483321947     0       0.000000000
                        0.502654825     0       0.000000000
                        0.523598776     0       0.000000000
                        0.54636394      0       0.000000000
                        0.571198664     0       0.000000000
                        0.598398601     0       0.000000000
                        0.628318531     0       0.000000000
                        0.661387927     0       0.000000000
                        0.698131701     0       0.000000000
                        0.785398163     0       0.000000000
                        0.897597901     0       0.000000000
                        1.047197551     0       0.000000000
                        1.256637061     0       0.000000000
                1.570796327     0       0

RAOPROP  pitch3  CURVE  0        0        0.000000000
                0.314159265     -0.00996583     -0.027925268
                0.34906585      -0.0108926      -0.027925268
                0.369599136     -0.011477285    -0.026179939
                0.392699082     -0.012126548    -0.02443461
                0.41887902      -0.012821189    -0.02443461
                0.448798951     -0.013494886    -0.013962634
                0.483321947     -0.014060372    -0.005235988
                0.502654825     -0.014254104    0.003490659
                0.523598776     -0.014327408    0.019198622
                0.54636394      -0.014241887    0.04712389
                0.571198664     -0.013894566    0.097738438
                0.598398601     -0.013158037    0.193731547
                0.628318531     -0.011445869    0.39618974
```

```
                0.661387927     -0.007897615     0.799360797
                0.698131701     -0.003136357     1.736602606
                0.785398163     -0.004256858     -2.331759881
                0.897597901     -0.000949459     1.123992038
                1.047197551     -0.001469567     1.052433539
                1.256637061     -0.001350885     -2.686061719
                1.570796327     -0.000439823     -1.466076572

RAOPROP  pitch4  CURVE  0        0        0.000000000
                        0.314159265      0        0.000000000
                        0.34906585       0        0.000000000
                        0.369599136      0        0.000000000
                        0.392699082      0        0.000000000
                        0.41887902       0        0.000000000
                        0.448798951      0        0.000000000
                        0.483321947      0        0.000000000
                        0.502654825      0        0.000000000
                        0.523598776      0        0.000000000
                        0.54636394       0        0.000000000
                        0.571198664      0        0.000000000
                        0.598398601      0        0.000000000
                        0.628318531      0        0.000000000
                        0.661387927      0        0.000000000
                        0.698131701      0        0.000000000
                        0.785398163      0        0.000000000
                        0.897597901      0        0.000000000
                        1.047197551      0        0.000000000
                        1.256637061      0        0.000000000
                        1.570796327      0        0

RAOPROP  pitch5  CURVE  0        0        0.000000000
                0.314159265     0.00996583      -0.027925268
                0.34906585      0.0108926       -0.027925268
                0.369599136     0.011477285     -0.026179939
                0.392699082     0.012126548     -0.02443461
                0.41887902      0.012821189     -0.02443461
                0.448798951     0.013494886     -0.013962634
                0.483321947     0.014060372     -0.005235988
                0.502654825     0.014254104     0.003490659
                0.523598776     0.014327408     0.019198622
                0.54636394      0.014241887     0.04712389
                0.571198664     0.013894566     0.097738438
```

```
0.598398601     0.013158037     0.193731547
0.628318531     0.011445869     0.39618974
0.661387927     0.007897615     0.799360797
0.698131701     0.003136357     1.736602606
0.785398163     0.004256858     -2.331759881
0.897597901     0.000949459     1.123992038
1.047197551     0.001469567     1.052433539
1.256637061     0.001350885     -2.686061719
1.570796327     0.000439823     -1.466076572
```

```
RAOPROP  yaw1    CURVE  0        0        0.000000000
                1.570796327  0    0

RAOPROP  yaw2    CURVE  0        0        0.000000000
                1.570796327  0    0

RAOPROP  yaw3    CURVE  0        0        0.000000000
                1.570796327  0    0

RAOPROP  yaw4    CURVE  0        0        0.000000000
                1.570796327  0    0

RAOPROP  yaw5    CURVE  0        0        0.000000000
                1.570796327  0    0
```